

ANALYSIS & PDE

Volume 9

No. 7

2016

FRANCISCO DE LA HOZ, ZINEB HASSAINIA,
TAOUFIK HMIDI AND JOAN MATEU

AN ANALYTICAL AND NUMERICAL STUDY
OF STEADY PATCHES IN THE DISC

AN ANALYTICAL AND NUMERICAL STUDY OF STEADY PATCHES IN THE DISC

FRANCISCO DE LA HOZ, ZINEB HASSAINIA, TAOUFIK HMIDI AND JOAN MATEU

We prove the existence of m -fold rotating patches for the Euler equations in the disc, for the simply connected and doubly connected cases. Compared to the planar case, the rigid boundary introduces rich dynamics for the lowest symmetries $m = 1$ and $m = 2$. We also discuss some numerical experiments highlighting the interaction between the boundary of the patch and the rigid one.

1. Introduction	1609
2. Preliminaries and background	1617
2.1. Function spaces	1617
2.2. Elements of bifurcation theory	1617
2.3. Boundary equations	1618
3. Simply connected V -states	1621
3.1. Regularity of the functional F	1622
3.2. Spectral study	1624
3.3. Proof of Theorem 1	1629
4. Doubly connected V -states	1630
4.1. Boundary equations	1631
4.2. Regularity of the functional G	1632
4.3. Structure of the linearized operator	1632
4.4. Eigenvalues study	1638
4.5. Bifurcation for $m \geq 1$	1649
5. Numerical experiments	1655
5.1. Simply connected V -states	1655
5.2. Doubly connected V -states	1660
Acknowledgements	1668
References	1668

1. Introduction

In this paper, we shall discuss some aspects of the vortex motion for the Euler system in the unit disc \mathbb{D} of the Euclidean space \mathbb{R}^2 . That system is described by the equations

$$\left\{ \begin{array}{l} \partial_t v + v \cdot \nabla v + \nabla p = 0, \\ \operatorname{div} v = 0, \\ v \cdot \nu = 0 \\ v|_{t=0} = v_0. \end{array} \right. \quad (t, x) \in \mathbb{R}_+ \times \mathbb{D}, \quad \text{on } \partial\mathbb{D}, \quad (1)$$

MSC2010: primary 35Q35, 37G40, 35Q31; secondary 76B47.

Keywords: Euler equations, V -states, bifurcation.

Here, $v = (v^1, v^2)$ is the velocity field, and the pressure p is a scalar potential that can be related to the velocity using the incompressibility condition. The boundary equation means that there is no matter flow through the rigid boundary $\partial\mathbb{D} = \mathbb{T}$; the vector ν is the outer unitary vector orthogonal to the boundary. The main feature of two-dimensional flows is that they can be illustrated through their vorticity structure; this can be identified with the scalar function $\omega = \partial_1 v_2 - \partial_2 v_1$, and its evolution is governed by the nonlinear transport equation

$$\partial_t \omega + v \cdot \nabla \omega = 0. \tag{2}$$

To recover the velocity from the vorticity, we use the stream function Ψ , which is defined as the unique solution of the Dirichlet problem on the unit disc:

$$\begin{cases} \Delta \Psi = \omega, \\ \psi|_{\partial\mathbb{D}} = 0. \end{cases}$$

Therefore, the velocity is given by

$$v = \nabla^\perp \Psi, \quad \nabla^\perp = (-\partial_2, \partial_1).$$

By using the Green function of the unit disc, we get the expression

$$\Psi(z) = \frac{1}{4\pi} \int_{\mathbb{D}} \log \left| \frac{z - \xi}{1 - z\bar{\xi}} \right|^2 \omega(\xi) dA(\xi), \tag{3}$$

with dA being the planar Lebesgue measure. In what follows, we shall identify the Euclidean and the complex planes, so the velocity field is identified with the complex function

$$v(z) = v_1(x_1, x_2) + i v_2(x_1, x_2), \quad z = x_1 + i x_2.$$

Therefore, we get the compact formula

$$\begin{aligned} v(t, z) &= 2i \partial_{\bar{z}} \Psi(t, z) \\ &= \frac{i}{2\pi} \int_{\mathbb{D}} \frac{|\xi|^2 - 1}{(\bar{z} - \bar{\xi})(\xi \bar{z} - 1)} \omega(t, \xi) dA(\xi) \\ &= \frac{i}{2\pi} \int_{\mathbb{D}} \frac{\omega(t, \xi)}{\bar{z} - \bar{\xi}} dA(\xi) + \frac{i}{2\pi} \int_{\mathbb{D}} \frac{\xi}{1 - \xi \bar{z}} \omega(t, \xi) dA(\xi). \end{aligned} \tag{4}$$

We recognize in the first part of the last formula the structure of the Biot–Savart law in the plane \mathbb{R}^2 , which is given by

$$v(t, z) = \frac{i}{2\pi} \int_{\mathbb{C}} \frac{\omega(t, \xi)}{\bar{z} - \bar{\xi}} dA(\xi), \quad z \in \mathbb{C}. \tag{5}$$

The second term of (4) is absent in the planar case. It describes the contribution of the rigid boundary \mathbb{T} , and our main task is to investigate the boundary effects on the dynamics of special long-lived vortex structures. Before going further into details, we recall first that, from the equivalent formulation (2)–(4) of the Euler system (1), Yudovich [1963] was able to construct a unique global solution in the weak sense, provided that the initial vorticity ω_0 is compactly supported and bounded. This result is very important because it allows one to deal rigorously with vortex patches, which are vortices uniformly distributed in a

bounded region D , i.e., $\omega_0 = \chi_D$. These structures are preserved by the evolution, and at each time t , the vorticity is given by χ_{D_t} , with $D_t = \psi(t, D)$ being the image of D by the flow. As we shall see later in (16), the contour dynamics equation of the boundary ∂D_t is described by the following nonlinear integral equation. Let $\gamma_t : \mathbb{T} \rightarrow \partial D_t$ be the Lagrangian parametrization of the boundary; then

$$\partial_t \gamma_t = -\frac{1}{2\pi} \int_{\partial D_t} \log|\gamma_t - \xi| d\xi + \frac{1}{4\pi} \int_{\partial D_t} \frac{|\xi|^2}{1 - \bar{\gamma}_t \xi} d\xi.$$

We point out that, when the initial boundary is smooth enough, roughly speaking more regular than C^1 , then the regularity is propagated for long times without any loss. This was first achieved by Chemin [1998] in the plane and extended in bounded domains by Depauw [1999]. Note also that we can find in [Bertozzi and Constantin 1993] another proof of Chemin’s result. It appears that the boundary dynamics of the patch is very complicate to tackle and, to our knowledge, the only known explicit example is the stationary one given by a small disc centered at the origin. Even though explicit solutions form a poor class, one can try to find implicit patches with prescribed dynamics, such as rotating patches, also known as V -states. These patches are subject to perpetual rotation around some fixed point that we can assume to be the origin and with uniform angular velocity Ω ; this means that $D_t = e^{it\Omega} D$. We shall see in Section 2.3 that the V -states equation, when D is symmetric with respect to the real axis, is given by

$$\operatorname{Re} \left\{ \left(2\Omega \bar{z} + \int_{\Gamma} \frac{\bar{z} - \bar{\xi}}{z - \xi} d\xi - \int_{\Gamma} \frac{|\xi|^2}{1 - z\xi} d\xi \right) z' \right\} = 0, \quad z \in \Gamma \triangleq \partial D, \tag{6}$$

with z' being a tangent vector to the boundary ∂D_0 at the point z ; note that we have used the notation $\int_{\Gamma} \equiv (1/2i\pi) \int_{\Gamma}$. In the flat case, the boundary equation (6) becomes

$$\operatorname{Re} \left\{ \left(2\Omega \bar{z} + \int_{\Gamma} \frac{\bar{z} - \bar{\xi}}{z - \xi} d\xi \right) z' \right\} = 0, \quad z \in \Gamma. \tag{7}$$

Note that circular patches are stationary solutions for (7); however, elliptical vortex patches perform a steady rotation about their centers without changing shape. This latter fact was discovered by Kirchhoff [1876], who proved that, when D is an ellipse centered at zero, $D_t = e^{it\Omega} D$, where the angular velocity Ω is determined by the semiaxes a and b through the formula $\Omega = ab/(a + b)^2$. These ellipses are often referred to in the literature as the Kirchhoff elliptic vortices; see for instance [Majda and Bertozzi 2002, p. 304] or [Lamb 1945, p. 232].

One century later, several examples of rotating patches were obtained by Deem and Zabusky [1978], using contour dynamics simulations. Burbea [1982] gave an analytical proof and showed the existence of V -states with m -fold symmetry for each integer $m \geq 2$. In this countable family, the case $m = 2$ corresponds to the Kirchhoff elliptic vortices. Burbea’s approach consists of using complex analysis tools, combined with bifurcation theory. It should be noted that, from this standpoint, the rotating patches are arranged in a collection of countable curves bifurcating from Rankine vortices (trivial disc solution) at the discrete angular velocities set $\{(m - 1)/2m : m \geq 2\}$. The numerical analysis of limiting V -states which are the ends of each branch is done in [Overman 1986; Wu et al. 1984] and reveals interesting behavior: the boundary develops corners at right angles. Recently, the C^∞ regularity and the convexity

of the patches near the trivial solutions have been investigated in [Hmidi et al. 2013]. More recently, this result has been improved by Castro, Córdoba and Gómez-Serrano [Castro et al. 2016b], who showed the analyticity of the V -states close to the disc. We point out that similar research has been carried out in the past few years for more singular nonlinear transport equations arising in geophysical flows, such as the surface quasigeostrophic equations or the quasigeostrophic shallow-water equations; see for instance [Castro et al. 2016a; 2016b; Hassainia and Hmidi 2015; Płotka and Dritschel 2012]. It should be noted that the angular velocities of the bifurcating V -states for (7) are contained in the interval $]0, \frac{1}{2}[$. However, it is not clear whether we can find a V -state when Ω does not lie in this range. Fraenkel [2000] proved, always in the simply connected case, that the solutions associated with $\Omega = 0$ are trivial and reduced to Rankine patches. This was established by using the moving plane method, which seems to be flexible and has been recently adapted in [Hmidi 2015] to $\Omega < 0$ but with a convexity restriction. The case $\Omega = \frac{1}{2}$ was also solved in that paper, using the maximum principle for harmonic functions.

Another related subject is to see whether a second bifurcation occurs at the branches discovered by Deem and Zabusky. This has been explored for the branch of the ellipses corresponding to $m = 2$. Kamm [1987] gave numerical evidence of the existence of some branches bifurcating from the ellipses; see also [Saffman 1992]. In [Luzzatto-Fegiz and Williamson 2010], one can find more details about the diagram for the first bifurcations and some illustrations of the limiting V -states. The proof of the existence and analyticity of the boundary has been recently investigated in [Castro et al. 2016b; Hmidi and Mateu 2016]. Another interesting topic which has been studied since the pioneering work of Love [1893] is the linear and nonlinear stability of the m -folds. For the ellipses, we mention [Guo et al. 2004; Tang 1987], and for the general case of the m -fold symmetric V -states, we refer to [Burbea and Landau 1982; Wan 1986]. For further numerical discussions, see also [Cerretelli and Williamson 2003; Dritschel 1986; Mitchell and Rossi 2008]. Recently [Hmidi et al. 2015; de la Hoz et al. 2016b] have shown a special interest in the study of doubly connected V -states which are bounded patches and delimited by two disjoint Jordan curves. For example, an annulus is doubly connected, and by rotation invariance, it is a stationary V -state. No other explicit doubly connected V -state is known in the literature. In [Hmidi et al. 2015], a full characterization of the V -states (with nonzero magnitude in the interior domain) with at least one elliptical interface has been achieved, complementing the results of Polvani and Flierl [1986]. As a byproduct, it is shown that the domain between two ellipses is a V -state only if it is an annulus. The proof of existence of nonradial doubly connected V -states has been achieved very recently in [de la Hoz et al. 2016b] by using bifurcation theory. More precisely, we get the following result. Let $0 < b < 1$ and $m \geq 3$, such that

$$1 + b^m - \frac{1 - b^2}{2}m < 0.$$

Then there exist two curves of m -fold symmetric doubly connected V -states bifurcating from the annulus $\{z \in \mathbb{C} : b < |z| < 1\}$ at each of the angular velocities

$$\Omega_m^\pm = \frac{1 - b^2}{4} \pm \frac{1}{2m} \sqrt{\left(\frac{m(1 - b^2)}{2} - 1\right)^2 - b^{2m}}. \quad (8)$$

The main goal of the current paper is to explore the existence of rotating patches (6) for Euler equations

posed on the unit disc \mathbb{D} . We shall focus on the simply connected and doubly connected cases and study the influence of the rigid boundary on these structures. Before stating our main results, we define the set $\mathbb{D}_b = \{z \in \mathbb{C} : |z| < b\}$. Our first result dealing with the simply connected V -states is:

Theorem 1. *Let $b \in]0, 1[$ and m be a positive integer. Then there exists a family of m -fold symmetric V -states $(V_m)_{m \geq 1}$ for (6) bifurcating from the trivial solution $\omega_0 = \chi_{\mathbb{D}_b}$ at the angular velocity*

$$\Omega_m \triangleq \frac{m - 1 + b^{2m}}{2m}.$$

The proof of this theorem is done in the spirit of [Burbea 1980; de la Hoz et al. 2016b], using the conformal mapping parametrization $\phi : \mathbb{T} \rightarrow \partial D$ of the V -states, combined with bifurcation theory. As we shall see later in (17), the function ϕ satisfies the following nonlinear equation, for all $w \in \mathbb{T}$:

$$\text{Im} \left\{ \left[2\Omega \overline{\phi(w)} + \int_{\mathbb{T}} \frac{\overline{\phi(w)} - \overline{\phi(\tau)}}{\phi(w) - \phi(\tau)} \phi'(\tau) d\tau - \int_{\mathbb{T}} \frac{|\phi(\tau)|^2 \phi'(\tau)}{1 - \phi(w)\phi(\tau)} d\tau \right] w \phi'(w) \right\} = 0.$$

Denote by $F(\Omega, \phi)$ the term in the left-hand side of the preceding equality. Then the linearized operator around the trivial solution $\phi = b \text{Id}$ can be explicitly computed and is given by the following Fourier multiplier: for $h(w) = \sum_{n \in \mathbb{N}} a_n \bar{w}^n$,

$$\partial_\phi F(\Omega, b \text{Id})h(w) = b \sum_{n \geq 1} n \left(\frac{n - 1 + b^{2n}}{n} - 2\Omega \right) a_{n-1} e_n, \quad e_n = \frac{1}{2i} (\bar{w}^n - w^n).$$

Therefore, the *nonlinear eigenvalues* leading to nontrivial kernels of dimension 1 are explicitly described by the quantity Ω_m appearing in Theorem 1. Later on, we check that all the assumptions of the Crandall–Rabinowitz theorem stated in Section 2.2 are satisfied, and our result follows easily. In Section 5.1, we implement some numerical experiments concerning the limiting V -states. We observe two regimes depending on the size of b : b small and b close to 1. In the first case, as expected, corners do appear as in the planar case. However, for b close to 1, the effect of the rigid boundary is not negligible. We observe that the limiting V -states are tangentially touching the unit circle; see Figure 5. Some remarks are in order.

Remark 2. For the Euler equations in the plane, there are no curves of 1-fold V -states close to Rankine vortices. However, we deduce from our main theorem that this mode appears for spherical bounded domains. Its existence is the result of the interaction between the patch and the rigid boundary \mathbb{T} . Moreover, according to the numerical experiments, these V -states are not necessarily centered at the origin, and this fact is completely new. For the symmetry $m \geq 2$, all the discovered V -states are necessarily centered at zero because they have at least two axes of symmetry passing through zero.

Remark 3. By a scaling argument, when the domain of the fluid is the ball $B(0, R)$, with $R > 1$, then from the preceding theorem, the bifurcation from the unit disc occurs at the angular velocities

$$\Omega_{m,R} \triangleq \frac{m - 1 + R^{-2m}}{2m}.$$

Therefore, we obtain Burbea’s result [1980] by letting R tend to $+\infty$.

Remark 4. From the numerical experiments done in [de la Hoz et al. 2016b], we note that, in the plane, the bifurcation is pitchfork and occurs to the left of Ω_m . Furthermore, the branches of bifurcation are “monotonic” with respect to the angular velocity. In particular, this means that, for each value of Ω , we have at most only one V -state with that angular velocity. This behavior is no longer true in the disc as will be discussed later in the numerical experiments; see Figure 3.

Remark 5. Due to the boundary effects, the ellipses are no longer solutions for the rotating patch equation (6). Whether explicit solutions can be found for this model is an interesting problem. However, we believe that the conformal mapping of any nontrivial V -state has a necessary infinite expansion. Note that Burbea [1982] proved that, in the planar case when the conformal mapping associated to the V -state has a finite expansion, it is necessarily an ellipse. His approach is based on Faber polynomials, and this could give insight to solving the same problem in the disc.

The second part of this paper deals with the existence of doubly connected V -states for the system (1), governed by (6). Note that the annular patches centered at zero, which are given by

$$\mathbb{A}_{b_1, b_2} = \{z \in \mathbb{C} : b_1 < |z| < b_2\}, \quad b_1 < b_2 < 1,$$

are indeed stationary solutions. Our main task is to study the bifurcation of the V -states from these trivial solutions in the spirit of the recent works [de la Hoz et al. 2016a; 2016b]. We shall first start by studying the existence with the symmetry $m \geq 2$, followed by the special case $m = 1$.

Theorem 6. *Let $0 < b_2 < b_1 < 1$, and set $b \triangleq b_2/b_1$. Let $m \geq 2$, such that*

$$m > \frac{2 + 2b^m - (b_1^m + b_2^m)^2}{1 - b^2}.$$

Then there exist two curves of m -fold symmetric doubly connected V -states bifurcating from the annulus \mathbb{A}_{b_1, b_2} at the angular velocities

$$\Omega_m^\pm = \frac{1 - b^2}{4} + \frac{b_1^{2m} - b_2^{2m}}{4m} \pm \frac{1}{2} \sqrt{\Delta_m},$$

with

$$\Delta_m = \left(\frac{1 - b^2}{2} - \frac{2 - b_1^{2m} - b_2^{2m}}{2m} \right)^2 - b^{2m} \left(\frac{1 - b_1^{2m}}{m} \right)^2.$$

Before outlining the ideas of the proof, a few remarks are necessary.

Remark 7. As was discussed in Remark 3, one can use a scaling argument and obtain the result previously established in [de la Hoz et al. 2016b] for the planar case. Indeed, when the domain of the fluid is the ball $B(0, R)$, with $R > 1$, then the bifurcation from the annulus $\mathbb{A}_{b, 1}$ amounts to making the changes $b_1 = 1/R$ and $b_2 = b/R$ in Theorem 6. Thus, by letting R tend to infinity, we get exactly the nonlinear eigenvalues of the Euler equations in the plane (8).

Remark 8. Unlike in the plane, where the frequency m is assumed to be larger than 3, we can reach $m = 2$ in the case of the disc. This can be checked for b_2 small with respect to b_1 . This illustrates once again the interaction between the rigid boundary and the V -states.

Now we shall sketch the proof of Theorem 6, which follows along the lines of [de la Hoz et al. 2016b] and stems from bifurcation theory. The first step is to write down the analytical equations of the boundaries of the V -states. This can be done for example through the conformal parametrization of the domains D_1 and D_2 , which are close to the discs $b_1\mathbb{D}$ and $b_2\mathbb{D}$, respectively. Set $\phi_j : \mathbb{D}^c \rightarrow D_j^c$, the conformal mappings which have the expansions,

$$\text{for all } |w| \geq 1, \quad \phi_1(w) = b_1 w + \sum_{n \in \mathbb{N}} \frac{a_{1,n}}{w^n}, \quad \phi_2(w) = b_2 w + \sum_{n \in \mathbb{N}} \frac{a_{2,n}}{w^n}.$$

In addition, we assume that the Fourier coefficients are real, which means that we are looking only for V -states that are symmetric with respect to the real axis. As we shall see later in Section 4.1, the conformal mappings are subject to two coupled nonlinear equations defined as follows: for $j \in \{1, 2\}$ and $w \in \mathbb{T}$,

$$F_j(\lambda, \phi_1, \phi_2)(w) \triangleq \text{Im}\left\{((1 - \lambda)\overline{\phi_j(w)} + I(\phi_j(w)) - J(\phi_j(w)))w\phi'_j(w)\right\} = 0,$$

with

$$\begin{aligned} I(z) &= \int_{\mathbb{T}} \frac{\bar{z} - \overline{\phi_1(\xi)}}{z - \phi_1(\xi)} \phi'_1(\xi) d\xi - \int_{\mathbb{T}} \frac{\bar{z} - \overline{\phi_2(\xi)}}{z - \phi_2(\xi)} \phi'_2(\xi) d\xi, \\ J(z) &= \int_{\mathbb{T}} \frac{|\phi_1(\xi)|^2}{1 - z\phi_1(\xi)} \phi'_1(\xi) d\xi - \int_{\mathbb{T}} \frac{|\phi_2(\xi)|^2}{1 - z\phi_2(\xi)} \phi'_2(\xi) d\xi, \end{aligned} \quad \lambda \triangleq 1 - 2\Omega.$$

In order to apply bifurcation theory, we should understand the structure of the linearized operator around the trivial solution $(\phi_1, \phi_2) = (b_1 \text{Id}, b_2 \text{Id})$ corresponding to the annulus with radii b_1 and b_2 and identify the range of Ω where this operator has a one-dimensional kernel. The computations of the linear operator $DF(\Omega, b_1 \text{Id}, b_2 \text{Id})$ with $F = (F_1, F_2)$ in terms of the Fourier coefficients are fairly lengthy, and we find that it acts as a Fourier multiplier matrix. More precisely, for

$$h_1(w) = \sum_{n \geq 1} \frac{a_{1,n}}{w^n}, \quad h_2(w) = \sum_{n \geq 1} \frac{a_{2,n}}{w^n},$$

we obtain the formula

$$DF(\lambda, b_1 \text{Id}, b_2 \text{Id})(h_1, h_2) = \sum_{n \geq 1} M_n(\lambda) \begin{pmatrix} a_{1,n-1} \\ a_{2,n-1} \end{pmatrix} e_n, \quad e_n(w) \triangleq \frac{1}{2i}(\bar{w}^n - w^n),$$

where the matrix M_n is given by

$$M_n(\lambda) = \begin{pmatrix} b_1[n\lambda - 1 + b_1^{2n} - n(b_2/b_1)^2] & b_2[(b_2/b_1)^n - (b_1 b_2)^n] \\ -b_1[(b_2/b_1)^n - (b_1 b_2)^n] & b_2[n\lambda - n + 1 - b_2^{2n}] \end{pmatrix}.$$

Therefore, the values of Ω associated with nontrivial kernels are the solutions of a second-degree polynomial in λ ,

$$P_n(\lambda) \triangleq \det M_n(\lambda) = 0. \tag{9}$$

The polynomial P_n has real roots when the discriminant $\Delta_n(\alpha, b)$ introduced in Theorem 6 is positive. The calculation of the dimension of the kernel is significantly more complicated than the cases considered before in [Burbea 1980; de la Hoz et al. 2016b]. The matter reduces to counting, for a given λ , the discrete set

$$\{n \geq 2 : P_n(\lambda) = 0\}.$$

Note that, in [Burbea 1980; de la Hoz et al. 2016b], this set has only one element, and therefore, the kernel is one-dimensional. This follows from the monotonicity of the roots of P_n with respect to n . In the current situation, we get similar results but with a more refined analysis.

Now we shall move on to the existence of 1-fold symmetries, which are completely absent in the plane. The study in the general case is slightly subtler, and we have only carried out partial results, so some other cases are left open and deserve to be explored. Before stating our main result, we need to do some preparation. As we shall see in Section 4.4.3, the equation $P_1(\lambda) = 0$ admits exactly two solutions

$$\lambda_1^- = (b_2/b_1)^2 \quad \text{or} \quad \lambda_1^+ = 1 + b_2^2 - b_1^2.$$

Similarly to the planar case [de la Hoz et al. 2016b], there is no hope of bifurcating from the first eigenvalue λ_1^- because the range of the linearized operator around the trivial solution has an infinite codimension, and thus, the Crandall–Rabinowitz theorem stated in Section 2.2 is useless. However, for the second eigenvalue λ_1^+ , the range is at most of codimension 2, and in order to bifurcate, we should avoid a special set of b_1 and b_2 that we shall describe now. Fix b_1 in $]0, 1[$, and set

$$\mathcal{E}_{b_1} \triangleq \{b_2 \in]0, b_1[: \text{there exists } n \geq 2 \text{ such that } P_n(1 + b_2^2 - b_1^2) = 0\},$$

where P_n is defined in (9). As we shall see in Proposition 20, this set is countable and composed of a strictly increasing sequence $(x_m)_{m \geq 1}$ converging to b_1 . Now we state our result.

Theorem 9. *Given $b_1 \in]0, 1[$, then for any $b_2 \notin \mathcal{E}_{b_1}$, there exists a curve of nontrivial 1-fold doubly connected V -states bifurcating from the annulus \mathbb{A}_{b_1, b_2} at the angular velocity*

$$\Omega_1 = \frac{b_1^2 - b_2^2}{2}.$$

The proof is done in the spirit of Theorem 6. When $b_2 \notin \mathcal{E}_{b_1}$, then all the conditions of the Crandall–Rabinowitz theorem are satisfied. However, when $b_2 \in \mathcal{E}_{b_1}$, then the range of the linearized operator has codimension 2. Whether the bifurcation occurs in this special case is an interesting problem which is left open here.

Notation. We need to collect some useful notation that will be frequently used along this paper. We shall use the symbol \triangleq to define an object. The unit disc is denoted by \mathbb{D} and its boundary, the unit circle, by \mathbb{T} . For a given continuous complex function $f : \mathbb{T} \rightarrow \mathbb{C}$, we set

$$\oint_{\mathbb{T}} f(\tau) d\tau \triangleq \frac{1}{2i\pi} \int_{\mathbb{T}} f(\tau) d\tau,$$

where $d\tau$ stands for complex integration.

Let X and Y be two normed spaces. We denote by $\mathcal{L}(X, Y)$ the space of all continuous linear maps $T : X \rightarrow Y$ endowed with its usual strong topology. We denote by $\text{Ker } T$ and $R(T)$ the null space and the range of T , respectively. Finally, if F is a subspace of Y , then Y/F denotes the quotient space.

2. Preliminaries and background

In this introductory section, we shall collect some basic facts on Hölder spaces and bifurcation theory and shall recall how to use conformal mappings to obtain the equations of V -states.

2.1. Function spaces. In this paper as well as in the preceding ones [Hmidi et al. 2013; de la Hoz et al. 2016b], we find it more convenient to think of a 2π -periodic function $g : \mathbb{R} \rightarrow \mathbb{C}$ as a function of the complex variable $w = e^{i\theta}$. To be more precise, let $f : \mathbb{T} \rightarrow \mathbb{R}^2$ be a smooth function; then it can be assimilated to a 2π -periodic function $g : \mathbb{R} \rightarrow \mathbb{R}^2$ via the relation

$$f(w) = g(\eta), \quad w = e^{i\eta}.$$

By Fourier expansion, there exist complex numbers $(c_n)_{n \in \mathbb{Z}}$ such that

$$f(w) = \sum_{n \in \mathbb{Z}} c_n w^n,$$

and the differentiation with respect to w is understood in the complex sense. Now we shall introduce Hölder spaces on the unit circle \mathbb{T} .

Definition. Let $0 < \gamma < 1$. We denote by $C^\gamma(\mathbb{T})$ the space of continuous functions f such that

$$\|f\|_{C^\gamma(\mathbb{T})} \triangleq \|f\|_{L^\infty(\mathbb{T})} + \sup_{\tau \neq w \in \mathbb{T}} \frac{|f(\tau) - f(w)|}{|\tau - w|^\gamma} < \infty.$$

For any nonnegative integer n , the space $C^{n+\gamma}(\mathbb{T})$ stands for the set of functions f of class C^n whose n -th order derivatives are Hölder continuous with exponent γ . It is equipped with the usual norm

$$\|f\|_{C^{n+\gamma}(\mathbb{T})} \triangleq \sum_{k=0}^n \left\| \frac{d^k f}{d^k w} \right\|_{L^\infty(\mathbb{T})} + \left\| \frac{d^n f}{d^n w} \right\|_{C^\gamma(\mathbb{T})}.$$

Recall that the Lipschitz seminorm is defined by

$$\|f\|_{\text{Lip}(\mathbb{T})} = \sup_{\tau \neq w \in \mathbb{T}} \frac{|f(\tau) - f(w)|}{|\tau - w|}.$$

Now we list some classical properties that will be useful later.

- (i) For $n \in \mathbb{N}$ and $\gamma \in]0, 1[$, the space $C^{n+\gamma}(\mathbb{T})$ is an algebra.
- (ii) For $K \in L^1(\mathbb{T})$ and $f \in C^{n+\gamma}(\mathbb{T})$, we have the convolution inequality

$$\|K \star f\|_{C^{n+\gamma}(\mathbb{T})} \leq \|K\|_{L^1(\mathbb{T})} \|f\|_{C^{n+\gamma}(\mathbb{T})}.$$

2.2. Elements of bifurcation theory. We shall now recall an important theorem of bifurcation theory which plays a central role in the proofs of our main results. This theorem was established by Crandall and Rabinowitz [1971]. Consider a continuous function $F : \mathbb{R} \times X \rightarrow Y$ with X and Y being two Banach spaces. Assume that $F(\lambda, 0) = 0$ for any λ belonging to nontrivial interval I . The Crandall–Rabinowitz theorem gives sufficient conditions for the existence of branches of nontrivial solutions to the equation $F(\lambda, x) = 0$ bifurcating at some point $(\lambda_0, 0)$. For more general results, we refer the reader to [Kielhöfer 2012].

Theorem 10. *Let X and Y be two Banach spaces and V a neighborhood of 0 in X , and let $F : \mathbb{R} \times V \rightarrow Y$. Set $\mathcal{L}_0 \triangleq \partial_x F(0, 0)$; then the following properties are satisfied.*

- (i) $F(\lambda, 0) = 0$ for any $\lambda \in \mathbb{R}$.
- (ii) The partial derivatives F_λ , F_x and $F_{\lambda x}$ exist and are continuous.
- (iii) The spaces $N(\mathcal{L}_0)$ and $Y/R(\mathcal{L}_0)$ are one-dimensional.
- (iv) The transversality assumption $\partial_\lambda \partial_x F(0, 0)x_0 \notin R(\mathcal{L}_0)$ holds, where

$$N(\mathcal{L}_0) = \text{span}\{x_0\}.$$

If Z is any complement of $N(\mathcal{L}_0)$ in X , then there is a neighborhood U of $(0, 0)$ in $\mathbb{R} \times X$, an interval $]-a, a[$ and continuous functions $\varphi :]-a, a[\rightarrow \mathbb{R}$ and $\psi :]-a, a[\rightarrow Z$ such that $\varphi(0) = 0$, $\psi(0) = 0$ and

$$F^{-1}(0) \cap U = \{(\varphi(\xi), \xi x_0 + \xi \psi(\xi)) : |\xi| < a\} \cup \{(\lambda, 0) : (\lambda, 0) \in U\}.$$

Before proceeding further with the consideration of the V -states, we shall recall the Riemann mapping theorem, a central result in complex analysis. To restate this result, we need to recall the definition of *simply connected* domains. Let $\widehat{\mathbb{C}} \triangleq \mathbb{C} \cup \{\infty\}$ denote the Riemann sphere. We say that a domain $\Omega \subset \widehat{\mathbb{C}}$ is *simply connected* if the set $\widehat{\mathbb{C}} \setminus \Omega$ is connected. Let \mathbb{D} denote the unit open disc and $\Omega \subset \mathbb{C}$ be a simply connected bounded domain. Then according to the Riemann mapping theorem, there is a unique biholomorphic map $\Phi : \mathbb{C} \setminus \overline{\mathbb{D}} \rightarrow \mathbb{C} \setminus \overline{\Omega}$ taking the form

$$\Phi(z) = az + \sum_{n \in \mathbb{N}} \frac{a_n}{z^n}, \quad a > 0.$$

In this theorem, the regularity of the boundary has no effect on the existence of the conformal mapping, but it plays a role in determining the boundary behavior of the conformal mapping. See for instance [Pommerenke 1992; Warschawski 1935]. Here, we shall recall the following result.

Kellogg and Warschawski's theorem ([Warschawski 1935] or [Pommerenke 1992, Theorem 3.6]). *If the conformal map $\Phi : \mathbb{C} \setminus \overline{\mathbb{D}} \rightarrow \mathbb{C} \setminus \overline{\Omega}$ has a continuous extension to $\mathbb{C} \setminus \mathbb{D}$ which is of class $C^{n+\beta}$, with $n \in \mathbb{N}$ and $0 < \beta < 1$, then the boundary $\Phi(\mathbb{T})$ is of class $C^{n+\beta}$.*

2.3. Boundary equations. Our next task is to write down the equations of V -states using the conformal parametrization. First recall that the vorticity $\omega = \partial_1 v_2 - \partial_2 v_1$ satisfies the transport equation

$$\partial_t \omega + v \cdot \nabla \omega = 0$$

and the associated velocity is related to the vorticity through the stream function Ψ as

$$v = 2i \partial_{\bar{z}} \Psi,$$

with

$$\Psi(z) = \frac{1}{4\pi} \int_{\mathbb{D}} \log \left| \frac{z - \xi}{1 - z\bar{\xi}} \right|^2 \omega(\xi) dA(\xi).$$

When the vorticity is a patch of the form $\omega = \chi_D$ with D a bounded domain strictly contained in \mathbb{D} , then

$$\Psi(z) = \frac{1}{4\pi} \int_D \log \left| \frac{z - \xi}{1 - z\bar{\xi}} \right|^2 dA(\xi).$$

For a complex function $\varphi : \mathbb{C} \rightarrow \mathbb{C}$ of class C^1 in the Euclidean variables (as a function of \mathbb{R}^2), we define

$$\partial_z \varphi = \frac{1}{2} \left(\frac{\partial \varphi}{\partial x} - i \frac{\partial \varphi}{\partial y} \right), \quad \partial_{\bar{z}} \varphi = \frac{1}{2} \left(\frac{\partial \varphi}{\partial x} + i \frac{\partial \varphi}{\partial y} \right).$$

As we have seen in the introduction, a rotating patch or V -state is a special solution of the vorticity equation (2) with initial data $\omega_0 = \chi_D$ and such that

$$\omega(t) = \chi_{D_t}, \quad D_t = e^{it\Omega} D.$$

In this definition and for simplicity, we have only considered patches rotating around zero. According to [Burbea 1980; Hmidi et al. 2013; de la Hoz et al. 2016b], the boundary equation of the rotating patches is

$$\operatorname{Re}\{(\Omega \bar{z} - 2\partial_{\bar{z}} \Psi)z'\} = 0, \quad z \in \Gamma \triangleq \partial D, \tag{10}$$

where z' denotes a tangent vector to the boundary at the point z . We point out that the existence of a rigid boundary does not alter this equation which in fact was established in the planar case. The purpose now is to transform (10) into an equation involving only the boundary ∂D of the V -state. To do so, we need to write $\partial_z \Psi$ as an integral on the boundary ∂D based on the use of the Cauchy–Pompeiu formula. Consider a finitely connected domain D bounded by finitely many smooth Jordan curves, and let Γ be the boundary ∂D endowed with the positive orientation; then

$$\text{for all } z \in \mathbb{C}, \quad \oint_{\Gamma} \frac{\varphi(z) - \varphi(\xi)}{z - \xi} d\xi = -\frac{1}{\pi} \int_D \partial_{\bar{\xi}} \varphi(\xi) \frac{dA(\xi)}{z - \xi}. \tag{11}$$

Differentiating (3) with respect to the variable z yields

$$\partial_z \Psi(z) = \frac{1}{4\pi} \int_D \frac{\bar{\xi}}{1 - z\bar{\xi}} dA(\xi) + \frac{1}{4\pi} \int_D \frac{1}{z - \xi} dA(\xi). \tag{12}$$

Applying the Cauchy–Pompeiu formula with $\varphi(z) = \bar{z}$, we find

$$\frac{1}{\pi} \int_D \frac{1}{z - \xi} dA(\xi) = -\oint_{\Gamma} \frac{\bar{z} - \bar{\xi}}{z - \xi} d\xi \quad \text{for all } z \in \bar{D}.$$

Using the change of variable $\xi \rightarrow \bar{\xi}$ which keeps the Lebesgue measure invariant,

$$\frac{1}{\pi} \int_D \frac{\bar{\xi}}{1 - z\bar{\xi}} dA(\xi) = \frac{1}{\pi z} \int_{\tilde{D}} \frac{\xi}{1/z - \xi} dA(\xi)$$

with \tilde{D} being the image of D by complex conjugation. A second application of the Cauchy–Pompeiu formula, using that $1/z \notin \mathbb{D}$ for $z \in D$, yields

$$\frac{1}{\pi z} \int_{\tilde{D}} \frac{\xi}{1/z - \xi} dA(\xi) = \oint_{\tilde{\Gamma}} \frac{|\xi|^2}{1 - z\xi} d\xi \quad \text{for all } z \in \bar{D}, \quad \tilde{\Gamma} = \partial \tilde{D}.$$

Using once again the change of variable $\xi \rightarrow \bar{\xi}$ which reverses the orientation,

$$\oint_{\Gamma} \frac{|\xi|^2}{1 - z\xi} d\xi = - \oint_{\Gamma} \frac{|\xi|^2}{1 - z\bar{\xi}} d\bar{\xi} \quad \text{for all } z \in \bar{D}.$$

Therefore, we obtain

$$4\partial_z \Psi(z) = - \oint_{\Gamma} \frac{|\xi|^2}{1 - z\bar{\xi}} d\bar{\xi} - \oint_{\Gamma} \frac{\bar{z} - \bar{\xi}}{z - \xi} d\xi. \tag{13}$$

Inserting the last identity in (10), we get an equation involving only the boundary

$$\text{Re} \left\{ \left(2\Omega \bar{z} + \oint_{\Gamma} \frac{\bar{z} - \bar{\xi}}{z - \xi} d\xi + \oint_{\Gamma} \frac{|\xi|^2}{1 - z\bar{\xi}} d\bar{\xi} \right) z' \right\} = 0 \quad \text{for all } z \in \Gamma.$$

It is more convenient in the formulas to replace the angular velocity Ω in the preceding equation by the parameter $\lambda = 1 - 2\Omega$, leading to the V -states equation

$$\text{Re} \left\{ \left((1 - \lambda) \bar{z} + \oint_{\Gamma} \frac{\bar{z} - \bar{\xi}}{z - \xi} d\xi + \oint_{\Gamma} \frac{|\xi|^2}{1 - z\bar{\xi}} d\bar{\xi} \right) z' \right\} = 0 \quad \text{for all } z \in \Gamma. \tag{14}$$

It is worth pointing out that (14) characterizes V -states among domains with C^1 boundary, regardless of the number of boundary components. If the domain is simply connected, then there is only one boundary component and so only one equation. However, if the domain is doubly connected, then (14) gives rise to two coupled equations, one for each boundary component. We note that all the V -states that we shall consider admit at least one axis of symmetry passing through zero and without loss of generality it can be supposed to be the real axis. This implies that the boundary ∂D is invariant by the reflection symmetry $\xi \rightarrow \bar{\xi}$. Therefore, using this change of variables, which reverses orientation, in the last integral term of the equation (14), we obtain

$$\text{Re} \left\{ \left((1 - \lambda) \bar{z} + \oint_{\Gamma} \frac{\bar{z} - \bar{\xi}}{z - \xi} d\xi - \oint_{\Gamma} \frac{|\xi|^2}{1 - z\xi} d\xi \right) z' \right\} = 0 \quad \text{for all } z \in \Gamma. \tag{15}$$

To end this section, we mention that in the general framework the dynamics of any vortex patch can be described by its Lagrangian parametrization $\gamma_t : \mathbb{T} \rightarrow \partial D_t \triangleq \Gamma_t$ as

$$\partial_t \gamma_t = v(t, \gamma_t).$$

Since Ψ is a real-valued function,

$$\partial_{\bar{z}} \Psi = \overline{\partial_z \Psi},$$

which implies according to (13)

$$\begin{aligned} v(t, z) &= 2i \partial_{\bar{z}} \Psi(t, z) \\ &= -\frac{1}{4\pi} \int_{\Gamma_t} \log|z - \xi|^2 d\xi + \frac{1}{4\pi} \int_{\Gamma_t} \frac{|\xi|^2}{1 - \bar{z}\xi} d\xi. \end{aligned}$$

Consequently, we find that the Lagrangian parametrization satisfies the nonlinear ODE

$$\partial_t \gamma_t = -\frac{1}{4\pi} \int_{\Gamma_t} \log|\gamma_t - \xi|^2 d\xi + \frac{1}{4\pi} \int_{\Gamma_t} \frac{|\xi|^2}{1 - \bar{\gamma}_t \xi} d\xi. \tag{16}$$

The ultimate goal of this section is to relate the V -states described above to stationary solutions for Euler equations when the rigid boundary rotates at some specific angular velocity. To do so, suppose that the disc \mathbb{D} rotates with a constant angular velocity Ω ; then the equations (1) written in the frame of the rotating disc take the form

$$\partial_t u + u \cdot \nabla u - \Omega y^\perp \cdot \nabla u + \Omega u^\perp + \nabla q = 0$$

with

$$y = e^{-it\Omega}x, \quad v(t, x) = e^{-it\Omega}u(t, y), \quad q(t, y) = p(t, x).$$

For more details about the derivation of this equation, we refer the reader for instance to [Farwig and Hishida 2011]. Here the variable in the rotating frame is denoted by y . Applying the *curl* operator to the equation of u , we find that the vorticity of u , which still denoted by ω , is governed by the transport equation

$$\partial_t \omega + (u - \Omega y^\perp) \cdot \nabla \omega = 0.$$

Consequently, any stationary solution in the patch form is actually a V -state rotating with the angular velocity Ω . Relating this observation to Theorems 1 and 6, we deduce that rotating the disc at some suitable angular velocities creates stationary patches with m -fold symmetry.

3. Simply connected V -states

In this section, we shall gather all the pieces needed for the proof of Theorem 1. The strategy is analogous to [Burbea 1980; Hmidi et al. 2013; de la Hoz et al. 2016b]. It consists of first writing down the V -states equation through the conformal parametrization and second applying the Crandall–Rabinowitz theorem. As can be noted from Theorem 1, the result is local meaning that we are looking for V -states which are smooth and cause a small perturbation of the Rankine patch $\chi_{\mathbb{D}_b}$ with $\mathbb{D}_b = b\mathbb{D}$. We also assume that the patch is symmetric with respect to the real axis, and this fact has been crucial in deriving (15). Note that as $D \Subset \mathbb{D}$ the exterior conformal mapping $\phi : \mathbb{D}^c \rightarrow D^c$ has the expansion

$$\phi(w) = bw + \sum_{n \geq 0} \frac{b_n}{w^n}, \quad b_n \in \mathbb{R},$$

and satisfies $0 < b < 1$. This latter fact follows from the Schwarz lemma. Indeed, let

$$\psi(z) \triangleq \frac{1}{\phi(1/z)};$$

then $\psi : \mathbb{D} \rightarrow \widehat{D}$ is conformal, with \widehat{D} the image of D by the map $z \mapsto 1/z$. Clearly $\mathbb{D} \subset \widehat{D}$, and therefore, the restriction $\psi^{-1} : \mathbb{D} \rightarrow \mathbb{D}$ is well defined and holomorphic and satisfies $\psi(0) = 0$. From the Schwarz lemma, we deduce that $|(\psi^{-1})'(0)| < 1$; otherwise D will coincide with \mathbb{D} . It suffices now to use that $(\psi^{-1})'(0) = b$.

Now we shall transform (15) into an equation on the unit circle \mathbb{T} . For this purpose, we make the change of variables $z = \phi(w)$ and $\xi = \phi(\tau)$. Note that for $w \in \mathbb{T}$ a tangent vector at the point $z = \phi(w)$

is given by

$$z' = iw\phi'(w)$$

and thus (15) becomes

$$\operatorname{Im} \left\{ \left[(1 - \lambda)\overline{\phi(w)} + \int_{\mathbb{T}} \frac{\overline{\phi(w)} - \overline{\phi(\tau)}}{\phi(w) - \phi(\tau)} \phi'(\tau) d\tau - \int_{\mathbb{T}} \frac{|\phi(\tau)|^2 \phi'(\tau)}{1 - \phi(w)\phi(\tau)} d\tau \right] w\phi'(w) \right\} = 0. \tag{17}$$

Set $\phi \triangleq b \operatorname{Id} + f$; then the foregoing functional can be split into three parts

$$\begin{aligned} F_1(f)(w) &\triangleq \operatorname{Im}\{\overline{\phi(w)}w\phi'(w)\}, \\ F_2(f)(w) &\triangleq \operatorname{Im} \left\{ \int_{\mathbb{T}} \frac{\overline{\phi(w)} - \overline{\phi(\tau)}}{\phi(w) - \phi(\tau)} \phi'(\tau) d\tau w\phi'(w) \right\}, \\ F_3(f)(w) &\triangleq \operatorname{Im} \left\{ \int_{\mathbb{T}} \frac{|\phi(\tau)|^2 \phi'(\tau)}{1 - \phi(w)\phi(\tau)} d\tau w\phi'(w) \right\}, \end{aligned} \tag{18}$$

and consequently, (17) becomes

$$F(\lambda, f) = 0, \quad F(\lambda, f) \triangleq (1 - \lambda)F_1(f) + F_2(f) - F_3(f). \tag{19}$$

Observe that we can decompose F into two parts $F(\lambda, f) = G(\lambda, f) - F_3(f)$ where $G(\lambda, f)$ is the functional appearing in the flat space \mathbb{R}^2 and the new term F_3 describes the interaction between the patch and the rigid boundary \mathbb{T} . Now it is easy from the complex formulation to check that the disc \mathbb{D}_b is a rotating patch for any $\Omega \in \mathbb{R}$. Indeed, as the disc is a trivial solution for the full space \mathbb{R}^2 , $G(\lambda, 0) = 0$. Moreover,

$$F_3(0)(w) \triangleq \operatorname{Im} \left\{ b^4 w \int_{\mathbb{T}} \frac{d\tau}{1 - b^2 w \tau} \right\} = 0$$

because the integrand is analytic in the open disc $(1/b^2)\mathbb{D}$ and therefore we apply residue theorem.

3.1. Regularity of the functional F . This section is devoted to the study of the regularity assumptions stated in the Crandall–Rabinowitz theorem for the functional F introduced in (19). The application of this theorem at this stage of the presentation requires one to fix the function spaces X and Y . We should look for Banach spaces X and Y of Hölder type in the spirit of [Hmidi et al. 2013; de la Hoz et al. 2016b], and they are given by

$$\begin{aligned} X &= \left\{ f \in C^{1+\alpha}(\mathbb{T}) : f(w) = \sum_{n \geq 0} a_n \bar{w}^n, \ a_n \in \mathbb{R}, \ w \in \mathbb{T} \right\}, \\ Y &= \left\{ g \in C^\alpha(\mathbb{T}) : g(w) = \sum_{n \geq 1} b_n e_n, \ b_n \in \mathbb{R}, \ w \in \mathbb{T} \right\}, \quad e_n \triangleq \frac{1}{2i}(\bar{w}^n - w^n), \end{aligned}$$

with $\alpha \in]0, 1[$. For $r \in]0, 1[$, we denote by B_r the open ball of X with center 0 and radius r

$$B_r = \{f \in X : \|f\|_{C^{1+\alpha}} \leq r\}.$$

It is straightforward to see that for any $f \in B_r$ the function $w \mapsto \phi(w) = bw + f(w)$ is conformal on

$\mathbb{C} \setminus \bar{\mathbb{D}}$ provided that $r < b$. Moreover, according to the Kellogg–Warschawski result [Warschawski 1935], the boundary of $\phi(\mathbb{C} \setminus \bar{\mathbb{D}})$ is a Jordan curve of class $C^{1+\alpha}$. We propose to prove the following result concerning the regularity of F .

Proposition 11. *Let $b \in]0, 1[$ and $0 < r < \min(b, 1 - b)$; then the following hold true:*

- (i) $F : \mathbb{R} \times B_r \rightarrow Y$ is C^1 (it is in fact C^∞).
- (ii) The partial derivative $\partial_\lambda \partial_f F : \mathbb{R} \times B_r \rightarrow \mathcal{L}(X, Y)$ exists and is continuous (it is in fact C^∞).

Proof. (i) We shall only sketch the proof because most of the details are done in [Hmidi et al. 2013; de la Hoz et al. 2016b]. First recall from (19) the decomposition

$$F(\lambda, f) = (1 - \lambda)F_1(f) + F_2(f) - F_3(f).$$

The part $(1 - \lambda)F_1(f) + F_2(f)$ coincides with the nonlinear functional appearing in the plane, and its regularity was studied in [Hmidi et al. 2013; de la Hoz et al. 2016b]. Therefore, it remains to check the regularity assumptions for the term F_3 given in (18). Since $C^\alpha(\mathbb{T})$ is an algebra, it suffices to prove that the mapping $F_4 : \phi \in b \text{Id} + B_r \rightarrow C^\alpha$ defined by

$$F_4(\phi(w)) = \int_{\mathbb{T}} \frac{|\phi(\tau)|^2 \phi'(\tau)}{1 - \phi(w)\phi(\tau)} d\tau \tag{20}$$

is C^1 and admits real Fourier coefficients. Observe that this functional is well defined and is given by the series expansion

$$F_4(\phi(w)) = \sum_{n \in \mathbb{N}} \phi^n(w) \int_{\mathbb{T}} \phi^n(\tau) |\phi(\tau)|^2 \phi'(\tau) d\tau.$$

This sum is defined pointwisely because $\|\phi\|_{L^\infty} \leq b + r < 1$. This series converges absolutely in $C^\alpha(\mathbb{T})$. To get this, we use the law product which can be proved by induction

$$\|\phi^n\|_{C^\alpha} \leq n \|\phi\|_{L^\infty}^{n-1} \|\phi\|_{C^\alpha},$$

and therefore, we obtain

$$\begin{aligned} \|F_4(\phi)\|_{C^\alpha} &\leq \sum_{n \in \mathbb{N}} n \|\phi\|_{L^\infty}^{n-1} \|\phi\|_{C^\alpha} \left| \int_{\mathbb{T}} \phi^n(\tau) |\phi(\tau)|^2 \phi'(\tau) d\tau \right| \\ &\leq \|\phi'\|_{L^\infty} \|\phi\|_{C^\alpha} \sum_{n \in \mathbb{N}} n \|\phi\|_{L^\infty}^{2n+1} \\ &\leq \|\phi'\|_{L^\infty} \|\phi\|_{C^\alpha} \sum_{n \in \mathbb{N}} n (b+r)^{2n+1} < \infty. \end{aligned}$$

From the completeness of $C^\alpha(\mathbb{T})$, we obtain that $F_4(\phi)$ belongs to this space. Again from the series expansion, we can check that $\phi \mapsto F_4(\phi)$ is not only C^1 but also C^∞ . To end the proof, we need to check that all the Fourier coefficients of $F_4(\phi)$ are real, and this fact is equivalent to showing that

$$\overline{F_4(\phi(w))} = F_4(\phi(\bar{w})) \quad \text{for all } w \in \mathbb{T}.$$

As $\overline{\phi(w)} = \phi(\bar{w})$ and $\overline{\phi'(w)} = \phi'(\bar{w})$, we may write successively

$$\begin{aligned} \overline{F_4(\phi(w))} &= - \int_{\mathbb{T}} \frac{|\phi(\bar{\tau})|^2 \phi'(\bar{\tau})}{1 - \phi(\bar{w})\phi(\bar{\tau})} d\bar{\tau} \\ &= \int_{\mathbb{T}} \frac{|\phi(\tau)|^2 \phi'(\tau)}{1 - \phi(w)\phi(\tau)} d\tau \end{aligned}$$

where in the last equality we have used the change of variable $\tau \mapsto \bar{\tau}$.

(ii) Following the arguments developed in [Hmidi et al. 2013; de la Hoz et al. 2016b], we get what is expected formally, that is

$$\begin{aligned} \partial_\lambda \partial_f F(\lambda, f)h &= -\partial_f F_1(f) \\ &= \text{Im}\{\overline{\phi(w)}wh'(w) + \overline{h(w)}w\phi'(w)\}, \end{aligned}$$

from which we deduce that $\partial_\lambda \partial_f F(\lambda, f) \in \mathcal{L}(X, Y)$ and the mapping $f \mapsto \partial_\lambda \partial_f F(\lambda, f)$ is in fact C^∞ , which is clearly better than the statement of the proposition. \square

3.2. Spectral study. This part is crucial for implementing the Crandall–Rabinowitz theorem. We shall in particular compute the linearized operator $\partial_f F(\lambda, 0)$ around the trivial solution and look for the values of λ associated with the nontrivial kernel. For these values of λ , we shall see that the linearized operator has a one-dimensional kernel and is in fact of Fredholm type with zero index. Before giving the main result of this subsection, we recall the notation $e_n = (\bar{w}^n - w^n)/2i$.

Proposition 12. *Let $h \in X$ take the form $h(w) = \sum_{n \geq 0} a_n/w^n$. Then the following hold true:*

(i) *The structure of $\partial_f F(\lambda, 0)$ is given by*

$$\partial_f F(\lambda, 0)h(w) = b \sum_{n \geq 1} n \left(\lambda - \frac{1 - b^{2n}}{n} \right) a_{n-1} e_n.$$

(ii) *The kernel of $\partial_f F(\lambda, 0)$ is nontrivial if and only if there exists $m \in \mathbb{N}^*$ such that*

$$\lambda = \lambda_m \triangleq \frac{1 - b^{2m}}{m}, \quad m \in \mathbb{N}^*,$$

and in this case, the kernel is one-dimensional and generated by $v_m(w) = \bar{w}^{m-1}$.

(iii) *The range of $\partial_f F(\lambda_m, 0)$ is of codimension 1.*

(iv) *The transversality condition holds: for $m \in \mathbb{N}^*$,*

$$\partial_\lambda \partial_f F(\lambda_m, 0)v_m \notin R\partial_f F(\lambda_m, 0).$$

Proof. (i) The computations of the terms $\partial_f F_i(\lambda, 0)h$ were almost done in [de la Hoz et al. 2016b], and we shall only give some details. By straightforward computations, we obtain

$$\begin{aligned} \partial_f F_1(0, 0)h(w) &= \text{Im}\{b\overline{h(w)}w + bh'(w)\} \\ &= b \text{Im}\left\{\sum_{n \geq 0} a_n w^{n+1} - \sum_{n \geq 1} n a_n \overline{w}^{n+1}\right\} \\ &= -\frac{b}{2i} \sum_{n \geq 0} (n+1)a_n (\overline{w}^{n+1} - w^{n+1}) \\ &= -b \sum_{n \geq 0} (n+1)a_n e_{n+1}. \end{aligned} \tag{21}$$

Concerning $\partial_f F_2(0, 0)$, one may write

$$\partial_f F_2(0, 0)h(w) = \text{Im}\left\{bw \int_{\mathbb{T}} \frac{\overline{h(\tau)} - \overline{h(w)}}{\tau - w} d\tau + b \int_{\mathbb{T}} \frac{h(\tau) - h(w)}{\tau - w} \bar{\tau} d\tau - b \int_{\mathbb{T}} h'(\tau) \bar{\tau} d\tau - bh'(w)\right\}.$$

Therefore, using the residue theorem at infinity,

$$\begin{aligned} \partial_f F_2(0, 0)h(w) &= \text{Im}\left\{bw \int_{\mathbb{T}} \frac{\overline{h(\tau)} - \overline{h(w)}}{\tau - w} d\tau - bh'(w)\right\} \\ &= -\text{Im}\{bh'(w)\}, \end{aligned}$$

where we have used in the last line the fact

$$\begin{aligned} \int_{\mathbb{T}} \frac{\overline{h(\tau)} - \overline{h(w)}}{\tau - w} d\tau &= \sum_{n \in \mathbb{N}} a_n \int_{\mathbb{T}} \frac{w^n - \tau^n}{\tau - w} d\tau \\ &= 0. \end{aligned}$$

Consequently, we obtain

$$\partial_f F_2(0, 0)h(w) = b \sum_{n \geq 1} n a_n e_{n+1}. \tag{22}$$

As for the third term $\partial_f F_3(0, 0)h$, we get by plain computation

$$\begin{aligned} \partial_f F_3(0, 0)h(w) &= \text{Im}\left\{b^3 w \int_{\mathbb{T}} \frac{d\tau}{1 - b^2 w \tau} h'(w) + b^3 w \int_{\mathbb{T}} \frac{h'(\tau) d\tau}{1 - b^2 w \tau} \right. \\ &\quad \left. + 2b^3 w \int_{\mathbb{T}} \frac{\text{Re}\{h(\tau)\bar{\tau}\}}{1 - b^2 w \tau} d\tau + b^5 w \int_{\mathbb{T}} \frac{wh(\tau) + \tau h(w)}{(1 - b^2 w \tau)^2} d\tau\right\} \\ &\triangleq \text{Im}\{I_1(w) + I_2(w) + I_3(w) + I_4(w)\}. \end{aligned} \tag{23}$$

By once again invoking the residue theorem,

$$I_1(w) = 0. \tag{24}$$

To compute the second term $I_2(w)$, we use the Taylor series of $1/(1 - \zeta)$, leading to

$$\begin{aligned} I_2(w) &= b^3 w \oint_{\mathbb{T}} \frac{h'(\tau) d\tau}{1 - b^2 w \tau} \\ &= \sum_{n \geq 0} b^{2n+3} w^{n+1} \oint_{\mathbb{T}} \tau^n h'(\tau) d\tau. \end{aligned}$$

From the Fourier expansions of h , we infer that

$$\oint_{\mathbb{T}} \tau^n h'(\tau) d\tau = -na_n,$$

which implies that

$$I_2(w) = - \sum_{n \geq 1} na_n b^{2n+3} w^{n+1}. \quad (25)$$

In regard to the third term $I_3(w)$, it may be written in the form

$$I_3(w) = b^3 w \oint_{\mathbb{T}} \frac{\tau \overline{h(\tau)}}{1 - b^2 w \tau} d\tau + b^3 w \oint_{\mathbb{T}} \frac{\bar{\tau} h(\tau)}{1 - b^2 w \tau} d\tau.$$

The first integral term is zero due to the fact that the integrand is analytic in the open unit disc and continuous up to the boundary. Therefore, we get similarly to $I_2(w)$

$$\begin{aligned} I_3(w) &= b^3 w \oint_{\mathbb{T}} \frac{\bar{\tau} h(\tau)}{1 - b^2 w \tau} d\tau \\ &= \sum_{n \geq 0} b^{2n+3} w^{n+1} \oint_{\mathbb{T}} \tau^{n-1} h(\tau) d\tau. \end{aligned}$$

Note that

$$\oint_{\mathbb{T}} \tau^{n-1} h(\tau) d\tau = a_n,$$

which implies in turn that

$$I_3(w) = \sum_{n \geq 0} a_n b^{2n+3} w^{n+1}. \quad (26)$$

Now we come back to the last term $I_4(w)$, and one may write using again the residue theorem

$$\begin{aligned} I_4(w) &= b^5 w^2 \oint_{\mathbb{T}} \frac{h(\tau) d\tau}{(1 - b^2 w \tau)^2} + b^5 w h(w) \oint_{\mathbb{T}} \frac{\tau d\tau}{(1 - b^2 w \tau)^2} \\ &= b^5 w^2 \oint_{\mathbb{T}} \frac{h(\tau) d\tau}{(1 - b^2 w \tau)^2} + 0. \end{aligned}$$

Using the Taylor expansion

$$\frac{1}{(1 - \zeta)^2} = \sum_{n \geq 1} n \zeta^{n-1}, \quad |\zeta| < 1, \quad (27)$$

we deduce that

$$\begin{aligned} I_4(w) &= \sum_{n \geq 1} n b^{2n+3} w^{n+1} \int_{\mathbb{T}} \tau^{n-1} h(\tau) d\tau \\ &= \sum_{n \geq 1} n a_n b^{2n+3} w^{n+1}. \end{aligned} \tag{28}$$

Inserting the identities (24), (25), (26) and (28) into (23), we find

$$\begin{aligned} \partial_f F_3(0, 0)h(w) &= \text{Im} \left\{ \sum_{n \geq 0} a_n b^{2n+3} w^{n+1} \right\} \\ &= - \sum_{n \geq 0} a_n b^{2n+3} e_{n+1}. \end{aligned} \tag{29}$$

Hence, by plugging (21), (22) and (29) into (19), we obtain

$$\begin{aligned} \partial_f F(\lambda, 0)h(w) &= b \sum_{n \geq 0} (n+1) \left(\lambda - \frac{1-b^{2n+2}}{n+1} \right) a_n e_{n+1} \\ &= b \sum_{n \geq 1} n \left(\lambda - \frac{1-b^{2n}}{n} \right) a_{n-1} e_n. \end{aligned} \tag{30}$$

This finishes the proof of the first part (i).

(ii) From (30), we immediately deduce that the kernel of $\partial_f F(\lambda, 0)$ is nontrivial if and only if there exists $m \geq 1$ such that

$$\lambda = \lambda_m \triangleq \frac{1-b^{2m}}{m}.$$

We shall prove that the sequence $n \mapsto \lambda_n$ is strictly decreasing, from which we conclude immediately that the kernel is one-dimensional. Assume that for two integers $n > m \geq 1$ one has

$$\frac{1-b^{2m}}{m} = \frac{1-b^{2n}}{n}.$$

This implies that

$$\frac{1-b^{2n}}{1-b^{2m}} = \frac{n}{m}.$$

Set $\alpha = n/m$ and $x = b^{2m}$; then the preceding equality becomes

$$f(x) \triangleq \frac{1-x^\alpha}{1-x} = \alpha.$$

If we prove that this equation has no solution $x \in]0, 1[$ for any $\alpha > 1$, then the result follows without difficulty. To do so, we get after differentiating f

$$f'(x) = \frac{(\alpha-1)x^\alpha - \alpha x^{\alpha-1} + 1}{(1-x)^2} \triangleq \frac{g(x)}{(1-x)^2}.$$

Now we note that

$$g'(x) = \alpha(\alpha-1)x^{\alpha-2}(x-1) < 0.$$

As $g(1) = 0$, then we deduce

$$g(x) > 0 \quad \text{for all } x \in]0, 1[.$$

Thus, f is strictly increasing. Furthermore,

$$\lim_{x \rightarrow 1} f(x) = \alpha.$$

This implies that,

$$\text{for all } x \in]0, 1[, \quad f(x) < \alpha.$$

Therefore, we get the strict monotonicity of the ‘‘eigenvalues’’, and consequently, the kernel of $\partial_f F(\lambda_m, 0)$ is a one-dimensional vector space generated by the function $v_m(w) = \bar{w}^{m-1}$.

(iii) We shall prove that the range of $\partial_f F(\lambda_m, 0)$ is described by

$$R\partial_f F(\lambda_m, 0) = \left\{ g \in Y : g(w) = \sum_{\substack{n \geq 1 \\ n \neq m}} b_n e_n \right\} \triangleq \mathcal{X}.$$

Combining Propositions 11 and 12(i), we conclude that the range is contained in the right space. So what is left is to prove the converse. Let $g \in \mathcal{X}$; we will solve in X the equation

$$\partial_f F(\lambda_m, 0)h = g, \quad h = \sum_{n \geq 0} a_n \bar{w}^n.$$

By virtue of (30), this equation is equivalent to

$$a_{n-1} = \frac{b_n}{bn(\lambda_m - \lambda_n)}, \quad n \geq 1, \quad n \neq m.$$

Thus, the problem reduces to showing that

$$h : w \mapsto \sum_{\substack{n \geq 1 \\ n \neq m}} \frac{b_n}{bn(\lambda_m - \lambda_n)} \bar{w}^{n-1} \in C^{1+\alpha}(\mathbb{T}).$$

Observe that

$$\inf_{n \neq m} |\lambda_n - \lambda_m| \triangleq c_0 > 0,$$

and thus, we deduce by Cauchy–Schwarz

$$\begin{aligned} \|h\|_{L^\infty} &\leq \frac{1}{b} \sum_{\substack{n \geq 1 \\ n \neq m}} \frac{|b_n|}{n|\lambda_m - \lambda_n|} \\ &\leq \frac{1}{c_0 b} \sum_{\substack{n \geq 1 \\ n \neq m}} \frac{|b_n|}{n} \\ &\lesssim \|g\|_{L^2} \lesssim \|g\|_{C^\alpha}. \end{aligned}$$

To finish the proof, we shall check that $h' \in C^\alpha(\mathbb{T})$ or equivalently $(\bar{w}h)' \in C^\alpha(\mathbb{T})$. It is obvious that

$$\begin{aligned} (\bar{w}h(w))' &= - \sum_{\substack{n \geq 1 \\ n \neq m}} \frac{b_n}{b(\lambda_m - \lambda_n)} \bar{w}^{n+1} \\ &= - \frac{1}{b\lambda_m} \sum_{\substack{n \geq 1 \\ n \neq m}} b_n \bar{w}^{n+1} + \frac{1}{b\lambda_m} \sum_{\substack{n \geq 1 \\ n \neq m}} \frac{\lambda_n}{\lambda_n - \lambda_m} b_n \bar{w}^{n+1}. \end{aligned}$$

We shall write the preceding expression with the Szegő projection

$$\Pi : \sum_{n \in \mathbb{Z}} a_n w^n \mapsto \sum_{n \in -\mathbb{N}} a_n w^n, \quad (\bar{w}h(w))' = - \frac{\bar{w}}{2ib\lambda_m} \Pi g(w) + \frac{\bar{w}}{2ib\lambda_m} (K \star \Pi g)(w),$$

with

$$K(w) \triangleq \sum_{\substack{n \geq 1 \\ n \neq m}} \frac{\lambda_n}{\lambda_n - \lambda_m} \bar{w}^n.$$

Notice that

$$\frac{\lambda_n}{|\lambda_n - \lambda_m|} \leq c_0^{-1} \frac{1}{n},$$

and therefore, $K \in L^2(\mathbb{T})$ which implies in particular that $K \in L^1(\mathbb{T})$. Now to complete the proof of $(\bar{w}h)' \in C^\alpha(\mathbb{T})$, it suffices to use the continuity of the Szegő projection on $C^\alpha(\mathbb{T})$ combined with $L^1 \star C^\alpha(\mathbb{T}) \subset C^\alpha(\mathbb{T})$.

(iv) To check the transversality assumption, we differentiate (30) with respect to λ :

$$\partial_\lambda \partial_f F(\lambda_m, 0)h = b \sum_{n \geq 1} n a_{n-1} e_n.$$

Therefore,

$$\partial_\lambda \partial_f F(\lambda_m, 0)v_m = b m e_m \notin R(\partial_f F(\lambda_m, 0)).$$

This completes the proof of the proposition. □

3.3. Proof of Theorem 1. According to Propositions 14 and 11, all the assumptions of the Crandall–Rabinowitz theorem are satisfied, and therefore, we conclude for each $m \geq 1$ the existence of only one nontrivial curve bifurcating from the trivial one at the angular velocity

$$\Omega_m = \frac{1 - \lambda_m}{2} = \frac{m - 1 + b^{2m}}{2m}.$$

To complete the proof, it remains to check the m -fold symmetry of the V -states. This can be done by including the required symmetry in the function spaces. More precisely, instead of dealing with X and Y ,

we should work with the spaces

$$X_m = \left\{ f \in C^{1+\alpha}(\mathbb{T}) : f(w) = \sum_{n=1}^{\infty} a_n \bar{w}^{nm-1}, a_n \in \mathbb{R} \right\},$$

$$Y_m = \left\{ g \in C^\alpha(\mathbb{T}) : g(w) = \sum_{n \geq 1} b_n e_{nm}, b_n \in \mathbb{R} \right\}, \quad e_n = \frac{1}{2i}(\bar{w}^n - w^n).$$

The conformal mapping describing the V -state takes the form

$$\phi(w) = bw + \sum_{n=1}^{\infty} a_n \bar{w}^{nm-1},$$

and the m -fold symmetry of the V -state means that

$$\phi(e^{2i\pi/m} w) = e^{2i\pi/m} \phi(w) \quad \text{for all } w \in \mathbb{T}.$$

The ball B_r is changed to $B_r^m = \{f \in X_m : \|f\|_{C^{1+\alpha}} < r\}$. Then Proposition 11 holds true according to this adaptation, and the only point that one must check is the stability of the spaces; that is, for $f \in B_r^m$, we have $F(\lambda, f) \in Y_m$. This result was checked in [de la Hoz et al. 2016b] for the terms F_1 and F_2 , and it remains to check that $F_3(f)$ belongs to Y_m . Recall that

$$F_3(f(w)) = \text{Im}\{F_4(\phi(w))w\phi'(w)\}, \quad \phi(w) = bw + f(w),$$

where F_4 is defined in (20). By change of variables and using the symmetry of ϕ ,

$$\begin{aligned} F_4(\phi(e^{i2\pi/m} w)) &= \int_{\mathbb{T}} \frac{|\phi(\xi)|^2 \phi'(\xi)}{1 - \phi(e^{i2\pi/m} w)\phi(\xi)} d\xi \\ &= e^{-i2\pi/m} \int_{\mathbb{T}} \frac{|\phi(e^{-i2\pi/m} \zeta)|^2 \phi'(e^{-i2\pi/m} \zeta)}{1 - \phi(e^{i2\pi/m} w)\phi(e^{-i2\pi/m} \zeta)} d\zeta \\ &= e^{-i2\pi/m} \int_{\mathbb{T}} \frac{|\phi(\tau)|^2 \phi'(\tau)}{1 - \phi(w)\phi(\tau)} d\tau \\ &= e^{-i2\pi/m} F_4(\phi(w)). \end{aligned}$$

Consequently, we obtain

$$F_3(f(e^{i2\pi/m} w)) = F_3(f(w)),$$

and this shows the stability result.

4. Doubly connected V -states

In this section, we shall establish all the ingredients required for the proofs of Theorems 6 and 9, and this will be carried out in several steps. First we shall write the equations governing the doubly connected V -states which are described by two coupled nonlinear equations. Second we briefly discuss the regularity of the functionals and compute the linearized operator around the trivial solution. The delicate part to which we will pay careful attention is the computation of the kernel dimension. This will be implemented through the study of the monotonicity of the nonlinear eigenvalues. As we shall see, the fact that we have

multiple parameters introduces many more complications to this study compared to the result of [de la Hoz et al. 2016b]. Finally, we shall prove Theorem 6 in Section 4.5.2.

4.1. Boundary equations. Let D be a doubly connected domain of the form $D = D_1 \setminus D_2$ with $D_2 \subset D_1$ two simply connected domains. Denote by Γ_j the boundary of the domain D_j . In this case, the V -states equation (15) reduces to two coupled equations, one for each boundary component Γ_j . More precisely,

$$\operatorname{Re}\{((1 - \lambda)\bar{z} + I(z) - J(z))z'\} = 0 \quad \text{for all } z \in \Gamma_1 \cup \Gamma_2, \tag{31}$$

with

$$\begin{aligned} I(z) &= \int_{\Gamma_1} \frac{\bar{z} - \bar{\xi}}{z - \xi} d\xi - \int_{\Gamma_2} \frac{\bar{z} - \bar{\xi}}{z - \xi} d\xi, \\ J(z) &= \int_{\Gamma_1} \frac{|\xi|^2}{1 - z\xi} d\xi - \int_{\Gamma_2} \frac{|\xi|^2}{1 - z\xi} d\xi. \end{aligned}$$

As for the simply connected case, we prefer using the conformal parametrization of the boundaries. Let $\phi_j : \mathbb{D}^c \rightarrow D_j^c$ satisfy

$$\phi_j(w) = b_j w + \sum_{n \geq 0} \frac{a_{j,n}}{w^n}$$

with $0 < b_j < 1$, $j = 1, 2$ and $b_2 < b_1$. We assume moreover that all the Fourier coefficients are real because we shall look for V -states which are symmetric with respect to the real axis. Then by change of variables, we obtain

$$\begin{aligned} I(z) &= \int_{\mathbb{T}} \frac{\bar{z} - \overline{\phi_1(\xi)}}{z - \phi_1(\xi)} \phi_1'(\xi) d\xi - \int_{\mathbb{T}} \frac{\bar{z} - \overline{\phi_2(\xi)}}{z - \phi_2(\xi)} \phi_2'(\xi) d\xi, \\ J(z) &= \int_{\mathbb{T}} \frac{|\phi_1(\xi)|^2}{1 - z\phi_1(\xi)} \phi_1'(\xi) d\xi - \int_{\mathbb{T}} \frac{|\phi_2(\xi)|^2}{1 - z\phi_2(\xi)} \phi_2'(\xi) d\xi. \end{aligned}$$

Setting $\phi_j = b_j \operatorname{Id} + f_j$, (31) becomes,

$$\text{for all } w \in \mathbb{T}, \quad G_j(\lambda, f_1, f_2)(w) = 0, \quad j = 1, 2,$$

where

$$G_j(\lambda, f_1, f_2)(w) \triangleq \operatorname{Im}\{((1 - \lambda)\overline{\phi_j(w)} + I(\phi_j(w)) - J(\phi_j(w)))w\phi_j'(w)\}.$$

Note that one can easily check that

$$G(\lambda, 0, 0) = 0 \quad \text{for all } \lambda \in \mathbb{R}.$$

This is consistent with the fact that the annulus is a stationary solution and therefore rotates with any angular velocity since the shape is rotational invariant.

4.2. Regularity of the functional G . In this short subsection, we shall quickly state the regularity result of the functional $G \triangleq (G_1, G_2)$ needed in the Crandall–Rabinowitz theorem. Following the simply connected case, the spaces X and Y involved in the bifurcation will be chosen in a similar way: set

$$X = \left\{ f \in (C^{1+\alpha}(\mathbb{T}))^2 : f(w) = \sum_{n \geq 0} A_n \bar{w}^n, A_n \in \mathbb{R}^2, w \in \mathbb{T} \right\},$$

$$Y = \left\{ g \in (C^\alpha(\mathbb{T}))^2 : g(w) = \sum_{n \geq 1} B_n e_n, B_n \in \mathbb{R}^2, w \in \mathbb{T} \right\}, \quad e_n \triangleq \frac{1}{2i}(\bar{w}^n - w^n),$$

with $\alpha \in]0, 1[$. For $r \in (0, 1)$, we denote by B_r the open ball of X with center 0 and radius r ,

$$B_r = \{f \in X : \|f\|_{C^{1+\alpha}} \leq r\}.$$

Similarly to Proposition 11, one can establish the regularity assumptions needed for the Crandall–Rabinowitz theorem. Compared to the simply connected case, the only terms that one should care about are those describing the interaction between the boundaries of the patches which are supposed to be disjoint. Therefore, the involved kernels are sufficiently smooth and actually do not cause significant difficulties in their treatment. For this reason, we prefer skip the details and restrict ourselves to the following statement.

Proposition 13. *Let $b \in]0, 1[$ and $0 < r < \min(b, 1 - b)$; then the following hold true:*

- (i) $G : \mathbb{R} \times B_r \rightarrow Y$ is C^1 (it is in fact C^∞).
- (ii) The partial derivative $\partial_\lambda \partial_f G : \mathbb{R} \times B_r \rightarrow \mathcal{L}(X, Y)$ exists and is continuous (it is in fact C^∞).

4.3. Structure of the linearized operator. In this subsection, we shall compute the linearized operator $\partial_f G(\lambda, 0)$ around the annulus \mathbb{A}_{b_1, b_2} of radii b_1 and b_2 . The study of the eigenvalues is postponed to the next subsections. From the regularity assumptions of G , we assert that the Fréchet derivative and Gâteaux derivatives coincide and

$$DG(\lambda, 0, 0)(h_1, h_2) = \frac{d}{dt} G(\lambda, th_1, th_2)|_{t=0}.$$

Note that $DG(\lambda, 0, 0)$ is nothing but the partial derivative $\partial_f G(\lambda, 0, 0)$. Our main result reads as follows.

Proposition 14. *Let $h = (h_1, h_2) \in X$ take the form $h_j(w) = \sum_{n \geq 0} a_{j,n} w^n$. Then*

$$DG(\lambda, 0, 0)(h_1, h_2) = \sum_{n \geq 1} M_n(\lambda) \begin{pmatrix} a_{1,n-1} \\ a_{2,n-1} \end{pmatrix} e_n,$$

where the matrix M_n is given by

$$M_n(\lambda) = \begin{pmatrix} b_1[n\lambda - 1 + b_1^{2n} - n(b_2/b_1)^2] & b_2[(b_2/b_1)^n - (b_1 b_2)^n] \\ -b_1[(b_2/b_1)^n - (b_1 b_2)^n] & b_2[n\lambda - n + 1 - b_2^{2n}] \end{pmatrix} \quad \text{and} \quad e_n(w) = \frac{1}{2i}(\bar{w}^n - w^n).$$

Proof. Since $G = (G_1, G_2)$, for a given couple of functions $(h_1, h_2) \in X$,

$$DG(\lambda, 0, 0)(h_1, h_2) = \begin{pmatrix} \partial_{f_1} G_1(\lambda, 0, 0)h_1 + \partial_{f_2} G_1(\lambda, 0, 0)h_2 \\ \partial_{f_1} G_2(\lambda, 0, 0)h_1 + \partial_{f_2} G_2(\lambda, 0, 0)h_2 \end{pmatrix}.$$

We shall split G_j into three terms

$$G_j(\lambda, f_1, f_2) = G_j^1(\lambda, f_j) + G_j^2(f_1, f_2) + G_j^3(f_1, f_2),$$

where

$$G_j^1(\lambda, f_j)(w) \triangleq \operatorname{Im} \left\{ \left[(1 - \lambda) \overline{\phi_j(w)} + (-1)^{j+1} \int_{\mathbb{T}} \frac{\overline{\phi_j(w)} - \overline{\phi_j(\tau)}}{\phi_j(w) - \phi_j(\tau)} \phi_j'(\tau) d\tau + (-1)^j \int_{\mathbb{T}} \frac{|\phi_j(\tau)|^2 \phi_j'(\tau)}{1 - \phi_j(w) \phi_j(\tau)} d\tau \right] w \phi_j'(w) \right\},$$

$$G_j^2(f_1, f_2) \triangleq (-1)^j \operatorname{Im} \left\{ \int_{\mathbb{T}} \frac{\overline{\phi_j(w)} - \overline{\phi_i(\tau)}}{\phi_j(w) - \phi_i(\tau)} \phi_i'(\tau) d\tau w \phi_j'(w) \right\}, \quad i \neq j,$$

$$G_j^3(f_1, f_2) \triangleq (-1)^{j+1} \operatorname{Im} \left\{ \int_{\mathbb{T}} \frac{|\phi_i(\tau)|^2 \phi_i'(\tau)}{1 - \phi_j(w) \phi_i(\tau)} d\tau w \phi_j'(w) \right\}, \quad i \neq j,$$

with $\phi_j = b_j \operatorname{Id} + f_j$, $j = 1, 2$.

• *Computation of $\partial_{f_j} G_j^1(\lambda, 0, 0)h_j$.* First observe that

$$G_1^1(\lambda, f_1)(w) = \operatorname{Im} \left\{ \left[(1 - \lambda) \overline{\phi_1(w)} + \int_{\mathbb{T}} \frac{\overline{\phi_1(w)} - \overline{\phi_1(\tau)}}{\phi_1(w) - \phi_1(\tau)} \phi_1'(\tau) d\tau - \int_{\mathbb{T}} \frac{|\phi_1(\tau)|^2 \phi_1'(\tau)}{1 - \phi_1(w) \phi_1(\tau)} d\tau \right] w \phi_1'(w) \right\}.$$

This functional is exactly the defining function in the simply connected case, and thus, using merely (30),

$$\partial_{f_1} G_1^1(\lambda, 0)h_1 = b_1 \sum_{n \geq 0} (\lambda(n + 1) - 1 + b_1^{2n+2}) a_{1,n} e_{n+1}. \tag{32}$$

In regard to $G_2^1(\lambda, f_2)$, we get from the definition

$$G_2^1(\lambda, f_2)(w) = \operatorname{Im} \left\{ \left[(1 - \lambda) \overline{\phi_2(w)} - \int_{\mathbb{T}} \frac{\overline{\phi_2(w)} - \overline{\phi_2(\tau)}}{\phi_2(w) - \phi_2(\tau)} \phi_2'(\tau) d\tau + \int_{\mathbb{T}} \frac{|\phi_2(\tau)|^2 \phi_2'(\tau)}{1 - \phi_2(w) \phi_2(\tau)} d\tau \right] w \phi_2'(w) \right\}.$$

It is easy to check the algebraic relation $G_2^1(\lambda, f_2) = -G_1^1(2 - \lambda, f_2)$, and thus, by applying (32),

$$\partial_{f_2} G_2^1(\lambda, 0)h_2 = b_2 \sum_{n \geq 0} (\lambda(n + 1) - 2n - 1 - b_2^{2n+2}) a_{2,n} e_{n+1}. \tag{33}$$

• *Computation of $\partial_{f_j} G_j^2(\lambda, 0, 0)h_j$.* This quantity is given by

$$\partial_{f_j} G_j^2(0, 0)h_j = (-1)^j \frac{d}{dt} \operatorname{Im} \left\{ b_i w \int_{\mathbb{T}} \frac{b_j \bar{w} - b_i \bar{\tau} + t \overline{h_j(w)}}{b_j w - b_i \tau + t h_j(w)} d\tau (b_j + t h_j'(w)) \right\} \Big|_{t=0}.$$

Straightforward computations yield

$$\begin{aligned} \partial_{f_j} G_j^2(0, 0)h_j = & (-1)^j b_i \operatorname{Im} \left\{ h_j'(w) w \int_{\mathbb{T}} \frac{b_j \bar{w} - b_i \bar{\tau}}{b_j w - b_i \tau} d\tau + b_j w \overline{h_j(w)} \int_{\mathbb{T}} \frac{d\tau}{b_j w - b_i \tau} \right. \\ & \left. - b_j w h_j(w) \int_{\mathbb{T}} \frac{b_j \bar{w} - b_i \bar{\tau}}{(b_j w - b_i \tau)^2} d\tau \right\}. \end{aligned}$$

According to the residue theorem,

$$\int_{\mathbb{T}} \frac{d\tau}{b_1 w - b_2 \tau} = 0, \quad \int_{\mathbb{T}} \frac{d\tau}{(b_1 w - b_2 \tau)^2} = 0 \quad \text{for all } w \in \mathbb{T},$$

and therefore,

$$\begin{aligned} \partial_{f_1} G_1^2(0, 0)h_1(w) &= -b_2^2 \operatorname{Im} \left\{ - \int_{\mathbb{T}} \frac{wh_1'(w)}{b_1 w - b_2 \tau} \frac{d\tau}{\tau} + b_1 \int_{\mathbb{T}} \frac{wh_1(w)}{(b_1 w - b_2 \tau)^2} \frac{d\tau}{\tau} \right\} \\ &= -b_2^2 \operatorname{Im} \left\{ -\frac{1}{b_1} h_1'(w) + \frac{1}{b_1} \bar{w} h_1(w) \right\} \\ &= -\frac{b_2^2}{b_1} \sum_{n \geq 0} (n+1) a_{1,n} e_{n+1}. \end{aligned} \tag{34}$$

Now using the vanishing integrals

$$\int_{\mathbb{T}} \frac{\bar{\tau} d\tau}{b_2 w - b_1 \tau} = 0, \quad \int_{\mathbb{T}} \frac{\bar{\tau} d\tau}{(b_2 w - b_1 \tau)^2} = 0, \quad \int_{\mathbb{T}} \frac{d\tau}{(b_2 w - b_1 \tau)^2} = 0,$$

we may obtain

$$\begin{aligned} \partial_{f_2} G_2^2(0, 0)h_2(w) &= b_1 \operatorname{Im} \left\{ b_2 h_2'(w) \int_{\mathbb{T}} \frac{d\tau}{b_2 w - b_1 \tau} + b_2 w \overline{h_2(w)} \int_{\mathbb{T}} \frac{d\tau}{b_2 w - b_1 \tau} \right\} \\ &= b_1 \operatorname{Im} \left\{ -\frac{b_2}{b_1} h_2'(w) - \frac{b_2}{b_1} w \overline{h_2(w)} \right\} \\ &= b_2 \sum_{n \geq 0} (n+1) a_{2,n} e_{n+1}. \end{aligned} \tag{35}$$

• *Computation of $\partial_{f_i} G_j^2(\lambda, 0, 0)h_i, i \neq j$.* By straightforward computations, we obtain

$$\begin{aligned} \partial_{f_i} G_j^2(0, 0)h_i(w) &= (-1)^j b_j \operatorname{Im} \left\{ w \int_{\mathbb{T}} \frac{(b_j \bar{w} - b_i \bar{\tau})}{b_j w - b_i \tau} h_i'(\tau) d\tau - b_i w \int_{\mathbb{T}} \frac{\overline{h_i(\tau)}}{b_j w - b_i \tau} d\tau \right. \\ &\quad \left. + b_i w \int_{\mathbb{T}} \frac{(b_j \bar{w} - b_i \bar{\tau}) h_i(\tau) d\tau}{(b_j w - b_i \tau)^2} \right\}. \end{aligned} \tag{36}$$

As \bar{h}_i is holomorphic inside the open unit disc, by the residue theorem, we deduce that

$$\int_{\mathbb{T}} \frac{\overline{h_i(\tau)}}{b_1 w - b_2 \tau} d\tau = 0, \quad w \in \mathbb{T}.$$

It follows that

$$\begin{aligned} \partial_{f_2} G_1^2(0, 0)h_2(w) &= -b_1 \operatorname{Im} \left\{ b_1 \int_{\mathbb{T}} \frac{h_2'(\tau)}{b_1 w - b_2 \tau} d\tau - b_2 w \int_{\mathbb{T}} \frac{\bar{\tau} h_2'(\tau)}{b_1 w - b_2 \tau} d\tau \right. \\ &\quad \left. + b_1 b_2 \int_{\mathbb{T}} \frac{h_2(\tau) d\tau}{(b_1 w - b_2 \tau)^2} - b_2^2 w \int_{\mathbb{T}} \frac{\bar{\tau} h_2(\tau) d\tau}{(b_1 w - b_2 \tau)^2} \right\} \\ &\triangleq -b_1 \operatorname{Im} \{ J_1 + J_2 + J_3 + J_4 \}. \end{aligned} \tag{37}$$

To compute the first term $J_1(w)$, we write after using the series expansion of $1/(1 - (b_2/b_1)\bar{w}\tau)$

$$\begin{aligned} J_1 &= \bar{w} \int_{\mathbb{T}} \frac{h'_2(\tau)}{1 - (b_2/b_1)\bar{w}\tau} d\tau \\ &= \sum_{n \geq 0} \left(\frac{b_2}{b_1}\right)^n \bar{w}^{n+1} \int_{\mathbb{T}} \tau^n h'_2(\tau) d\tau. \end{aligned}$$

Note that

$$\int_{\mathbb{T}} \tau^n h'_2(\tau) d\tau = -na_{2,n},$$

which us enables to get

$$J_1 = - \sum_{n \geq 1} na_{2,n} \left(\frac{b_2}{b_1}\right)^n \bar{w}^{n+1}. \tag{38}$$

As for the term $J_2(w)$, we write in a similar way

$$\begin{aligned} J_2 &= -\frac{b_2}{b_1} \int_{\mathbb{T}} \frac{\bar{\tau} h'_2(\tau)}{1 - (b_2/b_1)\bar{w}\tau} d\tau \\ &= - \sum_{n \geq 0} \left(\frac{b_2}{b_1}\right)^{n+1} \bar{w}^n \int_{\mathbb{T}} \tau^{n-1} h'_2(\tau) d\tau. \end{aligned}$$

Since $\int_{\mathbb{T}} \tau^{-k} h'_2(\tau) d\tau = 0$ for $k \in \{0, 1\}$, the preceding sum starts at $n = 2$ and by shifting the summation index

$$\begin{aligned} J_2 &= - \sum_{n \geq 1} \left(\frac{b_2}{b_1}\right)^{n+2} \bar{w}^{n+1} \int_{\mathbb{T}} \tau^n h'_2(\tau) d\tau \\ &= \sum_{n \geq 1} na_{2,n} \left(\frac{b_2}{b_1}\right)^{n+2} \bar{w}^{n+1}. \end{aligned} \tag{39}$$

Concerning the third term J_3 , we write by virtue of (27)

$$\begin{aligned} J_3 &= \frac{b_2}{b_1} \bar{w}^2 \int_{\mathbb{T}} \frac{h_2(\tau)}{(1 - (b_2/b_1)\bar{w}\tau)^2} d\tau \\ &= \sum_{n \geq 1} n \left(\frac{b_2}{b_1}\right)^n \bar{w}^{n+1} \int_{\mathbb{T}} \tau^{n-1} h_2(\tau) d\tau. \end{aligned}$$

Therefore, we find

$$J_3 = \sum_{n \geq 1} na_{2,n} \left(\frac{b_2}{b_1}\right)^n \bar{w}^{n+1}. \tag{40}$$

Similarly, we get

$$\begin{aligned}
 J_4 &= -\left(\frac{b_2}{b_1}\right)^2 \bar{w} \int_{\mathbb{T}} \frac{\bar{\tau} h_2(\tau)}{(1 - (b_2/b_1)\bar{w}\tau)^2} d\tau \\
 &= -\sum_{n \geq 1} n \left(\frac{b_2}{b_1}\right)^{n+1} \bar{w}^n \int_{\mathbb{T}} \tau^{n-2} h_2(\tau) d\tau \\
 &= -\sum_{n \geq 0} (n+1) a_{2,n} \left(\frac{b_2}{b_1}\right)^{n+2} \bar{w}^{n+1}.
 \end{aligned} \tag{41}$$

Inserting the identities (38), (39), (40) and (41) into (37), we find

$$\begin{aligned}
 \partial_{f_2} G_1^2(0, 0) h_2(w) &= b_1 \operatorname{Im} \left\{ \sum_{n \geq 0} a_{2,n} \left(\frac{b_2}{b_1}\right)^{n+2} \bar{w}^{n+1} \right\} \\
 &= b_1 \sum_{n \geq 0} a_{2,n} \left(\frac{b_2}{b_1}\right)^{n+2} e_{n+1}(w).
 \end{aligned} \tag{42}$$

Next, we shall move to the computation of $\partial_{f_1} G_2^2(0, 0) h_1$. In view of (36),

$$\begin{aligned}
 \partial_{f_1} G_2^2(0, 0) h_1(w) &= b_2 \operatorname{Im} \left\{ w \int_{\mathbb{T}} \frac{(b_2 \bar{w} - b_1 \bar{\tau})}{b_2 w - b_1 \tau} h_1'(\tau) d\tau - b_1 w \int_{\mathbb{T}} \frac{\overline{h_1(\tau)}}{b_2 w - b_1 \tau} d\tau \right. \\
 &\quad \left. + b_1 w \int_{\mathbb{T}} \frac{(b_2 \bar{w} - b_1 \bar{\tau}) h_1(\tau) d\tau}{(b_2 w - b_1 \tau)^2} \right\}.
 \end{aligned}$$

The residue theorem at infinity enables us to get rid of the first and third integrals in the right-hand side, and thus,

$$\partial_{f_1} G_2^2(0, 0) h_1(w) = -b_1 b_2 \operatorname{Im} \left\{ w \int_{\mathbb{T}} \frac{\overline{h_1(\tau)}}{b_2 w - b_1 \tau} d\tau \right\}.$$

A second application of the residue theorem in the disc yields

$$\begin{aligned}
 \partial_{f_1} G_2^2(0, 0) h_1(w) &= b_2 \operatorname{Im} \left\{ w \bar{h}_1 \left(\frac{b_2 w}{b_1}\right) \right\} \\
 &= -b_2 \sum_{n \geq 0} a_{1,n} \left(\frac{b_2}{b_1}\right)^n e_{n+1}(w).
 \end{aligned} \tag{43}$$

• *Computation of $\partial_{f_i} G_j^3(\lambda, 0, 0) h_i$.* The diagonal terms $i = j$ can be easily computed:

$$\begin{aligned}
 \partial_{f_i} G_i^3(0, 0) h_i(w) &= (-1)^{i+1} b_i^3 \operatorname{Im} \left\{ w \int_{\mathbb{T}} \frac{h_i'(w) d\tau}{1 - b_i^2 w \tau} + w h_i(w) \int_{\mathbb{T}} \frac{\tau d\tau}{(1 - b_i^2 w \tau)^2} \right\} \\
 &= 0.
 \end{aligned} \tag{44}$$

Let us now calculate $\partial_{f_i} G_j^3(\lambda, 0, 0)h_i$ for $i \neq j$. One can check with difficulty that

$$\partial_{f_i} G_j^3(0, 0)h_i(w) = (-1)^{j+1} b_j b_i^2 \operatorname{Im} \left\{ w \int_{\mathbb{T}} \frac{h'_i(\tau)}{1 - b_i b_j w \tau} d\tau + 2w \int_{\mathbb{T}} \frac{\operatorname{Re}\{\tau \overline{h_i(\tau)}\}}{1 - b_i b_j w \tau} d\tau + b_i b_j w^2 \int_{\mathbb{T}} \frac{h_i(\tau) d\tau}{(1 - b_i b_j w \tau)^2} \right\}.$$

Invoking once again the residue theorem, we find

$$\begin{aligned} \partial_{f_i} G_j^3(0, 0)h_i(w) &= (-1)^{j+1} b_j b_i^2 \operatorname{Im} \left\{ - \sum_{n \geq 0} n a_{i,n} (b_j b_i)^n w^{n+1} + \sum_{n \geq 0} a_{i,n} (b_j b_i)^n w^{n+1} + \sum_{n \geq 0} n a_{i,n} (b_j b_i)^n w^{n+1} \right\} \\ &= (-1)^j b_i \sum_{n \geq 0} a_{i,n} (b_j b_i)^{n+1} e_{n+1}. \end{aligned} \tag{45}$$

The details are left to the reader because most of them were done previously. Now putting together the identities (32), (34) and (44),

$$\partial_{f_1} G_1(\lambda, 0, 0)h_1 = \sum_{n \geq 0} b_1 \left[(n+1)\lambda - 1 + b_1^{2n+2} - (n+1) \left(\frac{b_2}{b_1} \right)^2 \right] a_{1,n} e_{n+1}. \tag{46}$$

From (33), (35) and (44), one obtains

$$\partial_{f_2} G_2(\lambda, 0, 0)h_2 = \sum_{n \geq 0} b_2 ((n+1)\lambda - n - b_2^{2n+2}) a_{2,n} e_{n+1}. \tag{47}$$

On the other hand, we observe that for $i \neq j$

$$\partial_{f_i} G_j^1(\lambda, 0)h_i(w) = 0. \tag{48}$$

Gathering the identities (48), (42) and (45) yields

$$\partial_{f_2} G_1(\lambda, 0, 0)h_2 = \sum_{n \geq 0} b_2 \left[\left(\frac{b_2}{b_1} \right)^{n+1} - (b_1 b_2)^{n+1} \right] a_{2,n} e_{n+1}.$$

Furthermore, combining (48), (43) and (45), we can assert that

$$\partial_{f_1} G_2(\lambda, 0, 0)h_1 = \sum_{n \geq 0} b_1 \left[(b_1 b_2)^{n+1} - \left(\frac{b_2}{b_1} \right)^{n+1} \right] a_{1,n} e_{n+1}.$$

Consequently, we get in view of the last two expressions combined with (47) and (48)

$$DG(\lambda, 0, 0)(h_1, h_2) = \sum_{n \geq 0} M_{n+1} \begin{pmatrix} a_{1,n} \\ a_{2,n} \end{pmatrix} e_{n+1}, \tag{49}$$

where the matrix M_n is given for each $n \geq 1$ by

$$M_n \triangleq \begin{pmatrix} b_1[n\lambda - 1 + b_1^{2n} - n(b_2/b_1)^2] & b_2[(b_2/b_1)^n - (b_1 b_2)^n] \\ -b_1[(b_2/b_1)^n - (b_1 b_2)^n] & b_2[n\lambda - n + 1 - b_2^{2n}] \end{pmatrix}. \tag{50}$$

This completes the proof of Proposition 14. □

4.4. Eigenvalues study. The current subsection will be devoted to the study of the structure of the *nonlinear eigenvalues* which are the values λ such that the linearized operator $DG(\lambda, 0, 0)$ given by (49) has a nontrivial kernel. Note that these eigenvalues correspond exactly to matrices M_n which are not invertible for some integer $n \geq 1$. In other words, λ is an eigenvalue if and only if there exists $n \geq 1$ such that $\det M_n = 0$, that is,

$$\begin{aligned} \det M_n(\lambda) &= b_1 b_2 \left[n^2 \lambda^2 - n \left(n + b_2^{2n} - b_1^{2n} + n \left(\frac{b_2}{b_1} \right)^2 \right) \lambda + (n-1) \left(1 - b_1^{2n} + n \left(\frac{b_2}{b_1} \right)^2 \right) \right. \\ &\quad \left. + \left(\frac{b_2}{b_1} \right)^{2n} + n b_2^{2n} \left(\frac{b_2}{b_1} \right)^2 - b_2^{2n} \right] \\ &= 0. \end{aligned}$$

This is equivalent to

$$\begin{aligned} P_n(\lambda) \triangleq \lambda^2 - \left[1 + \left(\frac{b_2}{b_1} \right)^2 - \left(\frac{b_1^{2n} - b_2^{2n}}{n} \right) \right] \lambda \\ + \left(\frac{b_2}{b_1} \right)^2 - \frac{1 - (b_2/b_1)^{2n}}{n^2} + \frac{1 - (b_2/b_1)^2}{n} - \frac{b_1^{2n} - b_2^{2n} (b_2/b_1)^2}{n} + \frac{b_1^{2n} - b_2^{2n}}{n^2} \\ = 0. \end{aligned} \tag{51}$$

The reduced discriminant of this second-degree polynomial in λ is given by

$$\Delta_n = \left(\frac{1 - (b_2/b_1)^2}{2} - \frac{2 - b_2^{2n} - b_1^{2n}}{2n} \right)^2 - \left(\frac{b_2}{b_1} \right)^{2n} \left(\frac{1 - b_1^{2n}}{n} \right)^2. \tag{52}$$

Thereby P_n admits two real roots if and only if $\Delta_n \geq 0$, and they are given by

$$\lambda_n^\pm = \frac{1 + (b_2/b_1)^2}{2} - \left(\frac{b_1^{2n} - b_2^{2n}}{2n} \right) \pm \sqrt{\Delta_n}.$$

To understand the structure of the eigenvalues and their dependence on the involved parameters, it would be better to fix the radius b_1 and to vary n and $b_2 \in]0, b_1[$. We shall distinguish the cases $n \geq 2$ from $n = 1$, which is very special. For given $n \geq 2$, we wish to draw the curves $b_2 \mapsto \lambda_n^\pm(b_2)$. As we shall see in Proposition 19, the maximal domains of existence of these curves are a common connected set of the form $[0, b_n^*]$ and b_n^* is defined as the unique $b_2 \in]0, b_1[$ such that $\Delta_n = 0$. We introduce the graphs \mathcal{C}_n^\pm of $\lambda_n^\pm(b_2)$:

$$\mathcal{C}_n^\pm \triangleq \{(b_2, \lambda_n^\pm(b_2)) : b_2 \in [0, b_n^*]\}, \quad \mathcal{C}_n = \mathcal{C}_n^- \cup \mathcal{C}_n^+, \quad n \geq 2. \tag{53}$$

It is not hard to check that \mathcal{C}_n^+ intersects \mathcal{C}_n^- at only one point whose abscissa is b_n^* , that is, when the discriminant vanishes. Furthermore, and this is not trivial, we shall see that the domain enclosed by the curve \mathcal{C}_n and located in the first quadrant of the plane is a strictly increasing set on n . This will give in particular the monotonicity of the eigenvalues with respect to n . Nevertheless, the dynamics of the first eigenvalues corresponding to $n = 1$ is completely different from the preceding ones. Indeed, according to

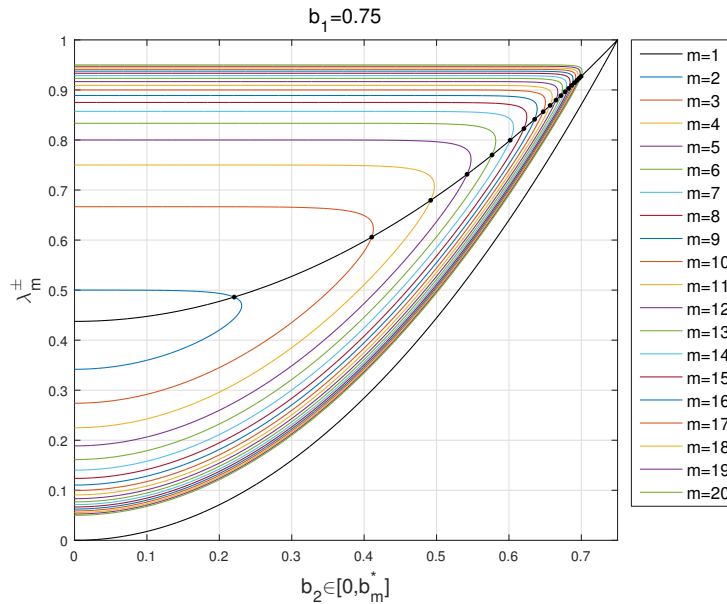


Figure 1. λ_m^\pm as a function of $b_2 \in [0, b_m^*]$, for $m = 2, \dots, 20$, together with the case $m = 1$ (black), for $b_1 = 0.75$.

Section 4.4.3, we find for $n = 1$ two eigenvalues given explicitly by

$$\lambda_1^- = (b_2/b_1)^2 \quad \text{or} \quad \lambda_1^+ = 1 + b_2^2 - b_1^2.$$

It turns out that for the first one the range of the linearized operator has an infinite codimension, and therefore, there is no hope to bifurcate using only the classical results of bifurcation theory. However, for the second eigenvalue, the range is “almost everywhere” of codimension 1 and the bifurcation is likely to happen. As for the structure of this eigenvalue, it is strictly increasing with respect to b_2 , and by working more, we prove that the curve \mathcal{C}_1^+ of $b_2 \in]0, b_1[\mapsto \lambda_1^+$ intersects \mathcal{C}_n if and only if $n \geq b_1^{-2}$. We can now make precise statements of these results, and for the complete ones, we refer the reader to Lemma 18 and Propositions 19 and 20.

Proposition 15. *Let $b_1 \in]0, 1[$; then the following hold true:*

- (i) *The sequence $n \geq 2 \mapsto b_n^*$ is strictly increasing.*
- (ii) *Let $2 \leq n < m$ and $b_2 \in [0, b_n^*]$; then*

$$\lambda_m^- < \lambda_n^- < \lambda_n^+ < \lambda_m^+.$$

- (iii) *The curve \mathcal{C}_1^+ intersects \mathcal{C}_n if and only if $n \geq 1/b_1^2$. In this case, we have a single point $(x_n, \lambda_1^+(x_n))$, with $x_n \in]0, b_n^*]$ being the only solution b_2 of the equation*

$$P_n(1 + b_2^2 - b_1^2) = 0,$$

where P_n is defined in (51).

The properties mentioned in the preceding proposition can be illustrated by Figure 1. Further illustrations will be given in Figure 7.

For the proof of Proposition 15, it appears to be more convenient to work with a continuous variable instead of the discrete one n . This is advantageous especially in the study of the variations of the eigenvalues with respect to n and the radius b_2 for b_1 fixed. To do so, we extend in a natural way $(\Delta_n)_{n \geq 1}$ to a smooth function defined on $[1, +\infty[$ as

$$\Delta_x = \left(\frac{1 - (b_2/b_1)^2}{2} - \frac{2 - b_2^{2x} - b_1^{2x}}{2x} \right)^2 - \left(\frac{b_2}{b_1} \right)^{2x} \left(\frac{1 - b_1^{2x}}{x} \right)^2, \quad x \in [1, +\infty[.$$

It is easy to see that Δ_x is positive if and only if

$$\left(1 - \left(\frac{b_2}{b_1} \right)^2 \right)^x - (2 - b_2^{2x} - b_1^{2x}) - 2 \left(\frac{b_2}{b_1} \right)^x (1 - b_1^{2x}) \geq 0 \tag{54}$$

or

$$E_x \triangleq \left(1 - \left(\frac{b_2}{b_1} \right)^2 \right)^x - (2 - b_2^{2x} - b_1^{2x}) + 2 \left(\frac{b_2}{b_1} \right)^x (1 - b_1^{2x}) < 0.$$

We shall prove that the last possibility $E_x < 0$ is excluded for $x \geq 2$. Indeed,

$$\begin{aligned} E_x &= (1 - (b_2/b_1)^2)^x - 2(1 - (b_2/b_1)^x) + (b_2^x - b_1^x)^2 \\ &= 2(1 - (b_2/b_1)^2) \left[\frac{x}{2} - \frac{1 - ((b_2/b_1)^2)^{x/2}}{1 - (b_2/b_1)^2} \right] + (b_2^x - b_1^x)^2 \\ &\geq (b_2^x - b_1^x)^2 > 0, \end{aligned}$$

where we have used the classical inequality,

$$\text{for all } b \in (0, 1) \text{ and } x \geq 1, \quad \frac{1 - b^x}{1 - b} \leq x.$$

Thus, for $x \geq 2$, the condition $\Delta_x \geq 0$ is equivalent to the first one of (54) or, in other words,

$$x \geq \frac{2 + 2(b_2/b_1)^x - (b_1^x + b_2^x)^2}{1 - (b_2/b_1)^2} \triangleq g_x(b_1, b_2). \tag{55}$$

In this case, the roots of the polynomial P_n can also be continuously extended as

$$\begin{aligned} \lambda_x^+ &= \frac{1 + (b_2/b_1)^2}{2} - \left(\frac{b_1^{2x} - b_2^{2x}}{2x} \right) + \sqrt{\Delta_x}, \\ \lambda_x^- &= \frac{1 + (b_2/b_1)^2}{2} - \left(\frac{b_1^{2x} - b_2^{2x}}{2x} \right) - \sqrt{\Delta_x}. \end{aligned}$$

4.4.1. Monotonicity for $n \geq 2$. To settle the proof of the second point (ii) of Proposition 15, we should look for the variations of the eigenvalues with respect to x but with fixed radii b_1 and b_2 . For this purpose, we need to first understand the topological structure of the domain of definition of $x \mapsto \lambda_x^\pm$

$$\mathcal{I}_{b_1, b_2} \triangleq \{x \geq 2 : \Delta_x > 0\}$$

and see in particular whether this set is connected. We shall establish the following:

Lemma 16. *Let $0 < b_2 < b_1 < 1$ be two fixed numbers; then the following hold true:*

- (i) *The set \mathcal{F}_{b_1, b_2} is connected and of the form $] \mu_{b_1, b_2}, \infty[$.*
- (ii) *The map $x \in \mathcal{F}_{b_1, b_2} \mapsto \Delta_x$ is strictly increasing.*

Remark 17. If the discriminant Δ_x admits a zero, then it is unique and coincides with the value μ_{b_1, b_2} . Otherwise, μ_{b_1, b_2} will be equal to 2.

Proof. To get this result, it suffices to check the following: for any $a \in \mathcal{F}_{b_1, b_2}$,

$$[a, +\infty[\subset \mathcal{F}_{b_1, b_2}.$$

By the continuity of the discriminant, there exists $\eta > a$ such that $[a, \eta[\subset \mathcal{F}_{b_1, b_2}$, and let $[a, \eta^*[$ be the maximal interval contained in \mathcal{F}_{b_1, b_2} . If η^* is finite, then necessarily $\Delta_{\eta^*} = 0$. If we could show that the discriminant is strictly increasing in this interval, then this will contradict the preceding assumption. To see this, observe that Δ_x can be rewritten in the form

$$\Delta_x = \frac{1}{4} \left(f_1 \left(\frac{b_2}{b_1} \right) - f_x(b_1) - f_x(b_2) \right)^2 - \left(\frac{b_2}{b_1} \right)^{2x} f_x^2(b_1) \tag{56}$$

with the notation

$$f_x(t) \triangleq \frac{1 - t^{2x}}{x}.$$

Differentiating Δ_x with respect to x ,

$$\begin{aligned} \partial_x \Delta_x = & -\frac{1}{2} (\partial_x f_x(b_1) + \partial_x f_x(b_2)) \left(f_1 \left(\frac{b_2}{b_1} \right) - f_x(b_1) - f_x(b_2) \right) \\ & - 2 f_x(b_1) \left(\frac{b_2}{b_1} \right)^{2x} \left(f_x(b_1) \log \left(\frac{b_2}{b_1} \right) + \partial_x f_x(b_1) \right). \end{aligned} \tag{57}$$

We shall prove that, for all $t \in]0, 1[$, the mapping $x \in [2, \infty[\mapsto f_x(t)$ is strictly decreasing. It is clear that

$$\partial_x f_x(t) = \frac{t^{2x} (1 - 2x \log t) - 1}{x^2} \triangleq \frac{g_x(t)}{x^2}. \tag{58}$$

To study the variation of $t \mapsto g_x(t)$, note that

$$g'_x(t) = -4x^2 t^{2x-1} \log t > 0 \quad \text{for all } t \in]0, 1[$$

and therefore g_x is strictly increasing, which implies that

$$\partial_x f_x(t) < \frac{g_x(1)}{x^2} = 0.$$

Using this fact, we deduce that the last term of (57) is positive and consequently

$$\partial_x \Delta_x \geq -\frac{1}{2} (\partial_x f_x(b_1) + \partial_x f_x(b_2)) \left(f_1 \left(\frac{b_2}{b_1} \right) - f_x(b_1) - f_x(b_2) \right).$$

Hence, to get $\partial_x \Delta_x > 0$ it suffices to establish that

$$f_1 \left(\frac{b_2}{b_1} \right) - f_x(b_1) - f_x(b_2) > 0, \tag{59}$$

which is equivalent to

$$x > \frac{2 - b_1^{2x} - b_2^{2x}}{1 - b^2}, \quad b = \frac{b_2}{b_1}.$$

Note that we have already seen that the positivity of Δ_x for $x \geq 2$ is equivalent to the condition (55) which actually implies the preceding one owing to the strict inequality

$$b^x - (b_1 b_2)^x > 0.$$

This shows that (59) is true and consequently,

$$\text{for all } x \in [a, \eta^*[, \quad \partial_x \Delta_x > 0.$$

This shows that the discriminant, which is positive, is strictly increasing in $[a, \eta^*[,$ and this excludes the fact that Δ_{η^*} vanishes. Therefore, $\eta^* = \infty$, and thus, (i) and (ii) are simultaneously proved. \square

The next goal is to establish the monotonicity of the eigenvalues.

Lemma 18. *Let $0 < b_2 < b_1 < 1$. Then:*

- (i) *The mapping $x \in \mathcal{F}_{b_1, b_2} \mapsto \lambda_x^+$ is strictly increasing.*
- (ii) *The mapping $x \in \mathcal{F}_{b_1, b_2} \mapsto \lambda_x^-$ is strictly decreasing.*
- (iii) *For any $x < y \in \mathcal{F}_{b_1, b_2}$,*

$$\lambda_y^- < \lambda_x^- < \lambda_x^+ < \lambda_y^+.$$

Proof. (i) Note that

$$\lambda_x^+ = \frac{1 + b^2}{2} - \frac{b_1^{2x}}{2} f_x(b) + \sqrt{\Delta_x}, \quad b = \frac{b_2}{b_1}.$$

We have already seen in the proof of Lemma 16 that for any $t \in]0, 1[$ the mapping $x \in [2, \infty[\mapsto f_x(t)$ is strictly decreasing, and therefore, $x \mapsto b_1^{2x} f_x(b_2/b_1)$ is also strictly decreasing. To get the strict increasing of $x \mapsto \lambda_x^+$, it suffices to combine this last fact with the increasing property of $x \mapsto \Delta_x$.

(ii) It is clear that

$$\lambda_x^- = \frac{1 + b^2}{2} + \frac{f_x(b_1) - f_x(b_2)}{2} - \sqrt{\Delta_x}.$$

The derivative of λ_x^- with respect to x is given by

$$\partial_x \lambda_x^- = \frac{1}{2} \partial_x f_x(b_1) - \frac{1}{2} \partial_x f_x(b_2) - \frac{\partial_x \Delta_x}{2\sqrt{\Delta_x}}.$$

By virtue of (57), we can split the preceding function into three parts:

$$\partial_x \lambda_x^- = \text{I} + \text{II} + \text{III},$$

where

$$\begin{aligned} \text{I} &\triangleq \frac{1}{2} \partial_x f_x(b_1) \left(1 + \frac{f_1(b) - f_x(b_1) - f_x(b_2)}{2\sqrt{\Delta_x}} \right), \\ \text{II} &\triangleq \frac{1}{2} \partial_x f_x(b_2) \left(-1 + \frac{f_1(b) - f_x(b_1) - f_x(b_2)}{2\sqrt{\Delta_x}} \right), \\ \text{III} &\triangleq \frac{b^{2x} f_x(b_1) (f_x(b_1) \log(b) + \partial_x f_x(b_1))}{\sqrt{\Delta_x}}. \end{aligned}$$

Keeping in mind the inequality (59) and $\partial_x f_x(t) < 0$ for any $t \in]0, 1[$, we can see that I is negative. To prove that the term II is also negative, it suffices to check that

$$\frac{f_1(b) - f_x(b_1) - f_x(b_2)}{2\sqrt{\Delta_x}} > 1.$$

From (59), we can deduce by squaring that the last expression is actually equivalent to

$$\frac{1}{4} \left(f_1\left(\frac{b_2}{b_1}\right) - f_x(b_1) - f_x(b_2) \right)^2 > \Delta_x.$$

From (56), we immediately conclude that the last inequality is always verified.

In regard to the negativity of the third term III, we just use the fact that $0 < b < 1$ and the decreasing of the function $x \mapsto f_x(t)$.

(iii) This follows easily from (i), (ii) and the obvious fact,

$$\text{for all } x \in \mathcal{J}_{b_1, b_2}, \quad \lambda_x^- < \lambda_x^+. \quad \square$$

4.4.2. Lifespan of the eigenvalues with respect to b_2 . We shall study in this section some properties of the eigenvalue functions $b_2 \mapsto \lambda_n^\pm$ for $n \geq 2$ and b_1 fixed. This will be crucial for studying the dynamics of the first eigenvalue λ_1^+ and especially in counting the intersections between the curves \mathcal{C}_1^+ and \mathcal{C}_n which has been the subject of the part (iii) of Proposition 15. Note that in this paragraph we shall give up using the continuous version λ_x^\pm of the roots λ_n^\pm as it has been done in the preceding section. The results that we shall state can actually be proved with the continuous parameter; however, this does not matter a lot for our final purpose. We define the following set: for $n \geq 2$ and $b_1 \in]0, 1[$,

$$\mathcal{J}_{n, b_1} \triangleq \left\{ b_2 \in [0, b_1[: n \geq \frac{2 + 2(b_2/b_1)^n - (b_1^n + b_2^n)^2}{1 - (b_2/b_1)^2} \right\}.$$

We shall prove the following:

Proposition 19. *Let $b_1 \in]0, 1[$ fixed and $n \geq 2$; then the following hold true:*

- (i) *The set \mathcal{J}_{n, b_1} is an interval of the form $[0, b_n^*]$, with $b_n^* \in]0, b_1[$.*
- (ii) *The eigenvalues $b_2 \mapsto \lambda_n^\pm$ are defined together in $[0, b_n^*]$.*
- (iii) *The sequence $n \mapsto b_n^*$ is strictly increasing, and we have the asymptotics*

$$b_n^* = b_1(1 - \alpha/n) + o(1/n), \quad e^{-\alpha} + 1 = \alpha, \quad \alpha \approx 1.27846.$$

(iv) The function $b_2 \in [0, b_n^*] \mapsto \lambda_n^-(b_2) - b_2^2$ is strictly increasing.

(v) The function $b_2 \in [0, b_n^*] \mapsto \lambda_n^+(b_2) - b_2^2$ is strictly decreasing.

Proof. (i) This follows from studying the function $h : [0, b_1] \rightarrow \mathbb{R}$, defined by

$$h(x) = n(1 - (x/b_1)^2) - 2 - 2(x/b_1)^n + (b_1^n + x^n)^2.$$

We claim that h is strictly decreasing. Indeed, by differentiating,

$$\begin{aligned} h'(x) &= \frac{2nx}{b_1^2}(-1 + b_1^2x^{2n-2}) + \frac{2nx^{n-1}}{b_1^n}(-1 + b_1^{2n}) \\ &< 0. \end{aligned}$$

As $h(0) = n - 2 + b_1^{2n} > 0$ and $h(b_1) = 4(-1 + b_1^{2n}) < 0$, we deduce from the intermediate value theorem that the set \mathcal{J}_{n,b_1} is in fact an interval of the form $[0, b_n^*]$. The number $b_n^* \in [0, b_1[$ is defined by the unique solution of the equation

$$h(b_n^*) = 0. \tag{60}$$

(ii) Observe that the domain of definition of the eigenvalues λ_n^\pm coincides with the domain of the discriminant Δ_n , which is in turn given by \mathcal{J}_{n,b_1} according to (55). Therefore, (60) implies the vanishing of Δ_n at the point b_n^* , and consequently both eigenvalues coincide.

(iii) Recall from (53) the definitions of the curves \mathcal{C}_n^\pm and $\mathcal{C}_n = \mathcal{C}_n^- \cup \mathcal{C}_n^+$. Since the eigenvalues $\lambda_n^+(b_n^*)$ and $\lambda_n^-(b_n^*)$ coincide, curves \mathcal{C}_n^+ and \mathcal{C}_n^- end at the same point which is a turning point for \mathcal{C}_n . Furthermore, we can see that \mathcal{C}_n lies on the left side of the vertical axis $x = b_n^*$. Now let $m > n \geq 2$, and we intend to check by some elementary geometric considerations that $b_m^* > b_n^*$. From the monotonicity of the eigenvalues $n \mapsto \lambda_n^\pm$,

$$\lambda_m^-(0) < \lambda_n^-(0), \quad \lambda_m^+(0) > \lambda_n^+(0).$$

If $b_m^* \leq b_n^*$, then the curve \mathcal{C}_m will intersect \mathcal{C}_n at some point and this contradicts the strict monotonicity of the eigenvalues with respect to n . Thus, we deduce that $n \mapsto b_n^*$ is strictly increasing and therefore should converge to some value $b^* \leq b_1$. Assume that $b^* < b_1$; then from (60) and the continuity of h , we find by letting $n \rightarrow +\infty$ that

$$\lim_{n \rightarrow +\infty} h(b_n^*) = 0.$$

On the other hand,

$$\begin{aligned} \lim_{n \rightarrow +\infty} h(b_n^*) &= \lim_{n \rightarrow +\infty} n(1 - (b_n^*/b_1)^2) - 2 \\ &= +\infty, \end{aligned}$$

which is clearly a contradiction, and thus, $b^* = b_1$. For the asymptotic behavior of b_n^* , which is a marginal part here, we shall settle for a formal reasoning by taking a first-order Taylor expansion of $1/n$. We shall look for α such that

$$b_n^* = b_1(1 - \alpha/n) + o(1/n).$$

At the first order of h ,

$$h(b_n^*) = \alpha(2 - \alpha/n) - 2 - 2(1 - \alpha/n)^n + o(1).$$

By taking the limit as $n \rightarrow \infty$, we find that α must satisfy

$$e^{-\alpha} + 1 = \alpha.$$

This equation admits a unique solution lying in the interval $]1, 2[$ and can be given explicitly by the Lambert W function:

$$\alpha = W(e^{-1}) + 1 \approx 1.27846.$$

(iv) Set $x = (b_2/b_1)^2$ and define the functions

$$f_{\pm}(x) = \lambda_n^{\pm}(b_2) = \frac{1+x}{2} + \frac{b_1^{2n}}{2n}(x^n - 1) \pm \sqrt{\Delta_n(x)}, \quad x \in \left[0, \frac{b_n^{*2}}{b_1^2}\right],$$

with

$$\Delta_n(x) = \left(\frac{1-x}{2} - \frac{2-b_1^{2n}(1+x^n)}{2n}\right)^2 - x^n \left(\frac{1-b_1^{2n}}{n}\right)^2.$$

Differentiating with respect to x yields

$$\Delta'_n(x) = -\left(\frac{1-x}{2} - \frac{2-b_1^{2n}(1+x^n)}{2n}\right)(1-b_1^{2n}x^{n-1}) - nx^{n-1}\left(\frac{1-b_1^{2n}}{n}\right)^2.$$

Note from the assumption (55), by switching the parameters n and x , that

$$\frac{1-x}{2} - \frac{2-b_1^{2n}(1+x^n)}{2n} > 0,$$

and therefore,

$$\Delta'_n(x) < 0 \quad \text{for all } x \in \left[0, \frac{b_n^{*2}}{b_1^2}\right] \subset [0, 1[.$$

Coming back to the function f_{\pm} and taking the derivative, we find

$$f'_{\pm}(x) = \frac{1}{2} + \frac{b_1^{2n}}{2}x^{n-1} \pm \frac{\Delta'_n(x)}{2\sqrt{\Delta_n(x)}}.$$

Using the definition of Δ_n and (54), one has

$$\left(\frac{1-x}{2} - \frac{2-b_1^{2n}(1+x^n)}{2n}\right) > \sqrt{\Delta_n(x)}$$

and consequently

$$\begin{aligned} \frac{\Delta'_n(x)}{\sqrt{\Delta_n(x)}} &\leq -\frac{(1-x)/2 - (2-b_1^{2n}(1+x^n))/2n}{\sqrt{\Delta_n(x)}}(1-b_1^{2n}x^{n-1}) \\ &< -(1-b_1^{2n}x^{n-1}). \end{aligned}$$

Therefore, we obtain that for all $x \in [0, b_n^{*2}/b_1^2]$

$$\begin{aligned} f'_-(x) &> 1, \\ f'_+(x) &\leq b_1^{2n} x^{n-1} < b_1^2. \end{aligned}$$

This shows that the function $g_- : x \mapsto f_-(x) - b_1^2 x$ is strictly increasing; however, $g_+ : x \mapsto f_+(x) - b_1^2 x$ is strictly decreasing. This finishes the proof of the desired result. \square

4.4.3. Dynamics of the first eigenvalue. We shall in this paragraph discuss the behavior of the first eigenvalues corresponding to $n = 1$. Note from (51) that these eigenvalues are in fact the solutions of the polynomial

$$P_1(\lambda) = \lambda^2 - (1 + b_2^2 - b_1^2 + (b_2/b_1)^2)\lambda + (b_2/b_1)^2 + b_2^2(b_2/b_1)^2 - b_2^2,$$

which vanishes exactly at the points

$$\lambda_1^- = (b_2/b_1)^2 \quad \text{or} \quad \lambda_1^+ = 1 + b_2^2 - b_1^2.$$

Recall from the preceding sections the definition

$$\mathcal{C}_n^\pm \triangleq \{(b_2, \lambda_n^\pm(b_2)) : b_2 \in [0, b_n^*]\}, \quad \mathcal{C}_n = \mathcal{C}_n^- \cup \mathcal{C}_n^+,$$

and the graph of the first eigenvalue λ_1^+ is given by

$$\mathcal{C}_1^+ \triangleq \{(b_2, 1 + b_2^2 - b_1^2) : b_2 \in [0, b_1]\}.$$

As we have already mentioned, it is not clear whether the bifurcation occurs with λ_1^- because the range of the linearized operator has an infinite codimension. The main result reads as follows.

Proposition 20. *Let $b_1 \in]0, 1[$ and $n \geq 2$. Then the following hold true:*

- (i) *For any $0 < b_2 < b_1$, we have $\lambda_1^- < \lambda_n^\pm$.*
- (ii) *If $n < b_1^{-2}$, then*

$$\mathcal{C}_n \cap \mathcal{C}_1^+ = \emptyset.$$

- (iii) *If $n \geq b_1^{-2}$, then $\mathcal{C}_n \cap \mathcal{C}_1^+$ is a single point, that is, there exists $x_n \in [0, b_n^*]$ such that*

$$\mathcal{C}_n \cap \mathcal{C}_1^+ = \{(x_n, \lambda_1^+(x_n))\}.$$

- (iv) *If $b_2 \notin \{x_m : m \geq b_1^{-2}\}$, then for all $n \geq 2$, $\lambda_1^+ \neq \lambda_n^\pm$.*

- (v) *The sequence $\{x_m\}_{m \geq b_1^{-2}}$ is increasing and converges to b_1 .*

Proof. (i) This follows easily from the monotonicity of the eigenvalue $n \mapsto \lambda_n^-$ and the fact that $\lambda_n^- \leq \lambda_n^+$. Indeed, for all $n \geq 2$,

$$\lambda_1^- = (b_2/b_1)^2 = \lim_{n \rightarrow +\infty} \lambda_n^- < \lambda_n^- \leq \lambda_n^+.$$

(ii) In view of (v) from Proposition 19, the mapping $b_2 \in [0, b_n^*] \mapsto \lambda_n^+(b_2) - \lambda_1^+(b_2)$ is strictly decreasing, and therefore, for $b_2 \in]0, b_n^*]$,

$$\lambda_n^+(b_2) - \lambda_1^+(b_2) < \lambda_n^+(0) - \lambda_1^+(0) = b_1^2 - \frac{1}{n}.$$

Therefore, for $n < b_1^{-2}$, the last term in the right-hand side is negative and consequently

$$\lambda_n^-(b_2) \leq \lambda_n^+(b_2) < \lambda_1^+(b_2) \quad \text{for all } b_2 \in]0, b_n^*].$$

(iii) When $n \geq b_1^{-2}$, then $\lambda_n^+(0) - \lambda_1^+(0) \geq 0$, and since $b_2 \in [0, b_n^*] \mapsto \lambda_n^+(b_2) - \lambda_1^+(b_2)$ is strictly decreasing, the equation $\lambda_n^+(b_2) - \lambda_1^+(b_2) = 0$ has at most one solution in $[0, b_n^*]$. We shall distinguish three cases. The first one is when $\lambda_n^+(b_n^*) - \lambda_1^+(b_n^*) < 0$, in which case the foregoing equation admits a unique solution denoted by x_n . This implies that $\mathcal{C}_n^+ \cap \mathcal{C}_1^+$ is a single point whose abscissa is x_n , and the next step is to check that $\mathcal{C}_n^- \cap \mathcal{C}_1^+$ is empty. Thus,

$$\lambda_n^+(b_n^*) - \lambda_1^+(b_n^*) \leq \lambda_n^+(x_n) - \lambda_1^+(x_n) = 0.$$

Combining the last inequality with the fact that $\lambda_n^+(b_n^*) = \lambda_n^-(b_n^*)$ and the monotonicity of the mapping $b_2 \in [0, b_n^*] \mapsto \lambda_n^-(b_2) - \lambda_1^+(b_2)$, which follows from (iv) of Proposition 19, we conclude that for all $b_2 \in]0, b_n^*]$

$$\begin{aligned} \lambda_n^-(b_2) - \lambda_1^+(b_2) &\leq \lambda_n^-(b_n^*) - \lambda_1^+(b_n^*) \\ &\leq \lambda_n^+(b_n^*) - \lambda_1^+(b_n^*) \\ &< 0. \end{aligned}$$

Therefore, $\mathcal{C}_n^- \cap \mathcal{C}_1^+ = \emptyset$ and the set $\mathcal{C}_n \cap \mathcal{C}_1^+$ reduces to a single point. The second case is when $\lambda_n^+(b_n^*) - \lambda_1^+(b_n^*) > 0$; then $\mathcal{C}_n^+ \cap \mathcal{C}_1^+$ is empty, and we shall prove that $\mathcal{C}_n^- \cap \mathcal{C}_1^+$ is a single point. Observe first that

$$\lambda_n^-(b_n^*) - \lambda_1^+(b_n^*) = \lambda_n^+(b_n^*) - \lambda_1^+(b_n^*) > 0.$$

Moreover,

$$\lambda_n^-(0) - \lambda_1^+(0) = \frac{1 - b_1^{2n}}{n} - (1 - b_1^2) < 0 \quad \text{for all } n \geq 2.$$

Since $b_2 \mapsto \lambda_n^-(b_2) - \lambda_1^+(b_2)$ is strictly increasing, by the intermediate value theorem, there exists only one solution $x_n \in]0, b_n^*[$ of the equation $\lambda_n^-(b_2) - \lambda_1^+(b_2) = 0$. The third and last case to analyze is when $\lambda_n^+(b_n^*) - \lambda_1^+(b_n^*) = 0$. This means that all the curves \mathcal{C}_n^+ , \mathcal{C}_n^- and \mathcal{C}_1^+ meet each other at the single point of abscissa b_n^* .

(iv) It follows immediately from (ii) and (iii).

(v) Let $n \geq b_1^{-1}$, and define the set enclosed by \mathcal{C}_n and located at the first quadrant of the plane:

$$\widehat{\mathcal{C}}_n \triangleq \{(x, y) \in \mathbb{R}^2 : x \in [0, b_n^*], \lambda_n^-(x) \leq y \leq \lambda_n^+(x)\}.$$

From the monotonicity of the eigenvalues $n \mapsto \lambda_n^\pm$ seen in Lemma 18, we note that,

$$\text{for all } (x, y) \in \widehat{\mathcal{C}}_n, \quad \lambda_{n+1}^-(x) < \lambda_n^-(x) \leq y \leq \lambda_n^+(x) < \lambda_{n+1}^+(x).$$

Hence,

$$\widehat{\mathcal{C}}_n \Subset \widehat{\mathcal{C}}_{n+1}, \quad \mathcal{C}_{n+1} \cap \widehat{\mathcal{C}}_n = \emptyset. \tag{61}$$

Now, from (iii) and the monotonicity of the mappings $b_2 \mapsto \lambda_n^\pm(b_2) - \lambda_1^\pm(b_2)$ stated in Proposition 19, we deduce that,

$$\text{for all } x \in [0, x_n[, \quad \lambda_n^-(x) < \lambda_1^+(x) < \lambda_n^+(x).$$

Then we have the inclusion

$$\mathcal{C}_{1,n}^+ \triangleq \{(x, \lambda_1^+(x)) : x \in [0, x_n]\} \subset \widehat{\mathcal{C}}_n.$$

It follows from (61) that $\mathcal{C}_{n+1} \cap \mathcal{C}_{1,n}^+ = \emptyset$ and consequently the abscissa of the single point intersection $\mathcal{C}_{n+1} \cap \mathcal{C}_1^+$ must satisfy $x_{n+1} > x_n$. This proves that $\{x_n\}_{n \geq b_1^{-2}}$ is strictly increasing, and thereby this sequence converges to some value $x_\star \leq b_1$. Assume that $x_\star < b_1$, and define the subsequences

$$\{x_n^\pm\}_{n \geq b_1^{-2}} \triangleq \{x_n : \lambda_n^\pm(x_n) = \lambda_1^\pm(x_n)\}.$$

Clearly one of the two sequences is infinite. Assume first that $\{x_n^+\}$ is infinite and up to an extraction this sequence converges also to x_\star , and for simplicity, we still denote this sequence by $\{x_n\}_{n \geq b_1^{-2}}$. Then from the definition of λ_n^+ , we can easily check that

$$\begin{aligned} \lim_{n \rightarrow +\infty} \lambda_n^+(x_n) &= \frac{1 + (x_\star/b_1)^2}{2} + \frac{1 - (x_\star/b_1)^2}{2} \\ &= 1. \end{aligned}$$

On the other hand,

$$\lim_{n \rightarrow +\infty} \lambda_1^+(x_n) = 1 + x_\star^2 - b_1^2.$$

This is possible only if $x_\star = b_1$, which is a contradiction, and thus, $x_\star = b_1$. Now in the case where only the sequence $\{x_n^-\}$ is infinite, then we follow the same reasoning as before. We suppose that $x_\star < b_1$, and one can verify that

$$\begin{aligned} \lim_{n \rightarrow +\infty} \lambda_n^-(x_n) &= (x_\star/b_1)^2, \\ \lim_{n \rightarrow +\infty} \lambda_1^+(x_n) &= 1 + x_\star^2 - b_1^2. \end{aligned}$$

By equating these numbers, we obtain

$$(1 - b_1^2)(x_\star^2 - b_1^2) = 0,$$

which is impossible since $b_1 < 1$ and consequently $x_\star = b_1$. Hence, the proof of (v) is finished. □

4.5. Bifurcation for $m \geq 1$. Now we shall see how to implement the preceding results to prove Theorems 6 and 9 by using the Crandall–Rabinowitz theorem. The proofs will be broken into several steps. First, we introduce the spaces of bifurcation which capture the m -fold symmetry, and they are of Hölderian type. Second, we rewrite Proposition 13 dealing with the regularity of the nonlinear functional defining the V -states in the new setting. We end this section with the proofs of the properties of the linearized operator around the annulus required by the Crandall–Rabinowitz theorem.

4.5.1. Function spaces. We shall make use of the same spaces as [de la Hoz et al. 2016b]. For $m \geq 1$, we introduce the spaces X_m and Y_m as follows:

$$X_m = C_m^{1+\alpha}(\mathbb{T}) \times C_m^{1+\alpha}(\mathbb{T}),$$

where $C_m^{1+\alpha}(\mathbb{T})$ is the space of the 2π -periodic functions $f \in C^{1+\alpha}(\mathbb{T})$ whose Fourier series is given by

$$f(w) = \sum_{n=1}^{\infty} a_n \bar{w}^{nm-1}, \quad w \in \mathbb{T}, \quad a_n \in \mathbb{R}.$$

This space is equipped with the usual strong topology of $C^{1+\alpha}(\mathbb{T})$. We can easily see that X_m is identified as

$$X_m = \left\{ f \in (C^{1+\alpha}(\mathbb{T}))^2 : f(w) = \sum_{n=1}^{\infty} A_n \bar{w}^{nm-1}, \quad A_n \in \mathbb{R}^2 \right\}. \tag{62}$$

We define the ball of radius $r \in (0, 1)$ by

$$B_r^m = \{ f \in (C_m^{1+\alpha}(\mathbb{T}))^2 : \|f\|_{C^{1+\alpha}(\mathbb{T})} < r \}.$$

Take $(f_1, f_2) \in B_r^m$; then the expansions of the associated conformal mappings ϕ_1 and ϕ_2 in the exterior unit disc $\{w \in \mathbb{C} : |w| > 1\}$ are given by

$$\begin{aligned} \phi_1(w) &= b_1 w + f_1(w) = w \left(b_1 + \sum_{n=1}^{\infty} \frac{a_{1,n}}{w^{nm}} \right), \\ \phi_2(w) &= b_2 w + f_2(w) = w \left(b_2 + \sum_{n=1}^{\infty} \frac{a_{2,n}}{w^{nm}} \right). \end{aligned}$$

This captures the m -fold symmetry of the associated boundaries $\phi_1(\mathbb{T})$ and $\phi_2(\mathbb{T})$ via the relation

$$\phi_j(e^{2i\pi/m} w) = e^{2i\pi/m} \phi_j(w), \quad j = 1, 2, \quad w \in \mathbb{T}. \tag{63}$$

Set

$$Y_m = \left\{ g \in (C^\alpha(\mathbb{T}))^2 : g = \sum_{n \geq 1} C_n e_{nm}, \quad C_n \in \mathbb{R}^2 \right\}. \tag{64}$$

With the help of Proposition 13, we deduce that the functional $G = (G_1, G_2)$ is well defined and smooth from $\mathbb{R} \times B_r^m$ to Y_m with r small enough. The only thing that one should care about, which has already been discussed in the simply connected case, is the persistence of the symmetry which comes from the

rotational invariance of the functional G . As the proofs are very close to the simply connected case without any substantial difficulties, we prefer to skip them and only state the desired results.

Proposition 21. *Let $b \in]0, 1[$ and $0 < r < \min(b, 1 - b)$; then the following hold true:*

- (i) $G : \mathbb{R} \times B_r^m \rightarrow Y_m$ is C^1 (it is in fact C^∞).
- (ii) The partial derivative $\partial_\lambda DG : \mathbb{R} \times B_r^m \rightarrow \mathcal{L}(X_m, Y_m)$ exists and is continuous (it is in fact C^∞).

Now using (49) and (50), we deduce that the restriction of $DG(\lambda, 0)$ to the space X_m leads to a well defined continuous operator $DG(\lambda, 0) : X_m \rightarrow Y_m$. It takes the form

$$DG(\lambda, 0)(h_1, h_2) = \sum_{n \geq 1} M_{nm}(\lambda) \begin{pmatrix} a_{1,n} \\ a_{2,n} \end{pmatrix} e_{nm}, \tag{65}$$

with $(h_1, h_2) \in X_m$ having the expansion

$$h_j(w) = \sum_{n \geq 1} a_{j,n} \bar{w}^{nm-1}$$

and the matrix M_n given for $n \geq 1$ by

$$M_n(\lambda) \triangleq \begin{pmatrix} b_1[n\lambda - 1 + b_1^{2n} - n(b_2/b_1)^2] & b_2[(b_2/b_1)^n - (b_1b_2)^n] \\ -b_1[(b_2/b_1)^n - (b_1b_2)^n] & b_2[n\lambda - n + 1 - b_2^{2n}] \end{pmatrix}. \tag{66}$$

4.5.2. Proof of Theorem 6. The main goal of this paragraph is to prove Theorem 6. This will be an immediate consequence of the Crandall–Rabinowitz theorem as soon as we check its conditions, which require a careful study. Concerning the regularity assumptions, they were discussed in Proposition 21. As to the properties required for the linearized operator, they are the object of following proposition.

Proposition 22. *Let $0 < b_2 < b_1 < 1$, and set $b \triangleq b_2/b_1$. Let $m \geq 2$ satisfy*

$$m \geq \frac{2 + 2b^m - (b_1^m + b_2^m)^2}{1 - b^2}.$$

Then the following results hold true:

- (i) *The kernel of $DG(\lambda_m^\pm, 0)$ is one-dimensional and generated by the vector*

$$v_m(w) = \begin{pmatrix} b_2[m\lambda_m^\pm - m + 1 - b_2^{2m}] \\ b_1[b^m - (b_1b_2)^m] \end{pmatrix} \bar{w}^{m-1}.$$

- (ii) *The range of $DG(\lambda_m^\pm, 0)$ is closed and of codimension 1.*
- (iii) *The transversality assumption holds: the condition*

$$\partial_\lambda DG(\lambda_m^\pm, 0)v_m \notin R(DG(\lambda_m^\pm, 0))$$

is satisfied if and only if

$$m > \frac{2 + 2b^m - (b_1^m + b_2^m)^2}{1 - b^2}.$$

Proof. (i) According to (55), the positivity of the discriminant Δ_n that guarantees the existence of real eigenvalues is equivalent for $m \geq 2$ to

$$m \geq \frac{2 + 2b^m - (b_1^m + b_2^m)^2}{1 - b^2}.$$

To prove that the kernel of $DG(\lambda_m^\pm, 0)$ is one-dimensional, it suffices to check that for $n \geq 2$ the matrix $M_{nm}(\lambda_m^\pm)$ defined in (66) is invertible. This follows from Lemma 18, which asserts that $\lambda_{nm}^\pm \neq \lambda_m^\pm$ for $n \geq 2$ and therefore

$$\det M_{nm}(\lambda_m^\pm) \neq 0.$$

To get a generator for the kernel, it suffices to take a vector orthogonal to the second row of $M_m(\lambda_m^\pm)$.

(ii) We are going to show that for any $m \geq 2$ the range $R(DG(\lambda_m^\pm, 0))$ coincides with the subspace

$$\mathcal{X}_m \triangleq \left\{ g \in Y_m : g(w) = \sum_{n \geq 1} C_n e_{nm}, \quad C_1 \in R(M_m), \quad C_n \in \mathbb{R}^2 \text{ for all } n \geq 2 \right\}. \tag{67}$$

Assume for now this result; then it is easy to check that $R(DG(\lambda_m^\pm, 0))$ is closed in Y_m and is of codimension 1. Now to get the description of the range, we first observe that from (65) and (66) the range is included in the space \mathcal{X}_m . Therefore, what is left is to check is the inclusion $\mathcal{X}_m \subset R(DG(\lambda_m^\pm, 0))$. Take $g = (g_1, g_2) \in \mathcal{X}_m$ with the form

$$g_j(w) = \sum_{n \geq 1} c_{j,n} e_{nm},$$

and let us prove that the equation

$$DG(\lambda_m^\pm, 0)h = g$$

admits a solution $h = (h_1, h_2)$ in the space X_m . Note that h_j has the structure

$$h_j(w) = \sum_{n \geq 1} a_{j,n} \bar{w}^{nm-1}.$$

According to (65), the preceding equation is equivalent to

$$M_{mn} \begin{pmatrix} a_{1,n} \\ a_{2,n} \end{pmatrix} = \begin{pmatrix} c_{1,n} \\ c_{2,n} \end{pmatrix} \quad \text{for all } n \geq 1.$$

For $n = 1$, this equation is satisfied because from the definition of \mathcal{X}_m we assume that the vector $C_1 \triangleq \begin{pmatrix} c_{1,1} \\ c_{2,1} \end{pmatrix}$ belongs to the range of the matrix M_m . With regard to $n \geq 2$, we use the fact that M_{nm} is invertible, and therefore, the sequences $(a_{j,n})_{n \geq 2}$ are uniquely determined by

$$\begin{pmatrix} a_{1,n} \\ a_{2,n} \end{pmatrix} = M_{nm}^{-1} \begin{pmatrix} c_{1,n} \\ c_{2,n} \end{pmatrix}, \quad n \geq 2. \tag{68}$$

By computing the matrix $M_{nm}^{-1}(\lambda_m^\pm)$, we deduce that for all $n \geq 2$

$$\begin{aligned} a_{1,n} &= \frac{b_2[nm(\lambda_m^\pm - 1) + 1 - b_2^{2nm}]}{\det(M_{nm}(\lambda_m^\pm))} c_{1,n} - \frac{b_2[(b_2/b_1)^{nm} - (b_1 b_2)^{nm}]}{\det(M_{nm}(\lambda_m^\pm))} c_{2,n}, \\ a_{2,n} &= \frac{b_1[(b_2/b_1)^{nm} - (b_1 b_2)^{nm}]}{\det(M_{nm}(\lambda_m^\pm))} c_{1,n} + \frac{b_1[nm(\lambda_m^\pm - (b_2/b_1)^2) - 1 + b_1^{2nm}]}{\det(M_{nm}(\lambda_m^\pm))} c_{2,n}. \end{aligned} \tag{69}$$

Hence, the proof of $(h_1, h_2) \in X_m$ amounts to showing that

$$w \mapsto \begin{pmatrix} h_1(w) - a_{1,1}\bar{w}^{m-1} \\ h_2(w) - a_{2,1}\bar{w}^{m-1} \end{pmatrix} \in C^{1+\alpha}(\mathbb{T}) \times C^{1+\alpha}(\mathbb{T}).$$

We shall develop the computations only for the first component, and the second one can be done in a similar way. Notice that $\det(M_{nm}(\lambda_m^\pm))$ does not vanish for $n \geq 2$ and behaves for large n like

$$\det(M_{nm}(\lambda_m^\pm)) = b_1 b_2 m^2 (\lambda_m^\pm - 1) [\lambda_m^\pm - (b_2/b_1)^2] n^2 + b_1 b_2 m (1 - (b_2/b_1)^2) n - 1 + o(1).$$

Since $\lambda_m^\pm \notin \{1, (b_2/b_1)^2\}$, by Taylor expansion,

$$a_{1,n} = \frac{1}{b_1 m (\lambda_m^\pm - (b_2/b_1)^2)} \frac{c_{1,n}}{n} + \gamma_{1,n} c_{1,n} + \gamma_{2,n} c_{2,n}$$

with

$$|\gamma_{j,n}| \leq \frac{C}{n^2}.$$

Set $\tilde{h}_1(w) = h_1(w) - a_{1,1}\bar{w}^{m-1}$, and define the functions

$$K_j(w) = \sum_{n \geq 2} n \gamma_{j,n} \bar{w}^{nm}, \quad \tilde{g}_j = \sum_{n \geq 2} \frac{c_{j,n}}{n} e_{nm}.$$

Then one can check that

$$\bar{w} \tilde{h}_1(w) = \frac{1}{mb_1(\lambda_m^\pm - (b_2/b_1)^2)} \sum_{n \geq 2} \frac{c_{1,n}}{n} \bar{w}^{nm} + \{K_1 \star (\Pi \tilde{g}_1)\}(w) + \{K_2 \star (\Pi \tilde{g}_2)\}(w). \tag{70}$$

The convolution is understood to be the usual one: for two continuous functions $f, g : \mathbb{T} \rightarrow \mathbb{C}$, we define,

$$\text{for all } w \in \mathbb{T}, \quad f \star g(w) = \int_{\mathbb{T}} f(\tau) g(\tau \bar{w}) \frac{d\tau}{\tau}.$$

The notation Π is used for the Szegő projection defined by

$$\Pi \left(\sum_{n \in \mathbb{Z}} c_n w^n \right) = \sum_{n \in -\mathbb{N}} c_n w^n,$$

which acts continuously on $C^{1+\alpha}(\mathbb{T})$. One can easily see that the first term in the right-hand side of (70) belongs to $C^{1+\alpha}(\mathbb{T})$. With regard to the last two terms, note that $K_j \in L^2(\mathbb{T}) \subset L^1(\mathbb{T})$ and $\tilde{g}_j \in C^{1+\alpha}(\mathbb{T})$; then using the classical convolution law $L^1(\mathbb{T}) \star C^{1+\alpha}(\mathbb{T}) \rightarrow C^{1+\alpha}(\mathbb{T})$ combined with the continuity of Π , we deduce that those terms belong to $C^{1+\alpha}(\mathbb{T})$ and the function $w \mapsto \bar{w} \tilde{h}_1(w)$ belongs to this space too. This finishes the proof of the range of $DG(\lambda_m^\pm, 0)$.

(iii) Recall from part (i) that the kernel of $DG(\lambda_m^\pm, 0)$ is one-dimensional and generated by the vector v_m defined by

$$w \in \mathbb{T} \mapsto v_m(w) = \begin{pmatrix} b_2[m\lambda_m^\pm - m + 1 - b_2^{2m}] \\ b_1[(b_2/b_1)^m - (b_1b_2)^m] \end{pmatrix} \bar{w}^{m-1}.$$

We shall prove that

$$\partial_\lambda DG(\lambda_m^\pm, 0)v_m \notin R(DG(\lambda_m^\pm, 0))$$

if and only if $\lambda_m^+ \neq \lambda_m^-$, which is equivalent to

$$m > \frac{2 + 2b^m - (b_1^m + b_2^m)^2}{1 - b^2}.$$

Let $(h_1, h_2) \in X_m$ with the expansion

$$h_j(w) = \sum_{n \geq 1} a_{j,n} \bar{w}^{nm-1}.$$

Then differentiating (65) with respect to λ ,

$$\partial_\lambda DG(\lambda, 0)(h_1, h_2) = m \sum_{n \geq 1} n \begin{pmatrix} b_1 a_{1,n} \\ b_2 a_{2,n} \end{pmatrix} e_{nm}. \tag{71}$$

Hence,

$$\begin{aligned} \partial_\lambda DG(\lambda_m^\pm, 0)v_m &= mb_1b_2 \begin{pmatrix} m\lambda_m^\pm - m + 1 - b_2^{2m} \\ (b_2/b_1)^m - (b_1b_2)^m \end{pmatrix} e_m \\ &\triangleq mb_1b_2 \mathbb{W}_m e_m. \end{aligned}$$

This pair of functions is in the range of $DG(\lambda_m^\pm, 0)$ if and only if the vector \mathbb{W}_m is a scalar multiple of the second column of the matrix $M_m(\lambda_m^\pm)$ defined by (66). This happens if and only if

$$(m\lambda_m^\pm - m + 1 - b_2^{2m})^2 - \left(\left(\frac{b_2}{b_1} \right)^m - (b_1b_2)^m \right)^2 = 0. \tag{72}$$

Combining this equation with $\det M_m = 0$, we find

$$(m\lambda_m^\pm - m + 1 - b_2^{2m})^2 + (m\lambda_m^\pm - m + 1 - b_2^{2m}) \left(m\lambda_m^\pm - 1 + b_1^{2m} - m \left(\frac{b_2}{b_1} \right)^2 \right) = 0,$$

which is equivalent to

$$(m\lambda - m + 1 - b_2^{2m}) \left(2m\lambda - m \left(1 + \left(\frac{b_2}{b_1} \right)^2 \right) - b_2^{2m} + b_1^{2m} \right) = 0.$$

Thus, we find that

$$m\lambda_m^\pm - m + 1 - b_2^{2m} = 0 \quad \text{or} \quad 2m\lambda_m^\pm - m \left(1 + \left(\frac{b_2}{b_1} \right)^2 \right) - b_2^{2m} + b_1^{2m} = 0.$$

The first possibility is excluded by (72), and the second one corresponds to a multiple eigenvalue condition: $\lambda_m^+ = \lambda_m^-$, that is, $\Delta_m = 0$. This completes the proof of Proposition 22. \square

4.5.3. Proof of Theorem 9. Our next task is to study the bifurcation of 1-fold rotating patches. Recall from Section 4.4.3 that for $m = 1$ there are two different eigenvalues given by

$$\lambda_1^- = (b_2/b_1)^2, \quad \lambda_1^+ = 1 + b_2^2 - b_1^2.$$

In that paragraph, we observed significant differences in their behaviors, and we shall see next how this fact does affect the bifurcation problem. It appears that the bifurcation with λ_1^- is very complicate due to the range of the linearized operator which is of infinite codimension. Nevertheless, with λ_1^+ , the situation is actually more tractable and the bifurcation occurs frequently. Before stating the basic results of this section, we need to define some notation. Let $b_1 \in]0, 1[$ be a fixed real number, and define the set

$$\mathcal{E}_{b_1} \triangleq \{b_2 \in]0, b_1[: \text{there exists } m \geq 2 \text{ such that } P_m(\lambda_1^+) = 0\}.$$

The polynomial P_m was defined in (51), which is up to a factor the characteristic polynomial of the matrix $M_m(\lambda)$. The set \mathcal{E}_{b_1} corresponds to the abscissa of the points of intersection between the collection of the curves $\{\mathcal{C}_m : m \geq 2\}$ and \mathcal{C}_1^+ , which were defined in (53). Recall from Proposition 20(ii–iii) that for each $m \geq 2$ there is at most one value x_m of b_2 such that $P_m(\lambda_1^+) = 0$. Moreover, the sequence $(x_m)_{m \geq b_1^{-2}}$ is strictly increasing and converges to b_1 . Now we will prove the following result.

Proposition 23. *The following assertions hold true.*

- (i) *The range of $DG(\lambda_1^-, 0)$ has an infinite codimension.*
- (ii) *If $b_2 \in \mathcal{E}_{b_1}$, then the kernel of $DG(\lambda_1^+, 0)$ is two-dimensional and generated by the vectors $v_1 = \begin{pmatrix} 1 \\ 1 \end{pmatrix}$ and v_m of Proposition 22, with $m \geq 2$ being the only integer such that $P_m(\lambda_1^+) = 0$. In addition, the range of $DG(\lambda_1^+, 0)$ is closed and has codimension 2.*
- (iii) *If $b_2 \notin \mathcal{E}_{b_1}$, then the kernel of $DG(\lambda_1^+, 0)$ is one-dimensional and is generated by the vector v_1 seen before. Furthermore, the range of $DG(\lambda_1^+, 0)$ has codimension 1 and the transversality assumption is satisfied:*

$$\partial_\lambda DG(\lambda_1^+, 0)v_1 \notin R(DG(\lambda_1^+, 0)).$$

Proof. (i) According to (66), we obtain

$$M_n(\lambda_1^-) \triangleq \begin{pmatrix} b_1[-1 + b_1^{2n}] & b_2[(b_2/b_1)^n - (b_1 b_2)^n] \\ -b_1[(b_2/b_1)^n - (b_1 b_2)^n] & b_2[n((b_2/b_1)^n - 1) + 1 - b_2^{2n}] \end{pmatrix}.$$

In this case, we get that the determinant of $M_n(\lambda_1^-)$ behaves for large n like $b_1 b_2 n$. Consequently, we deduce from (69) the existence of $\alpha \neq 0$ such that

$$a_{1,n} = \alpha c_{1,n} + o(1),$$

which means that the preimage of an element of Y_m by $DG(\lambda_1^-, 0)$ is not in general better than $C^\alpha(\mathbb{T})$. This implies that the range of the linearized operator is of infinite codimension. It follows that one important condition of the Crandall–Rabinowitz theorem is violated, and therefore, the bifurcation in this special case still unsolved.

(ii) Let $b_2 \in \mathcal{E}_{b_1}$. Then by definition, there exists $m \geq 2$ such that $P_m(\lambda_1^+) = 0$. This means that λ_1^+ coincides with one of the two numbers λ_m^\pm . Therefore, the kernel of $DG(\lambda_1^+, 0)$ is given by the two-dimensional vector space

$$\text{Ker } DG(\lambda_1^+, 0) = \text{Ker } M_1(\lambda_1^+) \oplus \text{Ker } M_m(\lambda_1^+) \bar{w}^{m-1}.$$

Easy computations give the expression

$$M_1(\lambda_1^+) = b_2(1 - b_1^2) \begin{pmatrix} -b_2/b_1 & b_2/b_1 \\ -1 & 1 \end{pmatrix}.$$

Obviously the kernel of $M_1(\lambda_1^+)$ is spanned by the vector $v_1 = \begin{pmatrix} 1 \\ 1 \end{pmatrix}$. However, we know that $\text{Ker } M_m(\lambda_1^+)$ is spanned by the vector v_m already seen in Proposition 22. To prove that the range is of codimension 2, we follow the same arguments of Proposition 22 bearing in mind that the determinant of $M_n(\lambda_1^+)$ behaves for large n like cn^2 with $c \neq 0$. We skip the details which are left to the reader.

(iii) Let $b_2 \notin \mathcal{E}_{b_1}$; then $P_m(\lambda_1^+)$ does not vanish for any $m \geq 2$. This means that the matrix $M_m(\lambda_1^+)$ is invertible, and therefore, the kernel of $DG(\lambda_1^+, 0)$ is one-dimensional and given by

$$\text{Ker } DG(\lambda_1^+, 0) = \text{Ker } M_1(\lambda_1^+) = \langle v_1 \rangle.$$

Similarly to Proposition 22, we get that the range is of codimension 1. In addition, the transversality condition is satisfied since the eigenvalue λ_1^+ is simple ($\lambda_1^+ \neq \lambda_1^-$) as has been discussed in the proof of Proposition 22(iii). The proof of Proposition 23 is now finished, and the result of Theorem 9 follows. \square

5. Numerical experiments

In order to obtain the V -states, we follow a similar procedure to that in [de la Hoz et al. 2016a; 2016b]; therefore, we shall omit some details, which can be consulted in those references.

5.1. Simply connected V -states.

5.1.1. Numerical derivation. Given a simply connected domain D with boundary $z(\theta)$, where $\theta \in [0, 2\pi[$ is the Lagrangian parameter and z is counterclockwise parametrized, the condition of D being a V -state rotating with angular velocity Ω is given by (15), i.e.,

$$\text{Re} \left\{ \left(2\Omega \overline{z(\theta)} + \frac{1}{2\pi i} \int_0^{2\pi} \frac{\overline{z(\theta) - z(\phi)}}{z(\theta) - z(\phi)} z_\phi(\phi) d\phi - \frac{1}{2\pi i} \int_0^{2\pi} \frac{|z(\phi)|^2}{1 - z(\theta)z(\phi)} z_\phi(\phi) d\phi \right) z_\theta(\theta) \right\} = 0. \tag{73}$$

As in [de la Hoz et al. 2016a; 2016b], we use a pseudospectral method to find m -fold V -states from (73). We discretize $\theta \in [0, 2\pi[$ in N equally spaced nodes $\theta_i = 2\pi i/N, i = 0, 1, \dots, N - 1$. Observe that the integrand in the first integral in (73) satisfies

$$\lim_{\phi \rightarrow \theta} \frac{\overline{z(\theta) - z(\phi)}}{z(\theta) - z(\phi)} \Big|_{\theta=\phi} = \frac{\overline{z_\theta(\theta)}}{z_\theta(\theta)}. \tag{74}$$

Therefore, bearing in mind (74), we can evaluate numerically with spectral accuracy the integrals in (73) at a node $\theta = \theta_i$ by means of the trapezoidal rule, provided that N is large enough:

$$\begin{aligned} \frac{1}{2\pi} \int_0^{2\pi} \frac{\overline{z(\theta_i) - z(\phi_j)}}{z(\theta_i) - z(\phi_j)} z_\phi(\phi_j) d\phi &\approx \frac{1}{N} \left(\frac{1}{z_\theta(\theta_i)} + \sum_{\substack{j=0 \\ j \neq i}}^{N-1} \frac{\overline{z(\theta_i) - z(\phi_j)}}{z(\theta_i) - z(\phi_j)} z_\phi(\phi_j) \right), \\ \frac{1}{2\pi} \int_0^{2\pi} \frac{|z(\phi)|^2}{1 - z(\theta_i)z(\phi)} z_\phi(\phi) d\phi &\approx \frac{1}{N} \sum_{j=0}^{N-1} \frac{|z(\phi_j)|^2}{1 - z(\theta_i)z(\phi_j)} z_\phi(\phi_j). \end{aligned} \tag{75}$$

In order to obtain m -fold V -states, we approximate the boundary z as

$$z(\theta) = e^{i\theta} \left[b + \sum_{k=1}^M a_k \cos(mk\theta) \right], \tag{76}$$

where the mean radius is b , and we are imposing that $z(-\theta) = \bar{z}(\theta)$; i.e., we are looking for V -states symmetric with respect to the x -axis. For sampling purposes, N has to be chosen such that $N \geq 2mM + 1$; additionally, it is convenient to take N a multiple of m , in order to be able to reduce the N -element discrete Fourier transforms to N/m -element discrete Fourier transforms. If we write $N = m2^r$, then $M = \lfloor (m2^r - 1)/(2m) \rfloor = 2^{r-1} - 1$.

We introduce (76) into (73) and approximate the error in (73) by an M -term sine expansion:

$$\begin{aligned} \operatorname{Re} \left\{ \left(2\Omega \overline{z(\theta)} + \frac{1}{2\pi i} \int_0^{2\pi} \frac{\overline{z(\theta) - z(\phi)}}{z(\theta) - z(\phi)} z_\phi(\phi) d\phi - \frac{1}{2\pi i} \int_0^{2\pi} \frac{|z(\phi)|^2}{1 - z(\theta)z(\phi)} z_\phi(\phi) d\phi \right) z_\theta(\theta) \right\} \\ \approx \sum_{k=1}^M b_k \sin(mk\theta). \end{aligned} \tag{77}$$

This last expression can be represented in a very compact way as

$$\mathcal{F}_{b,\Omega}(a_1, \dots, a_M) = (b_1, \dots, b_M) \tag{78}$$

for a certain $\mathcal{F}_{b,\Omega} : \mathbb{R}^M \rightarrow \mathbb{R}^M$. Remark that, for any Ω and any $b \in]0, 1[$, we trivially have $\mathcal{F}_{b,\Omega}(\mathbf{0}) = \mathbf{0}$, i.e., the circumference of radius b is a solution of the problem. Therefore, obtaining a simply connected V -state is reduced to numerically finding a nontrivial root (a_1, \dots, a_M) of (78). To do so, we discretize the $(M \times M)$ -dimensional Jacobian matrix \mathcal{J} of $\mathcal{F}_{b,\Omega}$ using first-order approximations. Fixing $|h| \ll 1$ (we have chosen $h = 10^{-10}$), we have that

$$\frac{\partial \mathcal{F}_{b,\Omega}(a_1, \dots, a_M)}{\partial a_1} \approx \frac{\mathcal{F}_{b,\Omega}(a_1 + h, \dots, a_M) - \mathcal{F}_{b,\Omega}(a_1, \dots, a_M)}{h}. \tag{79}$$

Hence, the first M coefficients of the sine expansion of (79) form the first row of \mathcal{J} , and so on. Therefore, if the n -th iteration is denoted by $(a_1, \dots, a_M)^{(n)}$, then the $(n + 1)$ -th iteration is given by

$$(a_1, \dots, a_M)^{(n+1)} = (a_1, \dots, a_M)^{(n)} - \mathcal{F}_{b,\Omega}((a_1, \dots, a_M)^{(n)}) \cdot [\mathcal{J}^{(n)}]^{-1},$$

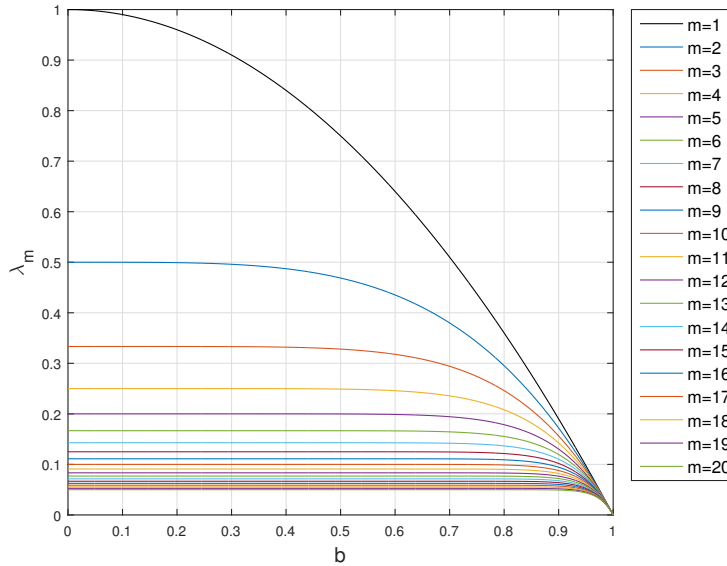


Figure 2. λ_m as a function of b , for $m = 1, \dots, 20$.

where $[\mathcal{F}^{(n)}]^{-1}$ denotes the inverse of the Jacobian matrix at $(a_1, \dots, a_M)^{(n)}$. This iteration converges in a small number of steps to a nontrivial root for a large variety of initial data $(a_1, \dots, a_M)^{(0)}$. In particular, it is usually enough to perturb the unit circumference by assigning a small value to $a_1^{(0)}$ and leave the other coefficients equal to zero. Our stopping criterion is

$$\max \left| \sum_{k=1}^M b_k \sin(mk\theta) \right| < \text{tol},$$

where $\text{tol} = 10^{-13}$. For the sake of coherence, we eventually change the sign of all the coefficients $\{a_k\}$, in order for, without loss of generality, $a_1 > 0$.

5.1.2. Numerical discussion. Given m and b , Proposition 14 defines the value λ_m at which we bifurcate from the circumference of radius b . Let us recall that $\lambda_m = 1 - 2\Omega_m$. Although working with λ is more convenient from an analytical point of view, we use $\Omega = (1 - \lambda)/2$ in the graphical representations of the V -states that follow because Ω is a more natural parameter from a physical point of view. Therefore, we bifurcate at $\Omega_m = (m - 1 + b^{2m})/(2m)$.

In Figure 2, we have plotted λ_m as a function of b , for $m = 1, \dots, 20$. Figure 2 suggests that there are two different situations: b close to 1 and b not so close to 1. Note that, in the latter case, the curves can be approximated by $\lambda_m \approx 1/m$, i.e., $\Omega_m \approx (m - 1)/(2m)$, which is in agreement with [Deem and Zabusky 1978].

In order to illustrate how the shape of the simply connected V -states depends on b , we consider the cases $1 \leq m \leq 4$; observe that everything said for $m = 3$ and $m = 4$ is valid for all $m \geq 3$. In general, fixing m and b , we bifurcate from the circumference with radius b at Ω_m . During the bifurcation process, there may be saddle-node bifurcation points [Kielhöfer 2012] appearing; in that case, we use the techniques

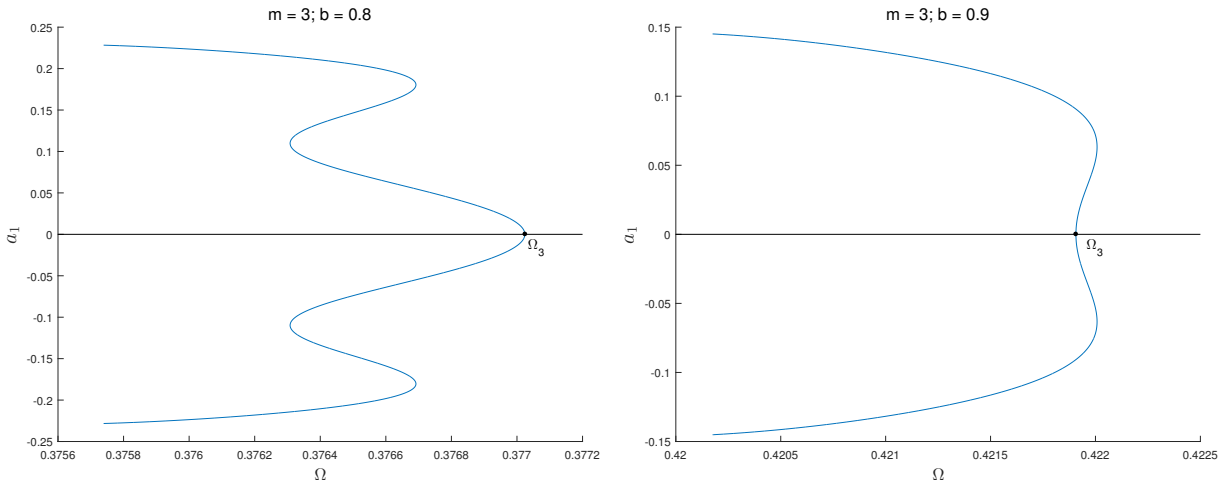


Figure 3. Bifurcation diagrams corresponding to $m = 3$ and $b = 0.8$ (left) and to $m = 3$ and $b = 0.9$ (right) with $N = 384$.

described in [de la Hoz et al. 2016a]. For instance, in Figure 3, we have plotted the bifurcation diagrams of the coefficient a_1 in (76) against Ω , for $m = 3$ and $b = 0.8$ (left) and for $m = 3$ and $b = 0.9$ (right). Note that, in the bifurcation diagrams, when starting to bifurcate at Ω_m , we sometimes take $\Omega < \Omega_m$ (left) and other times $\Omega > \Omega_m$ (right) although the latter case may appear only when b is *large enough*. Note also that we may have several saddle-node bifurcation points in the same bifurcation diagram, and hence more than two V -states corresponding to the same Ω , and in the same bifurcation branch. For instance, the left-hand side of Figure 3 tells us that there are three V -states corresponding to $m = 3$, $b = 0.8$ and $\Omega = 0.3765$, which we have plotted in Figure 4.

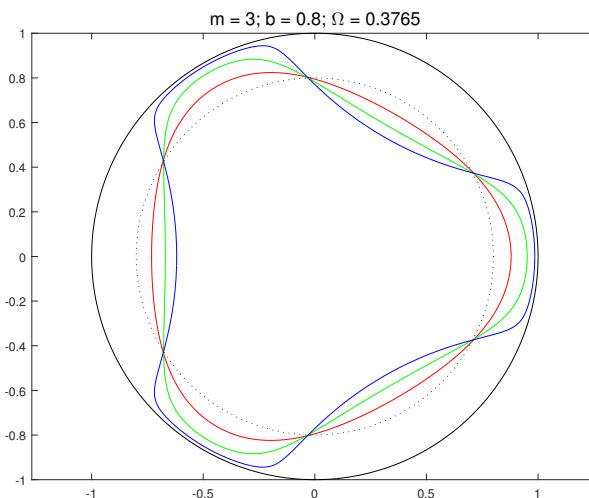


Figure 4. V -states from the same bifurcation branch (left side of Figure 3) corresponding to $m = 3$, $b = 0.8$ and $\Omega = 0.3765$ with $N = 768$.

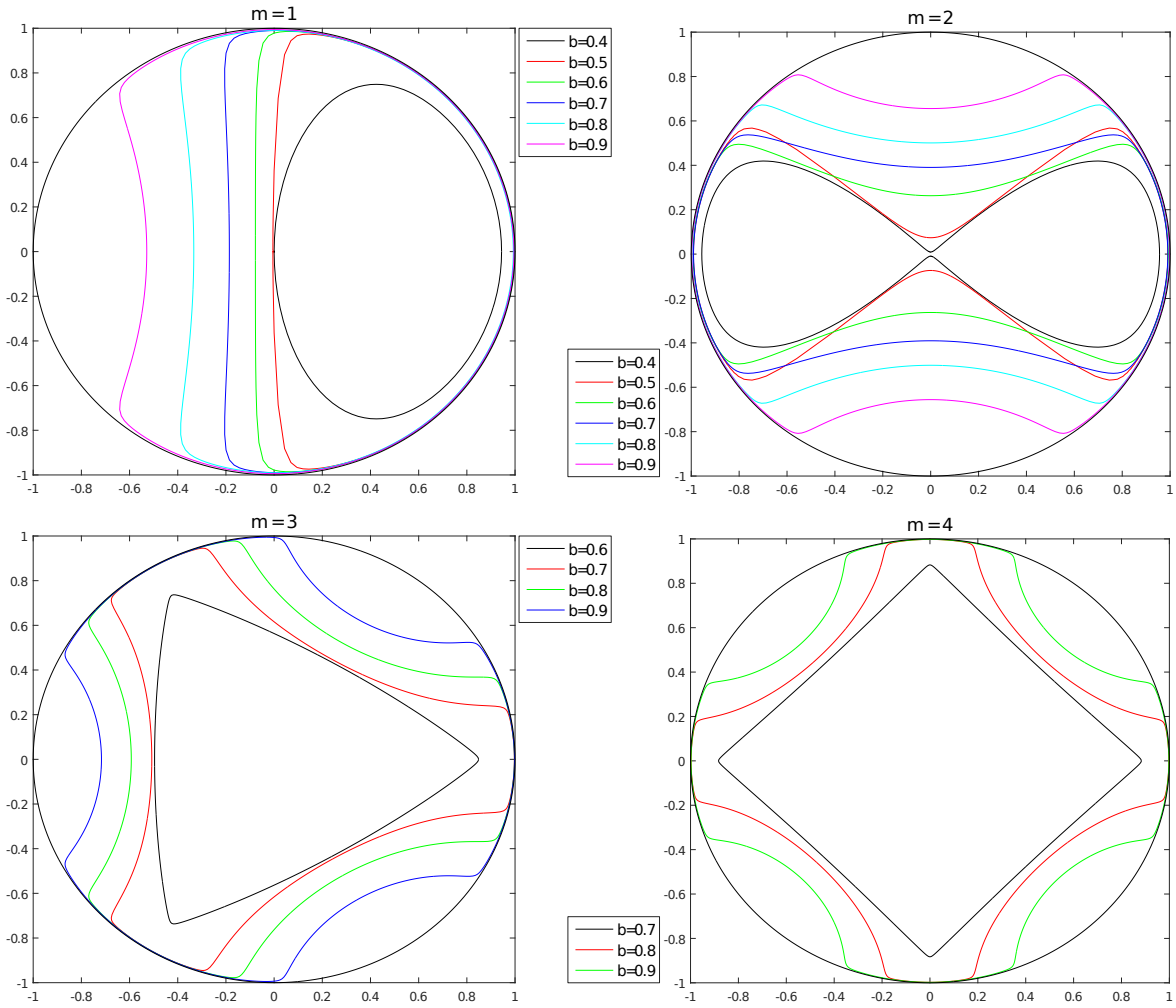


Figure 5. Approximations to the limiting V -states corresponding to $1 \leq m \leq 4$, for different b with $N = 256 \times m$. The values of Ω corresponding to the plots are given in Table 1.

We have approximated the limiting V -states occurring for $1 \leq m \leq 4$, which are depicted in Figure 5. Figure 5 confirms the observation on the size of b made from Figure 2. Loosely speaking, when b is far enough from 1, the rigid boundary does not have any remarkable effect on the shape of the V -states. Take for instance the cases $m = 1$ with $b = 0.4$, $m = 2$ with $b = 0.4$, $m = 3$ with $b = 0.6$ and $m = 4$ with $b = 0.7$: the approximations to the respective limiting V -states are clearly far away from the unit circumference whereas, in all the other cases, the distance to the unit circumference is smaller than 10^{-2} . In fact, Figure 5 suggests that, from a certain b on, we can obtain V -states arbitrarily close to the unit circumference and that the limiting V -state is precisely the one whose distance to the unit circumference is zero in the limit. Moreover, as b grows towards 1, the limiting V -states tend to cover an increasingly larger part of the unit circumference.

$b \downarrow m \rightarrow$	1	2	3	4
0.9	0.3749	0.4057	0.4199	0.4283
0.8	0.3251	0.3589	0.3755	0.3859
0.7	0.2900	0.3163	0.3321	0.3650
0.6	0.2640	0.2731	0.3144	0.3572
0.5	0.2459	0.2363		
0.4	0.1964	0.2018		

Table 1. Values of Ω for the V -states plotted in Figure 5.

Continuing with Figure 5, the cases $m = 1$ and $m = 2$ are pretty different from the other cases. Indeed, when $m \geq 3$ and b is small enough, the limiting V -states very closely resemble those in [Deem and Zabusky 1978] and corner-shaped singularities seem to develop. It is remarkable that the rigid boundary only affects the shape of the V -states for b pretty close to 1; furthermore, the larger m is, the larger b has to be, in order for the influence of the rigid boundary to become noticeable. On the other hand, when $m = 2$ and b is small enough, the limiting V -states are lemniscate-shaped; whether some self-intersection actually occurs deserves further study. Finally, when $m = 1$ and b is small enough, the limiting V -states seem to resemble an asymmetrical oval.

5.2. Doubly connected V -states.

5.2.1. Numerical derivation. Given a doubly connected domain D with outer boundary $z_1(\theta)$ and inner boundary $z_2(\theta)$, where $\theta \in [0, 2\pi[$ is the Lagrangian parameter and z_1 and z_2 are parametrized, D is a V -state if and only if its boundaries satisfy

$$\begin{aligned} \operatorname{Re} \left\{ \left(2\Omega_{z_1}(\theta) + \frac{1}{2\pi i} \int_0^{2\pi} \frac{\overline{z_1(\theta) - z_1(\phi)}}{z_1(\theta) - z_1(\phi)} z_{1,\phi}(\phi) d\phi - \frac{1}{2\pi i} \int_0^{2\pi} \frac{\overline{z_1(\theta) - z_2(\phi)}}{z_1(\theta) - z_2(\phi)} z_{2,\phi}(\phi) d\phi \right. \right. \\ \left. \left. - \frac{1}{2\pi i} \int_0^{2\pi} \frac{|z_1(\phi)|^2}{1 - z_1(\theta)z_1(\phi)} z_{1,\phi}(\phi) d\phi + \frac{1}{2\pi i} \int_0^{2\pi} \frac{|z_2(\phi)|^2}{1 - z_1(\theta)z_2(\phi)} z_{2,\phi}(\phi) d\phi \right) z_{1,\theta}(\theta) \right\} = 0, \quad (80) \end{aligned}$$

$$\begin{aligned} \operatorname{Re} \left\{ \left(2\Omega_{z_2}(\theta) + \frac{1}{2\pi i} \int_0^{2\pi} \frac{\overline{z_2(\theta) - z_1(\phi)}}{z_2(\theta) - z_1(\phi)} z_{1,\phi}(\phi) d\phi - \frac{1}{2\pi i} \int_0^{2\pi} \frac{\overline{z_2(\theta) - z_2(\phi)}}{z_2(\theta) - z_2(\phi)} z_{2,\phi}(\phi) d\phi \right. \right. \\ \left. \left. - \frac{1}{2\pi i} \int_0^{2\pi} \frac{|z_1(\phi)|^2}{1 - z_2(\theta)z_1(\phi)} z_{1,\phi}(\phi) d\phi + \frac{1}{2\pi i} \int_0^{2\pi} \frac{|z_2(\phi)|^2}{1 - z_2(\theta)z_2(\phi)} z_{2,\phi}(\phi) d\phi \right) z_{2,\theta}(\theta) \right\} = 0. \quad (81) \end{aligned}$$

As in the simply connected case, we use a pseudospectral method to find V -states. We discretize $\theta \in [0, 2\pi[$ in N equally spaced nodes $\theta_i = 2\pi i/N, i = 0, 1, \dots, N - 1$, where N has to be large enough. Then since z_1 and z_2 never intersect, all the integrals in (80) and (81) can be evaluated numerically with spectral accuracy at a node $\theta = \theta_i$ by means of the trapezoidal rule, exactly as in (75).

In order to obtain doubly connected m -fold V -states, we approximate z_1 and z_2 as in (76):

$$z_1(\theta) = e^{i\theta} \left[b_1 + \sum_{k=1}^M a_{1,k} \cos(mk\theta) \right], \quad z_2(\theta) = e^{i\theta} \left[b_2 + \sum_{k=1}^M a_{2,k} \cos(mk\theta) \right], \quad (82)$$

where the mean outer and inner radii are b_1 and b_2 , respectively, and we are imposing that $z_1(-\theta) = \bar{z}_1(\theta)$ and $z_2(-\theta) = \bar{z}_2(\theta)$, i.e., looking for V -states symmetric with respect to the x -axis. Again, if we choose N of the form $N = m2^r$, then $M = \lfloor (m2^r - 1)/(2m) \rfloor = 2^{r-1} - 1$.

We introduce (82) into (80) and (81), and as in (77), we approximate the errors in (80) and (81) by their M -term sine expansions, which are respectively $\sum_{k=1}^M b_{1,k} \sin(mk\theta)$ and $\sum_{k=1}^M b_{2,k} \sin(mk\theta)$. Then as in (78), the resulting systems of equations can be represented in a very compact way as

$$\mathcal{F}_{b_1, b_2, \Omega}(a_{1,1}, \dots, a_{1,M}, a_{2,1}, \dots, a_{2,M}) = (b_{1,1}, \dots, b_{1,M}, b_{2,1}, \dots, b_{2,M}) \quad (83)$$

for a certain $\mathcal{F}_{b_1, b_2, \Omega}: \mathbb{R}^{2M} \rightarrow \mathbb{R}^{2M}$. Remark that, for any Ω and any $0 < b_2 < b_1 < 1$, we have $\mathcal{F}_{b_1, b_2, \Omega}(\mathbf{0}) = \mathbf{0}$ trivially; i.e., any circular annulus is a solution of the problem. Therefore, obtaining a doubly connected V -state is reduced to numerically finding $\{a_{1,k}\}$ and $\{a_{2,k}\}$ such that $(a_{1,1}, \dots, a_{1,M}, a_{2,1}, \dots, a_{2,M})$ is a nontrivial root of (83). To do so, we discretize the $(2M \times 2M)$ -dimensional Jacobian matrix \mathcal{J} of $\mathcal{F}_{b_1, b_2, \Omega}$ as in (79), taking $h = 10^{-9}$:

$$\frac{\partial \mathcal{F}_{b_1, b_2, \Omega}(a_{1,1}, \dots, a_{1,M}, a_{2,1}, \dots, a_{2,M})}{\partial a_{1,1}} \approx \frac{\mathcal{F}_{b_1, b_2, \Omega}(a_{1,1} + h, a_{1,2}, \dots, a_{1,M}, a_{2,1}, \dots, a_{2,M}) - \mathcal{F}_{b_1, b_2, \Omega}(a_{1,1}, \dots, a_{1,M}, a_{2,1}, \dots, a_{2,M})}{h}. \quad (84)$$

Then the sine expansion of (84) gives us the first row of \mathcal{J} , and so on. Hence, if the n -th iteration is denoted by $(a_{1,1}, \dots, a_{1,M}, a_{2,1}, \dots, a_{2,M})^{(n)}$, then the $(n + 1)$ -th iteration is given by

$$(a_{1,1}, \dots, a_{1,M}, a_{2,1}, \dots, a_{2,M})^{(n+1)} = (a_{1,1}, \dots, a_{1,M}, a_{2,1}, \dots, a_{2,M})^{(n)} - \mathcal{F}_{b_1, b_2, \Omega}((a_{1,1}, \dots, a_{1,M}, a_{2,1}, \dots, a_{2,M})^{(n)}) \cdot [\mathcal{J}^{(n)}]^{-1},$$

where $[\mathcal{J}^{(n)}]^{-1}$ denotes the inverse of the Jacobian matrix at $(a_{1,1}, \dots, a_{1,M}, a_{2,1}, \dots, a_{2,M})^{(n)}$. To make this iteration converge, it is usually enough to perturb the annulus by assigning a small value to $a_{1,1}^{(0)}$ or $a_{2,1}^{(0)}$ and leave the other coefficients equal to zero. Our stopping criterion is

$$\left(\max_{k=1}^M \left| \sum_{k=1}^M b_{1,k} \sin(mk\theta) \right| < \text{tol} \right) \wedge \left(\max_{k=1}^M \left| \sum_{k=1}^M b_{2,k} \sin(mk\theta) \right| < \text{tol} \right),$$

where $\text{tol} = 10^{-13}$. As in [de la Hoz et al. 2016a; 2016b], $a_{1,1} \cdot a_{2,1} < 0$, so for the sake of coherence, we eventually change the sign of all the coefficients $\{a_{1,k}\}$ and $\{a_{2,k}\}$, in order for, without loss of generality, $a_{1,1} > 0$ and $a_{2,1} < 0$.

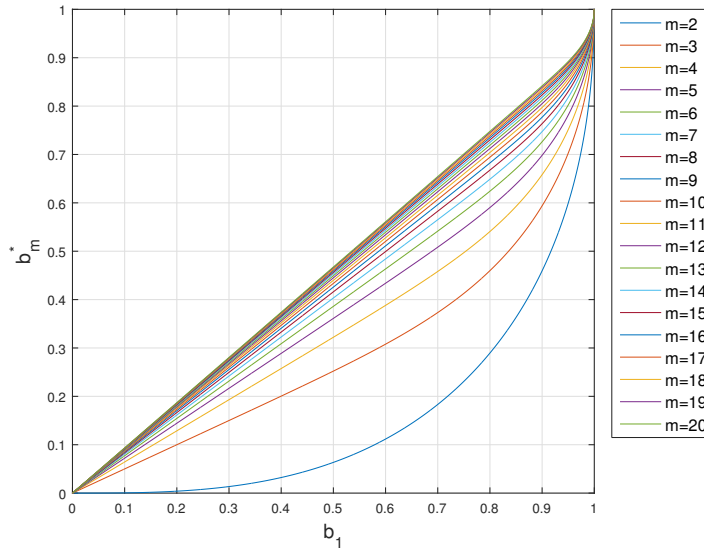


Figure 6. b_m^* as a function of b_1 , for $m = 2, \dots, 20$.

5.2.2. Numerical discussion. Proposition 19 states that, given $b_1 \in]0, 1[$ and $m \geq 2$, there is a certain b_m^* such that $b_2 \in [0, b_m^*]$. Let us recall that b_m^* is the only solution of

$$m = \frac{2 + 2(x/b_1)^m - (b_1^m + x^m)^2}{1 - (x/b_1)^2}.$$

In Figure 6, we have plotted b_m^* as a function of b_1 , for $m = 2, \dots, 20$.

If we make $b_2 = b_m^*$, then the discriminant Δ_m defined in Theorem 6 is equal to zero, and in that case, $\Omega_m^+ = \Omega_m^-$ or, equivalently, $\lambda_m^+ = \lambda_m^-$. Note that the relation between Ω^\pm and λ_m^\pm is given by

$$\Omega_m^\pm = \frac{1}{2}(1 - \lambda_m^\mp).$$

In Figure 7, we plotted λ_m^\pm as a function of $b_2 \in [0, b_m^*]$, for $m = 2, \dots, 20$ and $b_1 \in \{0.25, 0.5, 0.75, 0.99\}$. We have also plotted in black the special case $m = 1$, where $b_2 \in [0, b_1]$, $\lambda_1^+ = 1 + b_2^2 - b_1^2$ and $\lambda_1^- = (b_2/b_1)^2$. Observe that, whereas the curves λ_m^+ and λ_m^- are disjoint for $m \geq 2$, λ_1^+ may intersect λ_m^+ or λ_m^- . It is particularly interesting to see what happens when b_1 is close to 1; indeed, when $b_1 = 0.99$, the curves λ_m^- become practically indistinguishable.

Although Figure 7 gives a fairly good idea of the structure of λ_m^\pm , it may be clarifying to show globally how the curves in Figure 7 behave as b_1 changes, for a fixed m . In Figure 8, we have plotted λ_m^\pm as a function of $b_2 \in [0, b_m^*]$, for $m = 2, 3, 4$ and for all $b_1 \in]0, 1[$, in such a way that, for a given b_1 , the intersection between $z = b_1$ and the resulting surfaces yields curves equivalent to those in Figure 8. In general, the surfaces corresponding to $m \geq 3$ are very similar. On the other hand, Figure 8 shows that, when $m = 2$ and b_1 is *not too large*, the size of the curves (b_2, λ_2^\pm) is *very small*; indeed, in Figure 7, (b_2, λ_2^\pm) is hardly visible when $b_1 = 0.25$. A similar observation can be made with respect to the case $m = 2$ in Figure 6, which is markedly different from the others.

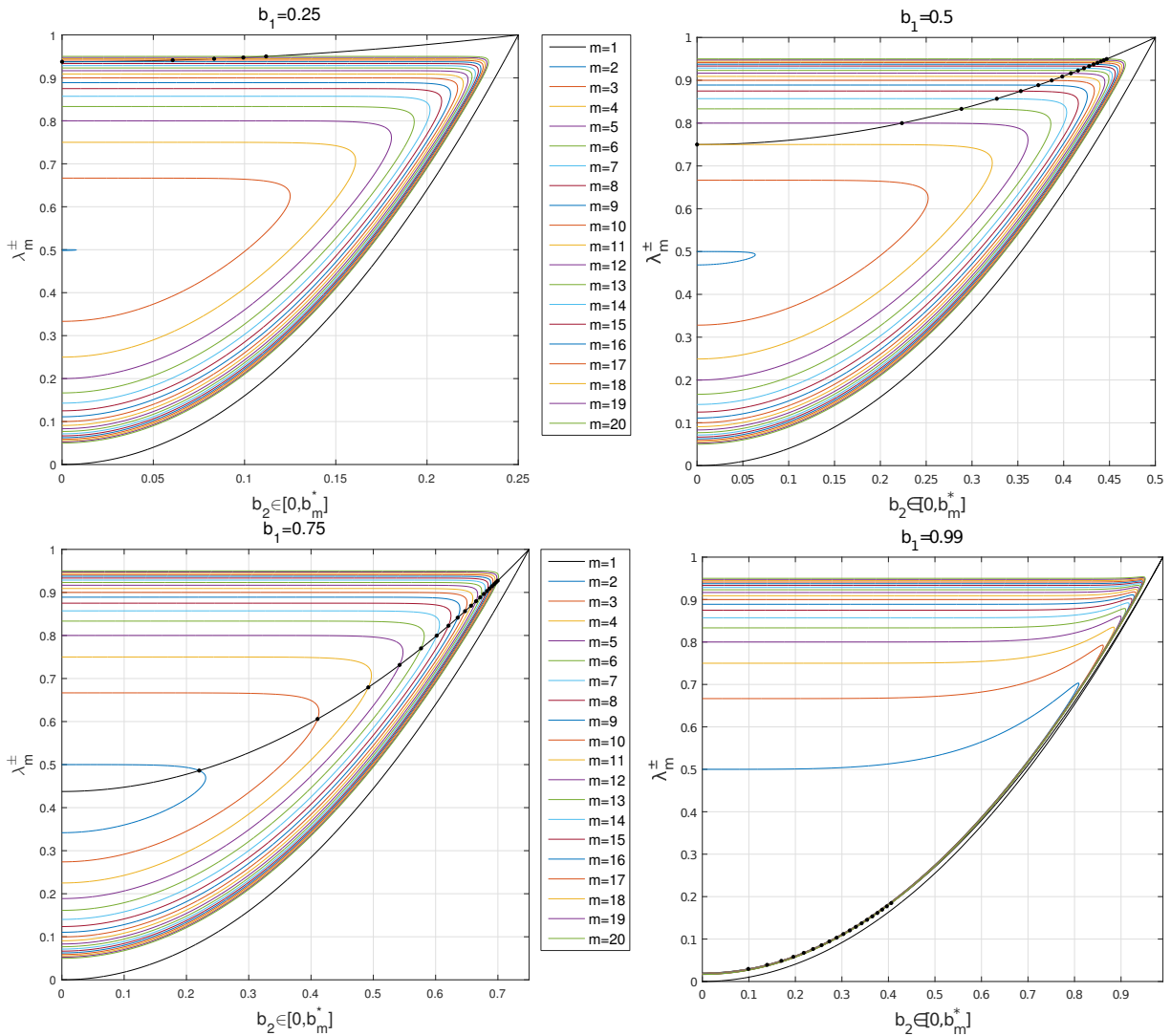


Figure 7. λ_m^\pm as a function of $b_2 \in [0, b_m^*]$, for $m = 2, \dots, 20$, together with the case $m = 1$ (black), for $b_1 \in \{0.25, 0.5, 0.75, 0.99\}$. We have marked with a small black dots the intersections happening between the case $m = 1$ and the other cases.

As in the simply connected case, we use $\Omega = (1 - \lambda)/2$ as our bifurcation parameter. In order to treat the saddle-node bifurcation points [Kielhöfer 2012] that may appear during the bifurcation process, we again use the techniques described in [de la Hoz et al. 2016a].

Before illustrating the shape of the doubly connected V -states, let us mention that the situation is much more involved than in the simply connected case, where there were roughly two situations for all m : b close to 1 and b not so close to 1. Indeed, we have to play now with both the proximity of b_1 to 1 and that of b_2 to b_m^* . Furthermore, we can start the bifurcation from the annulus of radii b_1 and b_2 at two

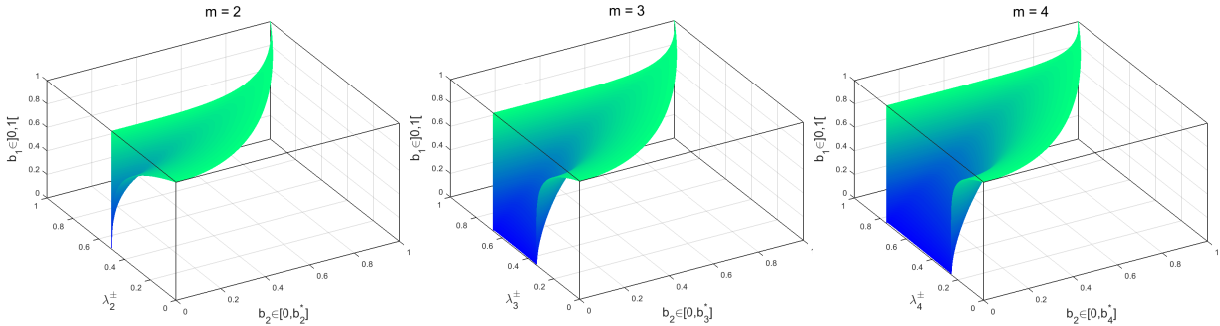


Figure 8. λ_m^\pm as a function of $b_2 \in [0, b_m^*]$, for $m = 2, 3, 4$ and for all $b_1 \in]0, 1[$.

different values of Ω , i.e., Ω_m^+ and Ω_m^- . Finally, the case $m = 1$ needs to be studied individually. All in all, we have detected the following scenarios.

When $m \geq 3$, there are roughly three cases when starting to bifurcate at Ω_m^+ and two cases when starting to bifurcate at Ω_m^- . More precisely, if we start to bifurcate at Ω_m^+ , we have to distinguish between the following:

- b_2 is very close to b_m^* . In that case, it seems possible to obtain V -states for all $\Omega \in]\Omega_m^-, \Omega_m^+[$, very much like in [de la Hoz et al. 2016b], irrespective of the size of b_1 . For example, in Figure 9, we have calculated the V -states corresponding to $m = 4, b_1 = 0.8$ and $b_2 = 0.53$. Observe that $b_4^* = 0.5407\dots$, i.e., we have chosen b_2 close enough to b_4^* . On the right-hand side, we have plotted the bifurcation diagram of the coefficients $a_{1,1}$ and $a_{2,1}$ in (82) against Ω , which shows that there is indeed a continuous bifurcation branch that joins Ω_m^- and Ω_m^+ , where $\Omega_4^- = 0.1335\dots$ and $\Omega_4^+ = 0.1671\dots$. On the left-hand side, we have plotted V -states for four different values of $\Omega \in]\Omega_m^-, \Omega_m^+[$.

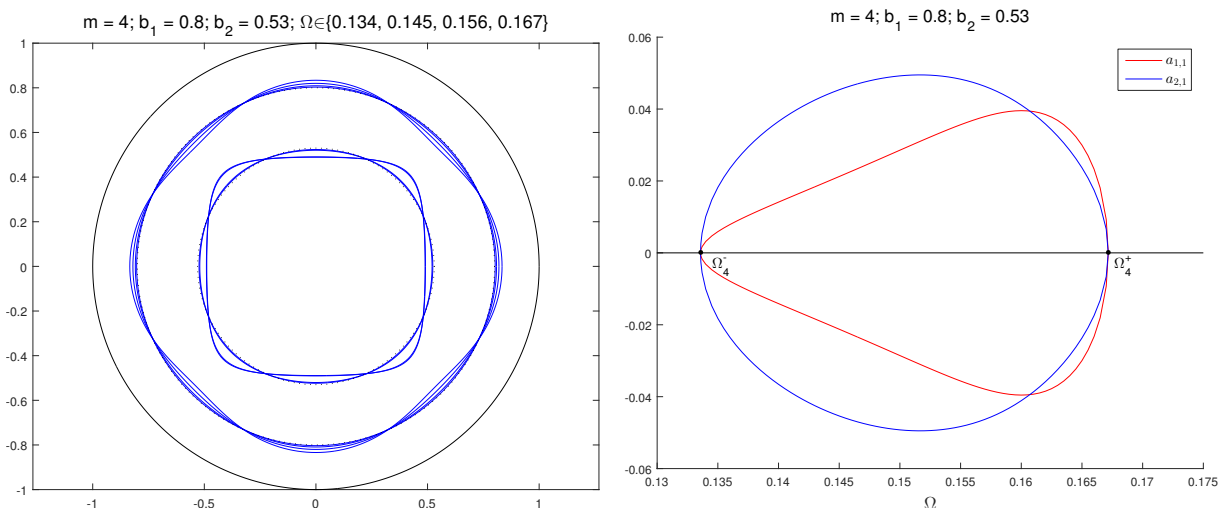


Figure 9. Left: V -states corresponding to $m = 4, b_1 = 0.8, b_2 = 0.53$ and several values of Ω . Right: bifurcation diagram. Here $N = 256$.

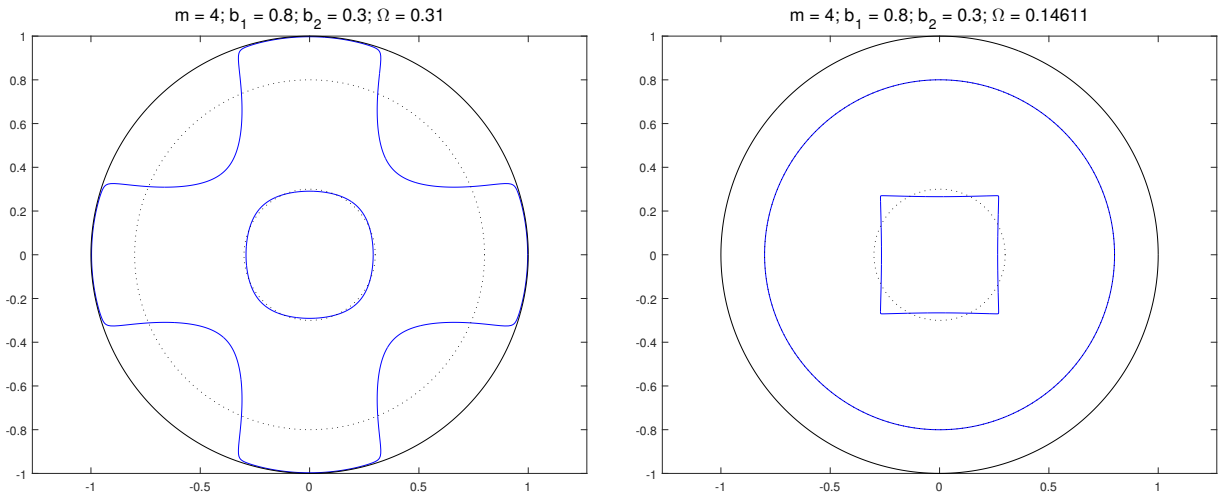


Figure 10. Approximation to the limiting V -states corresponding to $m = 4$, $b_1 = 0.8$ and $b_2 = 0.3$. Left: we have started to bifurcate at $\Omega_4^+ = 0.3256\dots$, taking $\Omega < \Omega_4^+$. Right: we have started to bifurcate at $\Omega_4^- = 0.1250\dots$, taking $\Omega > \Omega_4^-$. Here $N = 1024$.

- b_1 is close to 1, and b_2 is small enough. There are limiting V -states, for which the distance between the outer boundary z_1 and the unit circumference tends to zero, but the inner boundary z_2 does not deviate greatly from the circumference of radius b_2 . On the left-hand side of Figure 10, we have approximated the limiting V -state corresponding to $m = 4$, $b_1 = 0.8$ and $b_2 = 0.3$. The shape of z_1 is not very far from the case $m = 4$ and $b = 0.8$ of Figure 5.

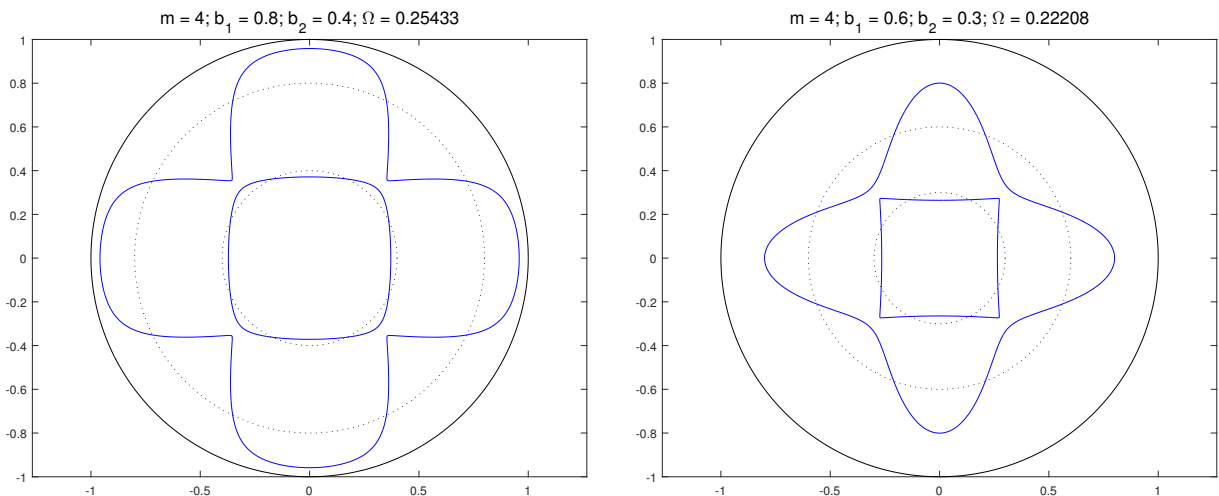


Figure 11. Left: approximation to the limiting V -state corresponding to $m = 4$, $b_1 = 0.8$ and $b_2 = 0.4$, starting to bifurcate at $\Omega_4^+ = 0.2706$, taking $\Omega < \Omega_4^+$. Right: approximation to the limiting V -state corresponding to $m = 4$, $b_1 = 0.6$ and $b_2 = 0.3$, starting to bifurcate at $\Omega_4^+ = 0.2516$, taking $\Omega < \Omega_4^+$. Here $N = 1024$.

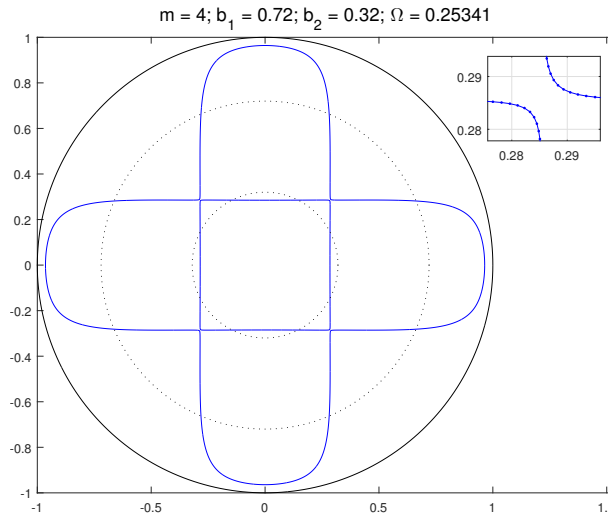


Figure 12. Approximation to the limiting V -state corresponding to $m = 4$, $b_1 = 0.72$ and $b_2 = 0.32$, starting to bifurcate at $\Omega_4^+ = 0.2851$, taking $\Omega < \Omega_4^+$. Here $N = 2048$. The zoom shows that the boundaries are very close from each other, but there is no intersection.

- b_1 and b_2 do not fit in the previous two cases. In that case, there are also limiting V -states, characterized by the appearance of corner-shaped singularities in z_1 or z_2 . In Figure 11, we have approximated the limiting V -states corresponding to $m = 4$, $b_1 = 0.8$ and $b_2 = 0.4$ (left) and to $m = 4$, $b_1 = 0.6$ and $b_2 = 0.3$ (right). Observe that the influence of the rigid boundary seems less perceptible in the second example, which accordingly does not differ too much from those in [de la Hoz et al. 2016b].

Although the distance between z_1 and the unit circumference is always strictly positive, the distance between z_1 and z_2 is sometimes very small, and we cannot exclude in advance the existence of limiting V -states where z_1 and z_2 actually touch each other. For instance, after playing with the values of b_1 and b_2 , we have found that the choice of $b_1 = 0.72$ and $b_2 = 0.32$ enables us to find a V -state such that the distance between z_1 and z_2 is of about 7×10^{-3} . This V -state is plotted in Figure 12, together with a zoom of one apparent intersection of the boundaries that shows that there is really no intersection and that the nodal resolution is adequate.

On the other hand, if we start to bifurcate at Ω_m^- , we have to distinguish between the following:

- b_2 is *very close* to b_m^* . This case has been explained above. In fact, it is irrelevant whether we start to bifurcate at Ω_m^- or at Ω_m^+ .
- b_2 is not *close enough* to b_m^* . In that case, there are limiting V -states, characterized by the appearance of corner-shaped singularities in z_2 whereas the outer boundary z_1 does not deviate greatly from the circumference of radius b_1 . On the right-hand side of Figure 10, we have approximated the limiting V -state corresponding to $m = 4$, $b_1 = 0.8$ and $b_2 = 0.3$. We have not bothered to plot the V -states

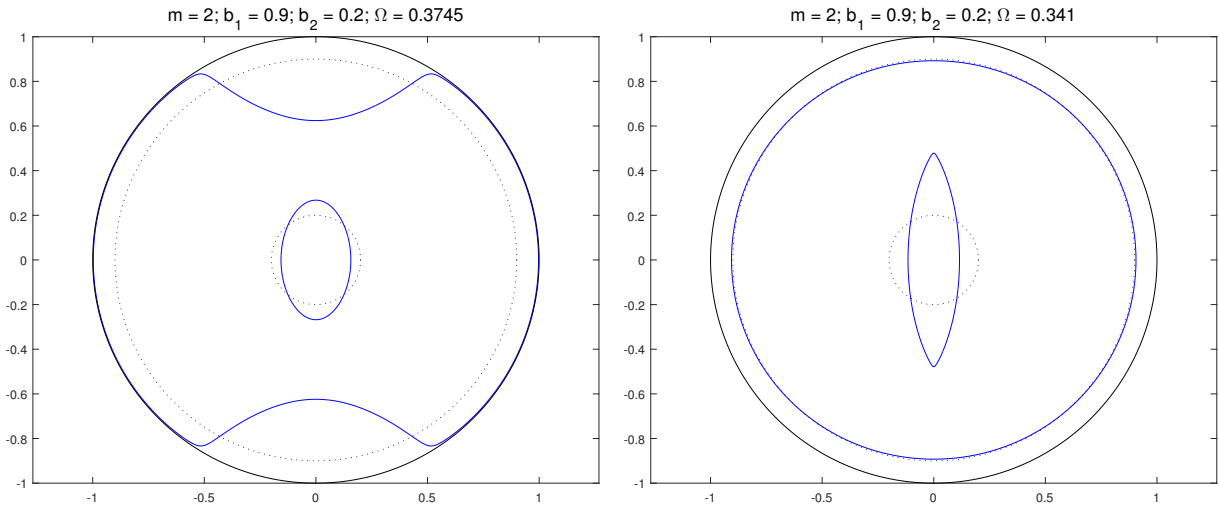


Figure 13. Left: approximation to the limiting V -states corresponding to $m = 2$, $b_1 = 0.9$ and $b_2 = 0.2$, starting to bifurcate at $\Omega_2^+ = 0.3892\dots$, taking $\Omega < \Omega_2^+$. Right: we have started to bifurcate at $\Omega_2^- = 0.2497\dots$, taking $\Omega > \Omega_2^-$. Here $N = 512$.

corresponding to those in Figures 11 and 12 but starting to bifurcate at Ω_m^- because they are virtually identical, up to a scaling of z_2 . This case closely matches that in [de la Hoz et al. 2016b], and the inner boundary resembles the simply connected V -states in [Deem and Zabusky 1978].

Summarizing, if we compare the doubly connected V -states just described with those in [de la Hoz et al. 2016b], we conclude that the truly unique case here is when b_1 is *close to 1* and b_2 is *small enough*.

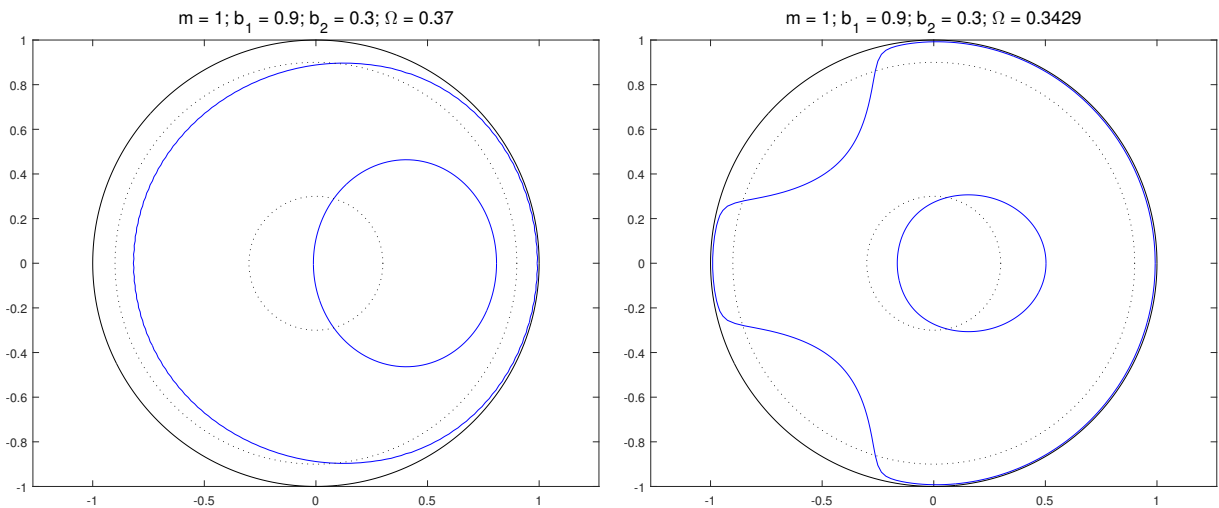


Figure 14. Approximation to the limiting V -states corresponding to $m = 1$, $b_1 = 0.9$ and $b_2 = 0.3$. Left: we have started to bifurcate at $\Omega_1^+ = \frac{4}{9}$, taking $\Omega < \Omega_1^+$. Right: we have started to bifurcate at $\Omega_1^- = 0.36$, taking $\Omega > \Omega_1^-$. Here $N = 256$.

Regarding the case $m = 2$, everything said above is applicable. For example, in Figure 13, we have taken $b_1 = 0.9$ and $b_2 = 0.2$, i.e., a value of b_1 close to 1 and a value of b_2 small enough. On the left-hand side, we show an approximation to the limiting V -state appearing when starting to bifurcate at Ω_2^+ ; note the clear parallelism with the case $m = 2$ and $b = 0.9$ of Figure 5 and with the left-hand side of Figure 10. On the right-hand side, we show an approximation to the limiting V -state appearing when starting to bifurcate at Ω_2^- ; as in the right-hand side of Figure 10, corner-shaped singularities seem to develop in z_2 whereas z_1 has barely deviated from a circumference.

The case $m = 1$ also deserves a comment. In Figure 14, we have approximated the limiting V -states corresponding to $m = 1$, taking again a value of b_1 close to 1 and a value of b_2 small enough, more precisely, $b_1 = 0.9$ and $b_2 = 0.3$. On the left-hand side, we have started to bifurcate at Ω_1^+ , and on the right-hand side, we have started to bifurcate at Ω_1^- . It is remarkable that, in both cases, the distance of z_1 to the unit circumference is smaller than 10^{-2} . Moreover, even if the V -state on the left-hand side is roughly in agreement with Figure 5 and with the left-hand sides of Figures 10 and 13, the V -state on the right-hand side exhibits a completely different, unexpected behavior.

Acknowledgements

Francisco de la Hoz was supported by the Basque Government, through the project IT641-13, and by the Ministerio de Economía y Competitividad, through the project MTM2014-53145-P. Taoufik Hmidi was partially supported by the Agence Nationale de la Recherche project Dyficolti ANR-13-BS01-0003-01. Joan Mateu was partially supported by the grants of Generalitat de Catalunya 2014SGR7, Ministerio de Economía y Competitividad MTM2013-4469 and ECPP7 Marie Curie project Metric Analysis for Emergent Technologies.

References

- [Bertozzi and Constantin 1993] A. L. Bertozzi and P. Constantin, “Global regularity for vortex patches”, *Comm. Math. Phys.* **152**:1 (1993), 19–28. MR 1207667 Zbl 0771.76014
- [Burbea 1980] J. Burbea, “Vortex motions and conformal mappings”, pp. 276–298 in *Nonlinear evolution equations and dynamical systems* (Lecce, Italy, 1979), edited by M. Boiti et al., Lecture Notes in Phys. **120**, Springer, Berlin, 1980. MR 581901
- [Burbea 1982] J. Burbea, “Motions of vortex patches”, *Lett. Math. Phys.* **6**:1 (1982), 1–16. MR 646163 Zbl 0484.76031
- [Burbea and Landau 1982] J. Burbea and M. Landau, “The Kelvin waves in vortex dynamics and their stability”, *J. Comput. Phys.* **45**:1 (1982), 127–156. MR 650429 Zbl 0488.76023
- [Castro et al. 2016a] A. Castro, D. Córdoba, and J. Gómez-Serrano, “Existence and regularity of rotating global solutions for the generalized surface quasi-geostrophic equations”, *Duke Math. J.* **165**:5 (2016), 935–984. MR 3482335 Zbl 1339.35234
- [Castro et al. 2016b] A. Castro, D. Córdoba, and J. Gómez-Serrano, “Uniformly rotating analytic global patch solutions for active scalars”, *Ann. PDE* **2**:1 (2016), Art. 1, 34. MR 3462104
- [Cerretelli and Williamson 2003] C. Cerretelli and C. H. K. Williamson, “A new family of uniform vortices related to vortex configurations before merging”, *J. Fluid Mech.* **493** (2003), 219–229. MR 2017951 Zbl 1063.76008
- [Chemin 1998] J.-Y. Chemin, *Perfect incompressible fluids*, Oxford Lecture Series in Mathematics and its Applications **14**, Clarendon, New York, 1998. MR 1688875 Zbl 0927.76002
- [Crandall and Rabinowitz 1971] M. G. Crandall and P. H. Rabinowitz, “Bifurcation from simple eigenvalues”, *J. Functional Analysis* **8** (1971), 321–340. MR 0288640 Zbl 0219.46015

- [Deem and Zabusky 1978] G. S. Deem and N. J. Zabusky, “Vortex waves: stationary “V states”, interactions, recurrence, and breaking”, *Phys. Rev. Lett.* **40**:13 (1978), 859–862.
- [Depauw 1999] N. Depauw, “Poche de tourbillon pour Euler 2D dans un ouvert à bord”, *J. Math. Pures Appl.* (9) **78**:3 (1999), 313–351. MR 1687165 Zbl 0927.76014
- [Dritschel 1986] D. G. Dritschel, “The nonlinear evolution of rotating configurations of uniform vorticity”, *J. Fluid Mech.* **172** (1986), 157–182. Zbl 0616.76069
- [Farwig and Hishida 2011] R. Farwig and T. Hishida, “Asymptotic profile of steady Stokes flow around a rotating obstacle”, *Manuscripta Math.* **136**:3–4 (2011), 315–338. MR 2844813 Zbl 1229.35172
- [Fraenkel 2000] L. E. Fraenkel, *An introduction to maximum principles and symmetry in elliptic problems*, Cambridge Tracts in Mathematics **128**, Cambridge University, 2000. MR 1751289 Zbl 0947.35002
- [Guo et al. 2004] Y. Guo, C. Hallstrom, and D. Spirn, “Dynamics near an unstable Kirchhoff ellipse”, *Comm. Math. Phys.* **245**:2 (2004), 297–354. MR 2039699 Zbl 1061.76012
- [Hassainia and Hmidi 2015] Z. Hassainia and T. Hmidi, “On the V-states for the generalized quasi-geostrophic equations”, *Comm. Math. Phys.* **337**:1 (2015), 321–377. MR 3324164 Zbl 1319.35188
- [Hmidi 2015] T. Hmidi, “On the trivial solutions for the rotating patch model”, *J. Evol. Equ.* **15**:4 (2015), 801–816. MR 3427065 Zbl 1338.35365
- [Hmidi and Mateu 2016] T. Hmidi and J. Mateu, “Bifurcation of rotating patches from Kirchhoff vortices”, *Discrete Contin. Dyn. Syst.* **36**:10 (2016), 5401–5422. MR 3543554
- [Hmidi et al. 2013] T. Hmidi, J. Mateu, and J. Verdera, “Boundary regularity of rotating vortex patches”, *Arch. Ration. Mech. Anal.* **209**:1 (2013), 171–208. MR 3054601 Zbl 1286.35201
- [Hmidi et al. 2015] T. Hmidi, J. Mateu, and J. Verdera, “On rotating doubly connected vortices”, *J. Differential Equations* **258**:4 (2015), 1395–1429. MR 3294351 Zbl 06396994
- [de la Hoz et al. 2016a] F. de la Hoz, Z. Hassainia, and T. Hmidi, “Doubly connected V-states for the generalized surface quasi-geostrophic equations”, *Arch. Ration. Mech. Anal.* **220**:3 (2016), 1209–1281. MR 3466846 Zbl 1334.35263
- [de la Hoz et al. 2016b] F. de la Hoz, T. Hmidi, J. Mateu, and J. Verdera, “Doubly connected V-states for the planar Euler equations”, *SIAM J. Math. Anal.* **48**:3 (2016), 1892–1928. MR 3507551 Zbl 1342.35239
- [Kamm 1987] J. R. Kamm, *Shape and stability of two-dimensional uniform vorticity regions*, Ph.D. thesis, California Institute of Technology, 1987, Available at <http://search.proquest.com/docview/303551772>. MR 2635730
- [Kielhöfer 2012] H. Kielhöfer, *Bifurcation theory: an introduction with applications to partial differential equations*, 2nd ed., Applied Mathematical Sciences **156**, Springer, New York, 2012. MR 2859263 Zbl 1230.35002
- [Kirchhoff 1876] G. Kirchhoff, *Vorlesungen über mathematische Physik: Mechanik*, Teubner, Leipzig, 1876. JFM 08.0542.01
- [Lamb 1945] H. Lamb, *Hydrodynamics*, 6th ed., Dover, Mineola, NY, 1945.
- [Love 1893] A. E. H. Love, “On the stability of certain vortex motions”, *Proc. London Math. Soc.* **25**:1 (1893), 18–43.
- [Luzzatto-Fegiz and Williamson 2010] P. Luzzatto-Fegiz and C. H. K. Williamson, “Stability of elliptical vortices from “Imperfect–Velocity–Impulse” diagrams”, *Theor. Comp. Fluid Dyn.* **24**:1 (2010), 181–188. Zbl 1191.76056
- [Majda and Bertozzi 2002] A. J. Majda and A. L. Bertozzi, *Vorticity and incompressible flow*, Cambridge Texts in Applied Mathematics **27**, Cambridge University, 2002. MR 1867882 Zbl 0983.76001
- [Mitchell and Rossi 2008] T. B. Mitchell and L. F. Rossi, “The evolution of Kirchhoff elliptic vortices”, *Phys. Fluids* **20** (2008), 054103. Zbl 1182.76523
- [Overman 1986] E. A. Overman, II, “Steady-state solutions of the Euler equations in two dimensions, II: Local analysis of limiting V-states”, *SIAM J. Appl. Math.* **46**:5 (1986), 765–800. MR 858995 Zbl 0608.76018
- [Plotka and Dritschel 2012] H. Plotka and D. G. Dritschel, “Quasi-geostrophic shallow-water vortex-patch equilibria and their stability”, *Geophys. Astrophys. Fluid Dyn.* **106**:6 (2012), 574–595. MR 2982526
- [Polvani and Flierl 1986] L. M. Polvani and G. R. Flierl, “Generalized Kirchhoff vortices”, *Phys. Fluids* **29**:8 (1986), 2376–2379. Zbl 0601.76015

- [Pommerenke 1992] C. Pommerenke, *Boundary behaviour of conformal maps*, Grundlehren der mathematischen Wissenschaften **299**, Springer, Berlin, 1992. MR 1217706 Zbl 0762.30001
- [Saffman 1992] P. G. Saffman, *Vortex dynamics*, Cambridge University, New York, 1992. MR 1217252 Zbl 0777.76004
- [Tang 1987] Y. Tang, “Nonlinear stability of vortex patches”, *Trans. Amer. Math. Soc.* **304**:2 (1987), 617–638. MR 911087 Zbl 0636.76019
- [Wan 1986] Y. H. Wan, “The stability of rotating vortex patches”, *Comm. Math. Phys.* **107**:1 (1986), 1–20. MR 861881 Zbl 0624.76055
- [Warschawski 1935] S. E. Warschawski, “On the higher derivatives at the boundary in conformal mapping”, *Trans. Amer. Math. Soc.* **38**:2 (1935), 310–340. MR 1501813 Zbl 0014.26707
- [Wu et al. 1984] H. M. Wu, E. A. Overman, II, and N. J. Zabusky, “Steady-state solutions of the Euler equations in two dimensions: rotating and translating V -states with limiting cases, I: Numerical algorithms and results”, *J. Comput. Phys.* **53**:1 (1984), 42–71. MR 734586 Zbl 0524.76029
- [Yudovich 1963] V. I. Yudovich, “Nonstationary flow of an ideal incompressible liquid”, *USSR Comp. Math. Math. Phys.* **3**:6 (1963), 1407–1456. Zbl 0129.19402

Received 20 Oct 2015. Revised 27 Apr 2016. Accepted 28 May 2016.

FRANCISCO DE LA HOZ: francisco.delahoz@ehu.eus

Department of Applied Mathematics and Statistics and Operations Research, Faculty of Science and Technology, University of the Basque Country UPV/EHU, Barrio Sarriena S/N, 48940 Leioa, Spain

ZINEB HASSAINIA: zineb.hassainia@cims.nyu.edu

Courant Institute for Mathematical Sciences, New York University, New York, NY 10012-1185, United States

TAOUFIK HMIDI: thmidi@univ-rennes1.fr

Institut de Recherche Mathématique de Rennes, Université de Rennes 1, Campus de Beaulieu, 35 042 Rennes CEDEX, France

JOAN MATEU: mateu@mat.uab.cat

Departament de Matemàtiques, Universitat Autònoma de Barcelona, 08193 Barcelona, Spain

Analysis & PDE

msp.org/apde

EDITORS

EDITOR-IN-CHIEF

Patrick Gérard
patrick.gerard@math.u-psud.fr
Université Paris Sud XI
Orsay, France

BOARD OF EDITORS

Nicolas Burq	Université Paris-Sud 11, France nicolas.burq@math.u-psud.fr	Werner Müller	Universität Bonn, Germany mueller@math.uni-bonn.de
Massimiliano Berti	Scuola Intern. Sup. di Studi Avanzati, Italy berti@sissa.it	Gilles Pisier	Texas A&M University, and Paris 6 pisier@math.tamu.edu
Sun-Yung Alice Chang	Princeton University, USA chang@math.princeton.edu	Tristan Rivière	ETH, Switzerland riviere@math.ethz.ch
Michael Christ	University of California, Berkeley, USA mchrist@math.berkeley.edu	Igor Rodnianski	Princeton University, USA irod@math.princeton.edu
Charles Fefferman	Princeton University, USA cf@math.princeton.edu	Wilhelm Schlag	University of Chicago, USA schlag@math.uchicago.edu
Ursula Hamenstaedt	Universität Bonn, Germany ursula@math.uni-bonn.de	Sylvia Serfaty	New York University, USA serfaty@cims.nyu.edu
Vaughan Jones	U.C. Berkeley & Vanderbilt University vaughan.f.jones@vanderbilt.edu	Yum-Tong Siu	Harvard University, USA siu@math.harvard.edu
Vadim Kaloshin	University of Maryland, USA vadim.kaloshin@gmail.com	Terence Tao	University of California, Los Angeles, USA tao@math.ucla.edu
Herbert Koch	Universität Bonn, Germany koch@math.uni-bonn.de	Michael E. Taylor	Univ. of North Carolina, Chapel Hill, USA met@math.unc.edu
Izabella Laba	University of British Columbia, Canada ilaba@math.ubc.ca	Gunther Uhlmann	University of Washington, USA gunther@math.washington.edu
Gilles Lebeau	Université de Nice Sophia Antipolis, France lebeau@unice.fr	András Vasy	Stanford University, USA andras@math.stanford.edu
Richard B. Melrose	Massachusetts Inst. of Tech., USA rbm@math.mit.edu	Dan Virgil Voiculescu	University of California, Berkeley, USA dvv@math.berkeley.edu
Frank Merle	Université de Cergy-Pontoise, France Frank.Merle@u-cergy.fr	Steven Zelditch	Northwestern University, USA zelditch@math.northwestern.edu
William Minicozzi II	Johns Hopkins University, USA minicozz@math.jhu.edu	Maciej Zworski	University of California, Berkeley, USA zworski@math.berkeley.edu
Clément Mouhot	Cambridge University, UK c.mouhot@dpms.cam.ac.uk		

PRODUCTION

production@msp.org
Silvio Levy, Scientific Editor

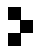
See inside back cover or msp.org/apde for submission instructions.

The subscription price for 2016 is US \$235/year for the electronic version, and \$430/year (+\$55, if shipping outside the US) for print and electronic. Subscriptions, requests for back issues from the last three years and changes of subscribers address should be sent to MSP.

Analysis & PDE (ISSN 1948-206X electronic, 2157-5045 printed) at Mathematical Sciences Publishers, 798 Evans Hall #3840, c/o University of California, Berkeley, CA 94720-3840, is published continuously online. Periodical rate postage paid at Berkeley, CA 94704, and additional mailing offices.

APDE peer review and production are managed by EditFlow® from MSP.

PUBLISHED BY

 **mathematical sciences publishers**
nonprofit scientific publishing

<http://msp.org/>

© 2016 Mathematical Sciences Publishers

ANALYSIS & PDE

Volume 9 No. 7 2016

The final-state problem for the cubic-quintic NLS with nonvanishing boundary conditions	1523
ROWAN KILLIP, JASON MURPHY and MONICA VISAN	
Magnetic wells in dimension three	1575
BERNARD HELFFER, YURI KORDYUKOV, NICOLAS RAYMOND and SAN VŨ NGỌC	
An analytical and numerical study of steady patches in the disc	1609
FRANCISCO DE LA HOZ, ZINEB HASSAINIA, TAOUFIK HMIDI and JOAN MATEU	
Isolated singularities of positive solutions of elliptic equations with weighted gradient term	1671
PHUOC-TAI NGUYEN	
A second order estimate for general complex Hessian equations	1693
DUONG H. PHONG, SEBASTIEN PICARD and XIANGWEN ZHANG	
Parabolic weighted norm inequalities and partial differential equations	1711
JUHA KINNUNEN and OLLI SAARI	
A double well potential system	1737
JAEYOUNG BYEON, PIERO MONTECCHIARI and PAUL H. RABINOWITZ	



2157-5045(2016)9:7;1-5